CHANGES IN *CRYPTOCOCCUS* GENE EXPRESSION IN RESPONSE TO THE ANTIFUNGAL ACTIVITY OF THE ANTIDEPRESSANT SERTRALINE

A Dissertation

by

ANANYA DASGUPTA

Submitted to the Graduate and Professional School of Texas
A&M University
in partial fulfillment of the requirements for the degree of

DOCTOR OF PHILOSOPHY

Chair of Committee,	Matthew S. Sachs
Committee Members,	Deborah Bell-Pedersen
	Jerome Menet
	Michael Polymenis
Head of Department,	Alex Keene

December 2021

Major Subject: Biology

ABSTRACT

Cryptococcus neoformans, a heterothallic basidiomycete fungus, is one of the most invasive, opportunistic pathogens. It predominantly affects immunocompromised patients and is the most common cause of fungal meningitis worldwide, accounting for half a million deaths each year. Current antifungal treatments are limited due to poor efficacy, toxicity with long-term use, and emerging resistance to drugs such as azoles: fluconazole (FLC). Therapies against cryptococcal meningitis are especially challenging because drugs must cross the blood-brain barrier and not be pumped out of the central nervous system. Ideally, existing drugs could be repurposed if they crossed the blood-brain barrier and had antifungal activity. Zoloft (sertraline or SRT) is a widely prescribed antidepressant that kills multiple microbes, including *C. neoformans*. Additionally, SRT and FLC act synergistically against *C. neoformans.* Combination treatment of cryptococcal meningitis with SRT and FLC together is being studied in clinical trials. However, the underlying mechanism employed by SRT to kill *C. neoformans* remains unclear. Therefore, we chose as a strategy to dissect the antifungal action of SRT to identify changes in gene expression following treatment of *C. neoformans* with SRT, FLC, and SRT+FLC using strand-specific RNA-seq and ribosome profiling. Our differential gene expression results indicate that SRT kills the pathogen by a different mechanism than FLC. Furthermore, combined treatment with SRT and FLC results in differential expression of specific genes that are not induced or repressed with individual drug treatments, indicating that combined treatment drives additional changes in the fungal cells. SRT is found to have a greater impact on genes involved in membrane transport. We hypothesize that SRT could kill cells by physiological imbalance due to membrane damage in *C. neoformans* in a manner distinct from FLC.

ACKNOWLEDGEMENTS

My long journey as a doctoral student has been filled with numerous experiences that has shaped me as a person and helped me grow as a researcher. Several individuals have impacted my academic and personal life and I would like to take this opportunity to recognize their ever-lasting contributions. I want to begin with my teachers and tutors through various phases of my education who have encouraged my curiosity and nurtured my quest for knowledge. I have been fascinated with biology from the days of school excursions to science and technology centers and remember being awestruck by the 3D model of DNA in one of these trips. My interest and curiosity in science peaked when I got admission for my bachelors in the University of Calcutta with honors in microbiology. I went on to complete my masters from the same University and was selected for a research internship at the Indian Institute of Chemical Biology (IICB), Kolkata. I am indebted to all my professors, lecturers, tutors, laboratory assistants, and peers in those formative years, who built our scientific foundation and instilled a sincere sense of passion which drives me till date. I gradually developed a love for molecular biology from my research experience under Professor Arun Bandopadhyay at the IICB and decided to pursue my doctoral degree in biology. After a brief stint of clinical research in India, I finally came to Texas A&M University (TAMU) and embarked on my doctoral program.

In all these 8 years I have been through highs and lows, but it was a journey worth taking. I grew as a researcher every time I planned and designed my experiments as well as when I trouble-shooted at any experimental failure. I really want to thank those projects that did not bear fruit but put my problem-solving skills to test and perseverance in the long run. I am grateful to my supervisor Professor Matthew S. Sachs for his support throughout my time in his lab and for allowing me to work on different types of scientific questions spanning different model organisms. My colleagues in the department had been instrumental in getting me started on new techniques, handling lab equipments and served as a wonderful platform to dissect and discuss research and learn from our shared experiences. Professor Xiaorong Lin who was a part of my graduate committee and later a co-advisor on my dissertation project, is a person I am especially thankful to, for her faith in my scientific abilities and for guiding me to reach the completion of my project. All the scientists whom I had the opportunity to collaborate with at various institutes such as Ruhr University in Germany, Duke University, USA and at the NIH have all been crucial in expanding my breadth of knowledge and enriched my academic experiences. I want to also thank my committee members, Professors Deb Bell-Pedersen, Michael Polymenis and Jerome Menet who had provided their valuable scientific feedback to improve my research. Finally, my journey towards my doctoral degree was made easy by the support from my department and their staff who were always by my side especially through my recent illness. Jennifer Bradford, who was our graduate coordinator, deserves special mention without whom I could not have navigated grad school. I must also acknowledge Dr. Mark Zoran for extending the Dean’s office scholarship and my supervisor who advocated for it. This was a much-needed financial help which allowed me to pull through my final semester.

In the last couple of years, I had battled trauma, pain and anxiety due to my temporary arm disability which seemed to be the nemesis of the worst kind. I want to recognize and appreciate the efforts of the doctors, physical therapists and my psychological counsellors who made sure that I could face the situation and be strong enough to accept what is beyond my control. I was in terrible agony as I identify myself as an experimental researcher and is unfortunately restricted to sedentary work. However, I have not given up hope and a major share of that mental strength is because of all my friends at TAMU, who are undoubtedly my family away from home! Yindrila needs a special mention here for hosting me in the last couple of months and relieving me from all the house chores that triggers pain in my arms. She and her family helped me settle down in their home and I will be forever grateful for this gesture. I definitely needed this support and could work on my dissertation with proper focus and concentration. I consider myself to be fortunate for the help, support and unconditional love from all of the friends who took time out to drive me to the clinics, cook for me or send me groceries. They made my life fun and made this journey happy and memorable for me. My best friends Antara, Ankita, Neelam and Manisha whom I have known from India, have been my morale booster in those dark days and cheered the loudest in my little accomplishments. I thank them for being themselves and listening to my constant chatter, bearing with my sob stories and making my life a lot brighter and happier with their love.

In this long list of acknowledgements, I want to now talk about those few people who made me who I am today. My family is of utmost importance in my life and the strong bond that I share with them grounds me and pushes me to achieve my goals. I lost my uncle, Piya who would have been the happiest today, as he was the one who taught me to lead my life on my terms without compromise. I owe my decision to him to be able to choose to leave my home and study abroad. Living thousands of miles away from home, I miss my cousin, Chota who has raised me, been more than a mother to me and always kept praying for my success and well-being. I cannot thank her enough for all that she has done for me. I must also mention Didiya, my cousin who is another foster parent to me and the one who had been a silent pillar holding me in my life. My aunt whom I refer to as Bordi, is an inspiration for me for holding her high in the face of any hardship. I want to thank my sibling, Dadabhai for teaching me how to be positive in any situation. I have lost my parents in the first year of grad school, but I hope they are blessing me from wherever they are. I come from a tightly knit, middle class family and have several extended relatives who have loved me and been my support.

Last but not the least, I want to acknowledge my friend, my mentor and my critic, Rajat for being with me in thick and thin and always encouraging me to be the best version of myself. He is a talented and successful chemist and his passion and dedication acts as my greatest inspiration. I can still stand confident and strong even after so many heath issues and all of that credit goes to him. I look forward to being equally supportive towards him throughout our lives.

CONTRIBUTORS AND FUNDING SOURCES

Contributors

This work was supervised by a dissertation committee consisting of Professor Matthew S. Sachs, Deb Bell-Pedersen and Jerome Menet of the Department of Biology and Professor Michael Polymenis of the Department of Biophysics and Biochemistry. The project was co-advised by Professor Xiaorong Lin from University of Georgia.

The RNA sequencing library preparation mentioned in Chapter 2 and 3 was conducted by Dr. Cheng Wu. The data analyzed for Chapter 3 was performed in collaboration with Professor Minou Nowrousian and Tim A. Dahlman from Ruhr-Universität Bochum, Germany. All other work conducted for the dissertation was completed by the student independently.

Funding Sources

This work was made possible by National Institute of Health [NIH] R21 Grant under Grant Number [AI138158]. Its contents are solely the responsibility of the authors and do not necessarily represent the official views of the NIH.

TABLE OF CONTENTS

Page

LIST OF FIGURES

Page

LIST OF TABLES

CHAPTER I

INTRODUCTION

CRYPTOCOCCUS NEOFORMANS, ITS PATHOGENICITY, TREATMENT AND CELLULAR RESPONSE

The basidiomycete *Cryptococcus neoformans* is an opportunistic pathogen the first mention of which dates back to 1894 [1]. *C. neoformans* var. *grubii* (serotype A) and *C. neoformans* var. *neoformans* (serotype D) are predominantly responsible for causing diseases in immunocompromised individuals. *C. neoformans* var. *gattii* (serotypes B and C) can also affect immunocompetent patients. With the advent of the HIV AIDs pandemic, over half a million patients are killed from cryptococcal meningitis each year worldwide, particularly in sub-Saharan Africa [2-7].

C. neoformans is ubiquitously distributed in nature and is usually isolated from plants, soil and avian excreta. Three well studied cryptococcal virulence factors include capsule, melanin and the ability to grow at human body temperature [2, 3]. The capsule is made up of glucuronoxylomannan and galactoxylomannan, and is thought to provide protection against desiccation [8-10]. Melanin pigment helps the organism to tolerate UV radiations in the environment [11]. *C. neoformans* is dimorphic and the yeast form is the highly potent, infective form, even in the desiccated state and can enter human lungs through inhalation and reside in dormancy until any severe trauma deranges the overall immune health of an individual [3, 5, 12]. Colonized yeasts can increase the fungal burden by evading host macrophage defense mechanisms and ensue the pulmonary disease, cryptococcosis. In immunocompromised hosts, the yeasts can penetrate the central nervous system crossing the blood brain barrier and develop the most dangerous, life threatening form of the infection, cryptococcal meningitis as depicted in Fig 1.1 [7, 12].

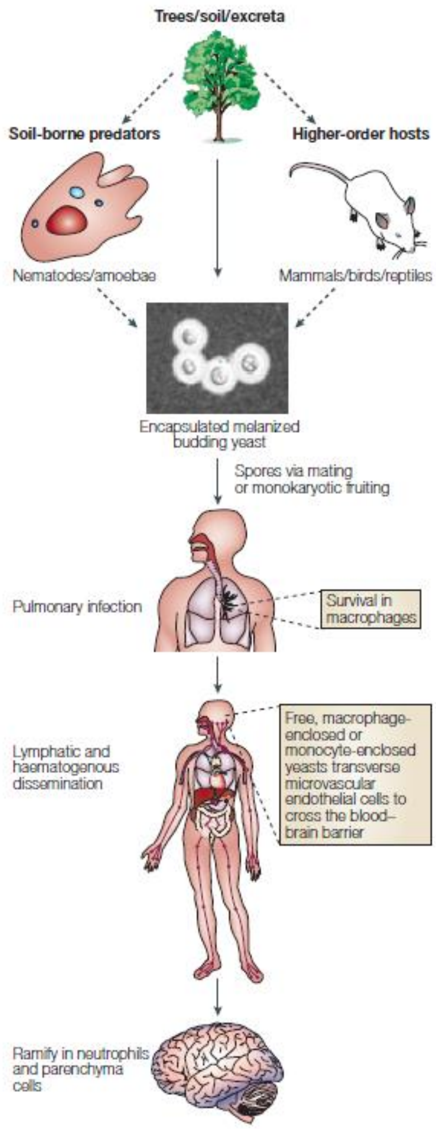

Figure I-1 Fig. 1.1. Pathogenic dissemination of Cryptococcus neoformans in humans [reproduced with permission from [12]

Antifungal therapies for invasive fungal infections are limited to a few classes of compounds: polyenes such as amphotericin B, echinocandins such as caspofungin, azoles such as fluconazole (FLC) and anti-metabolites such as flucytosine [3, 13-15]. Out of these, echinocandins are ineffective against *Cryptococcus spp.* [14, 16].

The first-line of treatment for cryptococcal infections involve amphotericin B, FLC and adjunct therapy in combination with flucytosine. The former affects ergosterol in fungal membranes and disrupts cellular integrity, killing the yeasts. However, long term toxicity of polyenes poses a problem and several kinds of lipid mediated delivery are introduced to the treatment regimen to improve efficacy and reduce toxic effects [14-17]. Azoles such as FLC inhibits the ergosterol biosynthetic enzyme ERG11, which belongs to the cytochrome P450 class of compounds. The major consequence of inhibition of ERG11, is the depletion of ergosterol, essential for maintaining cell structure and membrane permeability. The accumulation of the precursor sterols disrupts membrane function and affects cell growth [14-16, 18-20]. FLC is also well tolerated by patients and is widely preferred against *Cryptococcus spp*. However, this line of treatment is scarred by the emergence of antifungal resistance in the yeasts [3, 14, 15, 21, 22].

In order to mitigate the effects of drug resistance and expand the treatment regimen, drug combinations are being emphasized. [15, 23]. Amphotericin B has been combined with Flucytosine or FLC and polymyxin B and FLC combinations have been less toxic as lower doses for individual drugs are needed and additive or synergistic drug interactions increases efficacy of treatment [2, 13, 15, 23-25]. Antiproliferative effect of most drugs against *Cryptococcus* usually impairs ergosterol or decreases its availability thereby causing cell death due to cytosolic leakage, but some newer drugs such as triclosan have been shown to take a distinct route and induce apoptosis like features when used in combination with FLC or amphotericin B [25]. However, such combinations are usually difficult to reach the populations with maximal cryptococcal infections due to socioeconomic barriers and hence the need exists for newer antifungals to increase the available options for treatment. Drug discovery is itself a complex, lengthy, labor-intensive process and hence strategies are being investigated to screen for already approved, easily accessible drugs effective against invasive fungi [3, 19, 26, 27]. These approaches have led to the identification of anticryptococcal activity of sertraline (SRT), an antidepressant that has been under clinical trial [3, 4, 15, 28]. Sertraline being an antidepressant has good bioavalability in the brain which is a limitation for several drugs and so it can emerge as a potential therapeutic against cryptococcosis [29].

SRT has also been found to potentiate FLC and give synergistic advantage in killing *C. neoformans* [4, 30, 31]. However, the mechanism of function of SRT against *Cryptococcus* is not yet fully understood. Studies so far have implicated membrane damage, vesicular transport as antifungal targets and will be discussed in detail in the next section. It is also possible that SRT induces apoptosis-like processes to kill *Cryptococcus*. Nevertheless, all of the studied modes of action of SRT as an antifungal are distinct from common antifungals such as FLC and need further investigation to determine its molecular targets.

EFFECTS OF SERTRALINE

Background

SRT, marketed as Zoloft, is a selective serotonin reuptake inhibitor (SSRI) approved by the FDA (Food and Drug Administration) for treating depression and various types of mood disorders. It is a small molecule, used as first-line antidepressant treatment which is well tolerated and widely prescribed worldwide as shown in Fig. 1.2 [32, 33]. SRT primarily inhibits presynaptic reuptake of the neurotransmitter, serotonin (5-hydroxytryptamine 5-HT) which can then accumulate in the extracellular synapse, thus enhancing neuro-stimulation to increase signal transduction in the central nervous system. During nerve stimulation, serotonin released from pre-synaptic serotonergic neuron can bind to both pre- and post-synaptic transporters (SERT) on the nerve clefts. The blocking of pre-synaptic receptors to prevent reuptake of serotonin aids in post-synaptic uptake and augments neurotransmission as depicted in Fig 1.3. SRT and other SSRIs prevent the retrograde reuptake of serotonin and thus increase levels of post-synaptic serotonin, which can subsequently modulate behavior, improve mood and impact wakefulness, personality and overall cognition [4, 33, 34].

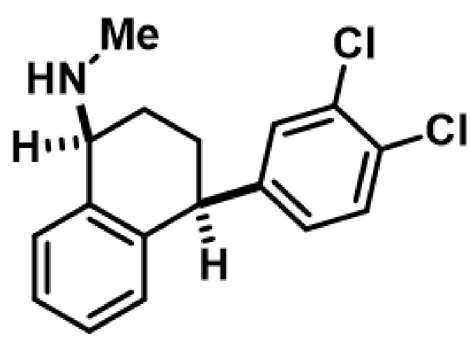

Figure I-2 Chemical structure of sertraline or Zoloft

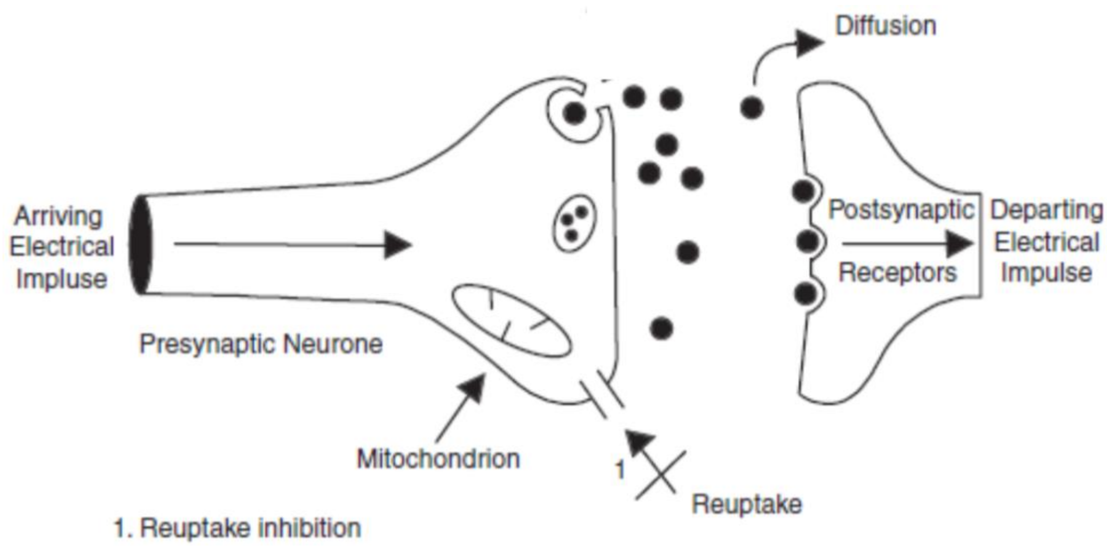

Figure I-3 Reuptake inhibition in neurotransmission; Solid Black circles represent serotonin [modified with permission from [33]

SRT has been widely studied for its psychoactive antidepressant properties and is found to achieve about 80% SERT occupancy [35]. Pre-synaptic reuptake inhibition results in substantial 5-HT accumulation in the synapse and increases transmission to the post-synaptic serotonergic neuron [32]. SRT is found to bind to the primary site of SERT which is closer to its substrate binding channel but away from its allosteric site. Since SRT can interact with residues of SERT both in the active site and primary ligand binding site of SERT, it has not been clearly defined as competitive or noncompetitive inhibitor [32]. This is explained in Fig 1.4. SRT can also bind to the bacterial homolog of SERT, leucine transporter (LeuT), and structural binding assays have been reported in the literature indicating interaction of SRT with residues near the substrate binding pocket of SERT [36]. Additionally, SRT is known to enter different cell types but the details of the uptake are not well established [32, 36].

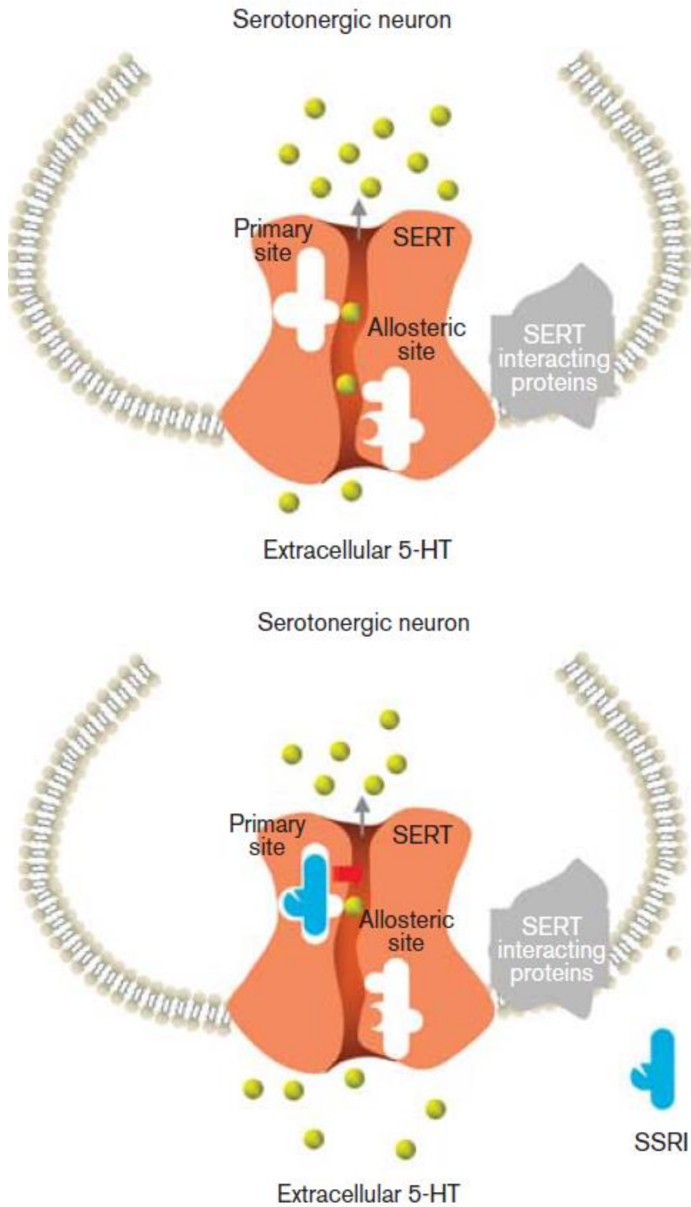

Figure I-4 Putative mechanism of interaction of SSRIs like SRT with the primary site of serotonin or 5-HT receptor, SERT and directing the increase in extracellular levels of 5-HT [reproduced with permission from [32]

Apart from its psychotropic functions, SRT has also been found to modulate a plethora of cellular interactions and activities. Serotonin also regulates physiological processes outside of the central nervous system, including cardiovascular, respiratory, gastro-intestinal, endocrine and genitourinary processes. Serotonin receptors are also widely distributed among various organ systems and hence the drugs targeting these receptors have been reported to impact various biological processes apart from their psychiatric effects [34]. While SRT is highly efficacious for treating major depressive disorder, obsessive compulsive disorder, post-traumatic stress disorder, anxiety and panic attacks, SRT treatment nonetheless shows transient side effects and may cause adverse reactions in certain cases. The major side effects of SSRIs including SRT are nausea, diarrhea, tremor, hallucinations, increased risk of bleeding, cardiovascular disorders and loss of urinary bladder control. The off target effects of these antidepressants can be attributed to their interactions with adrenergic, histamine and cholinergic receptors and dopamine transporters [32]. However SRT is often preferred as an SSRI of choice as it is one of the safest antidepressants in use because it shows a relatively good tolerance and a low index for overdose toxicity [37]. This makes it a powerful drug to be considered for a potential therapeutic for multiple conditions where treatment strategies are not yet established or suffer from issues such as low efficacy or adverse side effects. Thus, it is essential to better understand the impact of SRT on physiological processes and potentially help in the development of newer therapeutics.

Antimicrobial Activity of SRT

Numerous studies of SRT and its influence on various living organisms and their physiology have been published. One of the earliest reports of antibacterial activity came from the study of antidepressants effective against *Brucella spp* [38]. Most SSRIs are surprisingly active against Gram positive bacteria including staphylococci and streptococci. SRT has also shown to be active against *Haemophilus influenza, Campylobacter jejuni* and *Acinetobacter* [39]. In conjunction with antibiotics such as amoxicillin, clarithromycin, tetracycline, and metronidazole, sertraline has been found to be active against antibiotic resistant and sensitive *Helicobacter pylori* [40].

The antimicrobial activity of sertraline also extends to fungi. The study by Lass-Flörl *et.al* in 2001 described patients with recurrent vulvovaginal candidiasis, recovering from the condition and showing no acute episode of infection after SRT intervention for their premenstrual dysphoric disorder. SRT was observed to be effective against various isolates of *Candida* species: *Candida parapsilosis (*ATCC 22019), *Candida albicans, Candida glabrata* and *Candida tropicalis* [41, 42]. In other studies SRT has been found to exhibit anti-candida activity both *in vitro* and in biofilms, where cell membrane damage has been consistently observed after treatment with SRT [27, 43, 44]. It also exhibits anti-proliferative activity against the model yeast, *Saccharomyces cerevisiae,* where it has been found to target vesiculogenic membranes, increase lipid droplet formation and is thought to trigger an adaptive autophagic response [45, 46]. SSRIs including sertraline showed time and dose dependent fungicidal effect on *Aspergillus fumigatus, Aspergillus flavus* and *Aspergillus terreus* [42]. Similar to its activity when administered with antibacterial antibiotics, SRT can act synergistically with Amphotericin B, an important antifungal drug, against some isolates of *Aspergillus fumigatus* [47]. SRT is reported to be effective against *Cryptococcus neoformans* (H99), *C. gattii* (R265) and *C. albicans* (Caf2-1) and is seen to potentiate the antifungal fluconazole or amphotericin B in combinatorial treatments [4, 19, 30, 48, 49]. Antifungal activity of SRT is also observed against some less common fungal pathogens: *Lomentospora prolificans*, *Scedosporium spp., Fusarium spp., Paecilomyces spp., Alternaria spp. and Curvularia spp*. Either alone or in combination with amphotericin B [50].

Antiparasitic Activity of SRT

The inhibitory activity of SRT is also extended to parasitic protozoa such as *Leishmania* and *Trypanosoma*. There are several published articles in the literature advocating for repurposing of SRT as anti-protozoal drug candidate. This could expand the available treatment regimens and curb the development of antibiotic resistance in such difficult to treat parasitic infections. In the case of visceral leishmaniasis, SRT has been found to derange metabolic processes to limit the parasitic burden [51-53]. SRT is also reported to be effective against *Trypanosoma cruzi*, the causative agent of Chagas disease, where it causes oxidative damage and membrane alterations [54].

Caenorhabditis elegans which are resistant to known anthelmintic drugs are found to be more susceptible to SSRIs including SRT. Different life stages of worms including embryos, developing larvae and adult stages of *C. elegans* are inhibited within minutes of exposure. SRT and other SSRIs also reduces mobility of adult *Trichuris muris* whipworms, impede hatching and development of *Ancylostoma caninum* hookworms and kill *Schistosoma mansoni* flatworms, three highly disparate parasitic helminth species [53].

For the treatment of parasitic infections which are endemic in many parts of the world, SRT might become an easily accessible and affordable therapeutic [53].

Anti-cancer Activity of SRT

Oncogenesis and serotonin signaling pathways have been reported to be intertwined [55-59]. Prevention of serotonin reuptake by blocking the respective transporters has been studied for the purpose of inhibiting malignant brain tumors, lung cancer, breast cancer, prostate cancer, colorectal carcinoma, hepatocellular carcinoma and leukemia [60-65]. Several studies have documented the role of SRT alone or in combination with other chemotherapeutics and neuromodulatory drugs in killing or reducing tumors, via various mechanisms, indicating that a large network of pathways can be influenced by SRT [60-65]. In different human cancers such as melanoma, subcutaneous myeloid tumors, solid tumors in colon or lungs as well as in transgenic mice with breast cancer, tumor reduction mediated by SRT and other pharmaceutical compounds is associated with tumor reversion and downregulation of translationally controlled tumor protein (TCTP) [60, 61]. Treatment with SRT in combination with thioridazine, an antipsychotic drug for mental disorders, results in the reciprocal regulation of P53 with TCTP and exerts their anti-tumor and apoptotic responses. Each drug inhibits TCTP induced P53 protein degradation and increases the abundance of P53 protein which in turn represses the transcription of TCTP [61].

SRT may act on these pathways by interacting with other cross functional networks in the cancer cells. Initially direct binding of SRT to TCTP was observed by binding analysis and this was thought to provide a mechanism for regulation of TCTP activity by SRT. A more recent study using multiple ligand interaction techniques argues against this idea and suggests an indirect association of SRT and TCTP, potentially through the mammalian target of rapamycin complex 1 (mTORC1) pathway [61, 62]. SRT has been reported to reduce ATP levels, promote phosphorylation of AMP-activated protein kinase (AMPK), ribosomal protein S6 kinase (S6K) and ribosomal protein S6 and subsequently inhibiting mTOR pathway. On the other hand, TCTP has been found to be translationally upregulated by Phosphoinositide 3-kinases (PI3Ks)/ Protein kinase B (PKB), also known as Akt /mTORC1 pathway, thus tying the two together [64, 66-73]. AMPK/mTOR/S6K signaling pathway is regulated by SRT alone or in combination with other antineoplastic drugs and pharmacological inhibition of AMPK has been shown to significantly compromise the anti-cancer activity of SRT [67]. Thus the mTOR pathway and its downstream candidates can be a major molecular target for the anticancer activity of SRT [59].

Several studies have demonstrated the potential role of SRT in inducing apoptotic pathways in leukemia, prostate and colon cancer. [74-77]. The pro-apoptotic effect of SRT has been implicated in a vast array of cellular processes including cell cycle arrest, generation of reactive oxygen species (ROS), inhibition of phosphorylation of Akt, downregulation of anti-apoptotic factors such as TCTP and survivin and increase in the caspase 3 activity induced apoptosis. SRT treatment also causes increase in levels of autophagic markers such as double membraned vacuoles and levels of microtubule-associated protein 1A/1B-light chain 3 (LC3). [76, 78-85]. Also in non-small cell lung cancer cells SRT acts synergistically with the chemotherapeutic agent, erlotinib to stimulate autophagy as inferred from autolysosome formation and LC3-II accumulation [67, 86]. The various physiological effects of SRT are summarized in Fig.1.5.

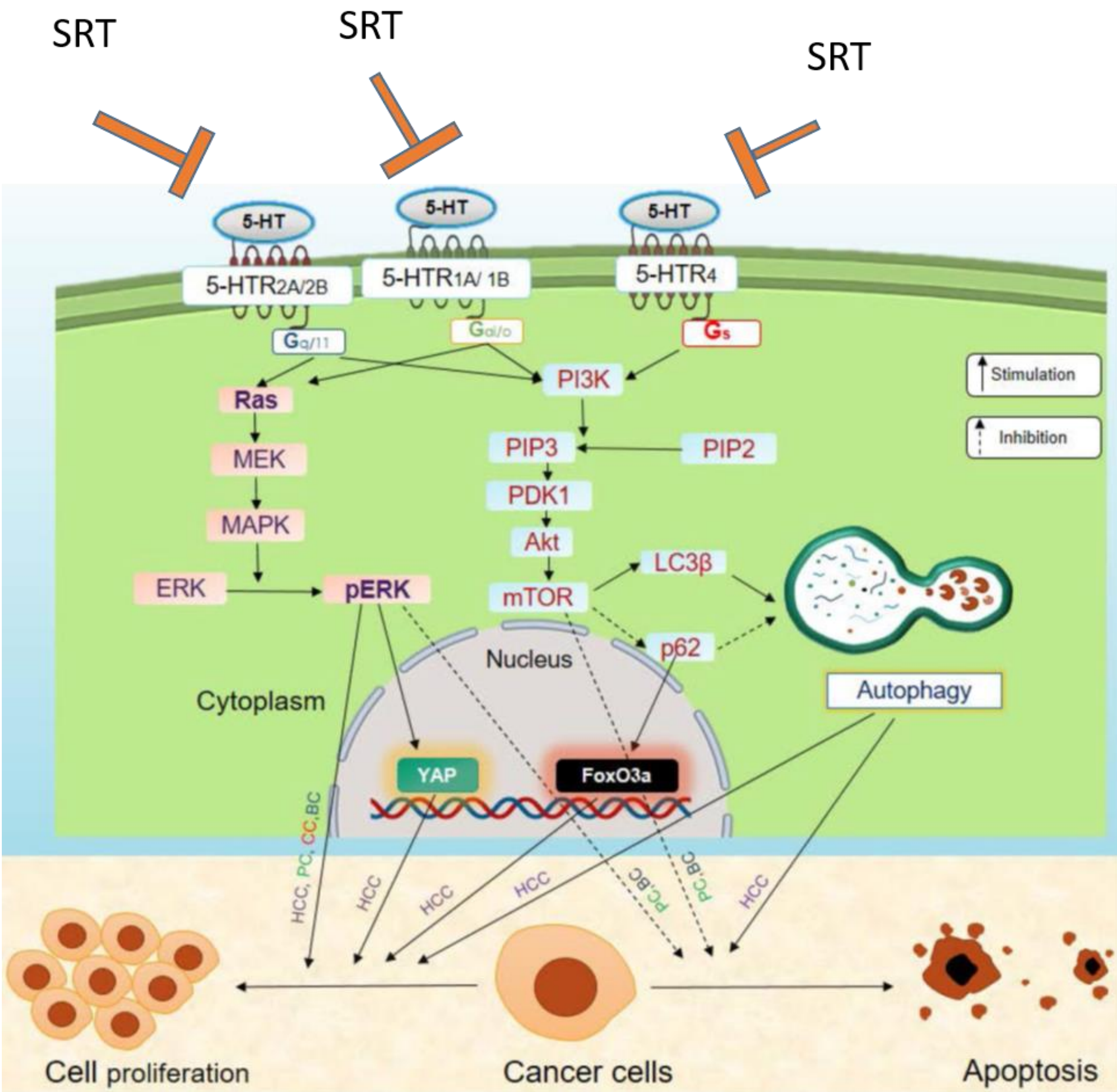

Figure I-5 Effects of SRT in disrupting serotonin signaling resulting in physiological consequences in cancer cells. BC, Breast cancer; CC, Colon cancer; HCC, Hepatocellular carcinoma; PC, Prostate cancer. Reproduced with permission from [59]

MOLECULAR BASIS OF ACTION

SRT has been widely investigated for its potential involvement in genetic, epigenetic, metabolic and cellular signaling pathways.

Membrane damage

Several biochemical analyses of SRT in vivo and in vitro have revealed the affinity of SRT towards cell membrane components such as lipids, efflux pumps, ABC transporters and proton coupled amino acid transporters in multidrug resistant bacteria and antifungal resistant fungi [87-91] Outer membrane permeabilization and cell shrinkage were observed in case on *Candida auris* treated with SRT [27]. In Gram negative bacteria membrane blebbing and perturbations in glycerophospholipids were observed as markers for lack of cell integrity caused due to drug treatment [27, 92]. SRT is reported to dock into bilayers, changing membrane conformation and interact with cell membranes and intracellular vesicles [93]. Studies in yeast cells suggest involvement of vacuolar ATPases and clathrin in uptake or intracellular accumulation of cationic amphipathic drugs such as SRT which leads to induction of phospholipidosis and could trigger autophagy [45, 46]. In another report showing Leishmanicidal effects of SRT, a morphological characteristic of multivesicular vacuole with altered membrane structure was observed in the promastigotes after SRT treatment [52].

Mitochondrial Dysfunction

Reduction in the level of ATP has often been associated with SRT treatment. Some reports suggest involvement of the drug in depolarization of the mitochondrial membrane, changes in mitochondrial membrane morphology, generation of ROS and induction of apoptosis through association of SRT with the mitochondrial outer membrane protein, VDAC I (voltage dependent anion channel protein I) [52, 73, 94, 95].

ER Stress / Calcium imbalance

Studies in certain cancers such as prostate cancer and other reports studying cytotoxicity of SRT in pancreatic β cells, hepatocytes and osteosarcoma, reveal the impact of SRT on processes involving the endoplasmic reticulum (ER). The rise of calcium ions is frequently observed in the cytosol during SRT treatment and is attributed to the action of membrane pumps in ER including phospholipase C regulated Ca^{+2} pumps, which can be reversed by inhibitors of ER Ca^{+2} channels [74, 78, 94]. SRT has also been shown to increase ER stress markers such as nitric oxide synthase, activating transcription factor (ATF) and C/EBP homology protein (CHOP), which can potentially be involved in the apoptotic effects of the drug [74, 77, 78, 96].

Oxidative stress / DNA damage

In several studies, SRT has been found to derail redox signaling by creating an imbalance between oxidants and antioxidants, resulting in oxidative stress and molecular damage. Elevated reactive oxygen species, lipid peroxidation and depletion of antioxidant enzymes in SRT-treated rats, mice and *Leishmania*, and elevated F2 isoprostane excretion in patients recovering from depressive disorders on SRT administration, are strong evidence of oxidative stress generation [52, 74, 97-105]. On the other hand, low doses of SRT have been found to reduce reactive oxygen species or oxidative status in rats or patients of depression [106-111]. SRT has also been implicated in increased oxidative stress index and decreased nuclear division index in human peripheral lymphocytes [112] . A study on *Drosophila* larvae showed double stranded DNA breaks were induced by SRT treatment on a mitotically active tissue and SRT treatment delayed larval development independent of its effect on serotonin signaling [75]. SRT's cytotoxicity was rescued by the addition of the antioxidant ascorbic acid, consistent with production of ROS and DNA damage being the result of SRT treatment [75].

Inhibition of translation

SRT is reported to inhibit translation both in vivo and in vitro. Cell free translation assays using fungal cell extracts show inhibition of protein synthesis by SRT in a dose dependent manner [4]. In breast cancer cells, SRT treatment is associated with decreased levels of eIF4E-associated eIF4G and eIF4A and increased levels of eIF4E binding proteins, thus effectively reducing the eIF4F complex, responsible for initiation of protein synthesis [66]. In the aforementioned cancer cell study, it is found that SRT promotes phosphorylation of eukaryotic initiation factor-2α (eIF2α) which is a hallmark of global suppression of translation. SRT also stimulates the expression of regulated in development and DNA damage response 1 (REDD1) protein, which is a negative regulator of mTOR pathway which in turn influences eIF4F assembly. Thus SRT could modulate translation by utilizing at least two targets: eIF2α phosphorylation and eIF4F assembly [66].

SIGNIFICANCE

The available treatment regimens for cryptococcal meningitis and cryptococcal pneumonia are highly restricted due to lack of efficacy, poor absorption and toxicity with long term use of existing antifungals. Antifungal resistance is also emerging as an obstruction to treat cryptococcal infections [4, 13]. Thus the current medical arsenal is limited to amphotericin B, flucytosine and fluconazole (FLC) [18, 113] . Treating cryptococcal meningitis is particularly challenging because drugs have to be able to cross the blood brain barrier and not be substrates for efflux pumps which are well-distributed in the central nervous system [113]. SRT penetrates to the brain and is found its antifungal activity synergizes with FLC [4, 114, 115]. The sheer effort, time and financial burden of *de novo* drug discovery can be relaxed if efficient use of existing resources can be carried out. Using already FDA approved drugs such as SRT that has overall social acceptance and biological relevance, antifungal therapies could be developed at a faster pace, saving numerous lives in return.

However, in spite of research conducted for over 50 years, the exact mode of action by which SRT kills fungal cells alone or in combination with other drugs is not clear. To explore the mechanism of growth inhibition, this dissertation uses genetic approaches including RNA sequencing and ribosome profiling of SRT-treated and FLC-treated *C.*

neoformans cells. The results suggest, similar to the common antifungal, FLC, SRT can also increase the levels of ergosterol genes albeit lesser number of genes than FLC, which is crucial in maintaining membrane integrity. While both drugs are found to repress ribosome biogenesis and potentially impact translation, SRT alters different sets of genes. SRT is found to have a greater impact on genes involved in membrane transport and can possibly kill cells by physiological imbalance as a consequence of membrane damage.

CHAPTER II

MATERIALS AND METHODS

Strains and media

Cryptococcus neoformans H99α wild type strain is used in this study. It was obtained from the lab of Prof. Xiaorong Lin, University of Georgia. Yeast form was maintained on YPD Yeast Peptone Dextrose agar petriplates and RPMI 1640 was used for broth culture with or without drug compounds.

YPD medias

Bacto agar (Invitrogen), Bacto peptone (Becton, Dickinson and Company),Glucose Powder or 40%, w/v (Fisher Scientific), Yeast extract (Becton, Dickinson and Company)

Method

For making 1L media, the following reagents are added to an autoclavable flask and mixed using a magnetic stirrer:

Reagents	**Amount for liquid media**	**Amount for agar plates**
Bacto agar	-	15g
Bacto peptone	20g	20g
Yeast extract	10g	10g
Glucose (dextrose)	20g	20g
Milli-Q Water	Upto 1000 mL	Upto 1000 mL

The mixture is autoclaved to sterilize media. Liquid media is used after cooling and at appropriate temperatures required. In a Biosafety Level 2 (BSL2) cabinet, warm media is poured in plastic petridishes to let it cool and solidify.

RPMI 1640 media

Reagents	**Amount**
MOPS	34.53g
Glucose	20g
RPMI1640 (+ Glu, -bicarb; Sigma R1383)	8.4g
Milli-Q water	Upto 1000 mL
1M NaOH as a buffering agent	40ml

Method

For making 1L media, all reagents except NaOH are added to 800ml Milli-Q water in an autoclavable flask and mixed using a magnetic stirrer.The pH of the media is adjusted to 7.0 +/- 0.1 @25^{0}C by adding 40 ml 1M NaOH and using a pH meter**.** Volume is adjusted to 1L by adding Milli-Q water**.** The media is sterilized by vacuum filtration using Nalgene Rapid-Flow sterile disposable bottle-top filters from Thermofisher.

Compounds

Sertraline hydrochloride (from Matrix Scientific) is dissolved in 1% dimethyl sulfoxide (DMSO) at a working concentration of 20 mg/ml and sterile filtered. During experiments, it is diluted with sterile filtered DMSO.

Fluconazole (from Sigma) is dissolved in 1% dimethyl sulfoxide (DMSO) at a working concentration of 2 mg/ml and sterile filtered. During experiments, it is also diluted with sterile filtered DMSO.

Growth Condition

10^5 cells/ml H99 cells were inoculated in RPMI 1640 media at 37^0C with 150 rpm shaking and OD was measured every 3h at 600 nm.

Antifungal Assays

All inoculations: streaking, spreading and broth culture addition are performed inside a Biosafety Level 2 cabinet

MIC_{50} or Minimum Inhibitory Concentration required to inhibit 50% of the growth of organisms is measured as follows:

H99 cells were inoculated at a concentration of 10^5 cells/ml in RPMI 1640 media at 37^0 C with 150 rpm shaking and cultured without any drug (1%DMSO as control) or in the presence of increasing concentrations of SRT - 6-8μg/ml, FLC - 0.5-1μg/ml and in the presence of varying concentrations of the combination of SRT and FLC . After 12h aliquots of cell suspensions were transferred and plated onto drug-free agar medium to determine Colony Forming Units after 2 more days of incubation and checked for 50% inhibition in drug treated plates compared to controls. The results are obtained from triplicate set of experiments for each treatment.

Total RNA extraction

H99 cells at a concentration of 10^5 cells/ml in RPMI 1640 media at 37^0 C with 150 rpm shaking were treated for 4h with 7 μg/ml SRT, 0.7 μg/ml FLC, or 4 μg/ml SRT and 0.25 μg/ml FLC in combination, and DMSO as vehicle control. (1%DMSO). Cells were harvested and flash frozen in liquid N_2. Frozen Cell pellets in 2 ml screw cap tubes (~50-100mg) were lyophilized overnight, usually six tubes. Holes were punched on fresh sterile caps with needles aseptically and replaced on the tubes with cells before lyophilization. Centrifuge is set at 4^0C and let to cool down. In BSL2 hood, about 100mg of sterile/baked 0.5mm diameter zirconium beads were added to Lyophilized cells and caps without holes were screwed on the tubes. Cells were powdered for 30 seconds in the bead beater, taking 3 tubes per beating cycle. The PureLink RNA Mini Kit (Catalog numbers: 12183025 from Ambion) lysis buffer containing 1% βME (2-mercaptoethanol) is freshly prepared and carefully 1.2ml is added to each of the tubes with pulverized cells inside BL2 hood. Cells are broken in the bead beater for 1 min taking 3 tubes / cycle. Each 2ml tube is placed over a sterile 5ml culture tube. Aseptically holes are made at the bottom of the tube and carefully placed upright on the culture tube. Also holes are made on the caps of the tubes to avoid pressure build up during the next spin. The tubes with the above set up are placed in 50ml conical tube holders inside the swing bucket centrifuge and spun at 4000rpm for 5 mins at 4^0C. The supernatant is collected in a sterile 15ml tube and re-centrifuged to get clarified supernatant. 1.2ml of 70% ethanol is added to each set of supernatants and vortex to mix thoroughly. They are then transferred to the spin column from the kit 700ul at a time and further steps were followed as per the kit protocol. Yield was measured spectrophotometrically at 260/280nm

RNA-seq

H99 cells at a concentration of 10^5 cells/ml in RPMI 1640 media at 37^0 C with 150 rpm shaking were treated for 4h with 7 μg/ml SRT, 0.7 μg/ml FLC, or 4 μg/ml SRT and 0.25 μg/ml FLC in combination, and DMSO as vehicle control. (1%DMSO). Triplicate sets were grown for each treatment. RNA extraction was performed as stated earlier. Corall total RNA-seq library prep kit from Lexogen (Catalog Numbers: 095) was used as per manufacturer instructions.

Ribosome Profiling

H99 cells at a concentration of 10^5 cells/ml in RPMI 1640 media at 37^0 C with 150 rpm shaking were treated for 1h, 2h and 4h with 7 μg/ml SRT, 0.7 μg/ml FLC, or 4 μg/ml SRT and 0.25 μg/ml FLC in combination, and DMSO as vehicle control. (1%DMSO). Triplicate sets were grown for each treatment time point. Ribosomal profiling workflow for *C. neoformans* cultures was modified from published methods from Ingolia lab [116].

Briefly, harvesting was adapted for *C. neoformans*. Cells were centrifugation at 8000 rpm at4^0C. Cell pellets were suspended in lysis buffer (2 :1 ; 500µl for 1g pellet). The lysis buffer cell mixture was added dropwise into LN_2 using a sterile Pasteur pipette to form small frozen cell beads. Precooled SPEX Sample Prep 6850 Freezer Mill was used to grind frozen beads in the respective cryogenic grinding vials with metal stoppers. Pulverized and broken cells were collect quickly in polycarbonate tubes and thawed on ice (~30 mins for 4-6 samples in an ice slurry). Then they were centrifuged at 4ºC for 15 min at 16,000 rpm. The supernatant is carefully collected with a sterile Pasteur pipette. The cell lysates were then processed as per ribosome profiling protocol mentioned above.

Bioinformatics Pipeline

Texas A&M Institute for Genome Sciences and Society facility provided Illumina Next Generation Sequencing to generate the reads from the RNA-seq and ribo-seq libraries.

Trimming and Cutting adapter: After demultiplexing the RNAseq or Riboseq reads, the sequencing adapters using CutAdapt to make them fit for mapping purposes to the respective H99 genome.

Read Quality Check: The read quality is assessed using the FastQC software which analyses: correct base calling using statistical parameters such as Phred scores, flags overrepresented sequences, checks Sequence length distribution, checks sequence duplications and checks GC content.

Mapping reads to the transcriptome STAR Aligner: STAR (Spliced Transcripts Alignment to a Reference), a mapping software specifically developed to handle transcript mapping is used to align the sequence reads to H99 genome. Soft clipping was used to remove random nucleotides such as 5Ns in the linker for ribo-seq and only two mismatches are allowed for mapping.

Differentially expressed genes DEseq2: Differential gene expression analysis is carried out by using DEseq2 software which generates read count tables, computes the normalization factor which is applied to all reads and fold changes are calculated.

Functional Analysis using FungiDB tools: Gene domains and functional searches and Gene ontology enrichments were performed using FungiDB tools [117].

CHAPTER III

RESULTS

We aimed to determine the effects of drugs SRT, FLC and their combination on gene expression of *C. neoformans* by performing RNA-seq and ribo-seq. To accomplish this we first determined the generation time for *C. neoformans* in RPMI 1640 media. Growth experiments were performed using *C. neoformans* H99 wildtype strain in RPMI 1640 media at 37^0C with shaking at 150 rpm. The generation time was measured to be 200 mins (Fig. 3.1). Antifungal assays established conditions for SRT and FLC in cells grown in RPMI 1640 media that would reduce colony-forming units by 50% (MIC_{50}) after 12 h incubation using these conditions. These concentrations were 7 μg/ml SRT and 0.7 μg/ml FLC added separately, and 4 μg/ml SRT and 0.25 μg/ml FLC when added together. Adding 4 μg/ml SRT or 0.25 μg/ml FLC alone did not reduce viable cell numbers under these growth conditions (Fig.3.2 and Fig.3.3). H99 cells were grown under the above conditions and DMSO as vehicle control for 4h (approximately 4h was considered as one generation time) in case of RNA-seq. 1h, 2h and 4h cultures from independently grown H99 cells under similar conditions as above were used in case of ribo-seq . We harvested the cultures and prepared sequencing libraries. The resulting reads were processed through a bioinformatics pipeline of read quality assessment, mapping to the H99 genome with STAR aligner and run through Deseq2 to obtain differentially expressed gene abundance with their statistical significance parameters, in drug treated samples compared to DMSO.

Growth Curve

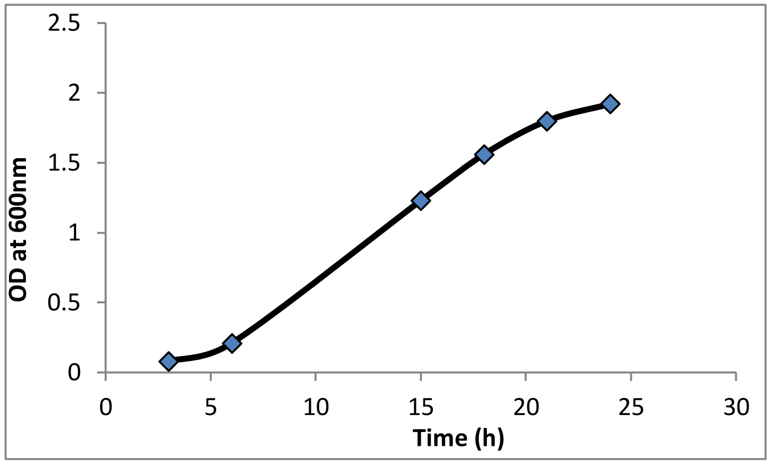

Figure III-1 Fig. 3.1. Growth Curve. H99α growth curve in RPMI 1640 at 37^{0}C with 150 rpm shaking.

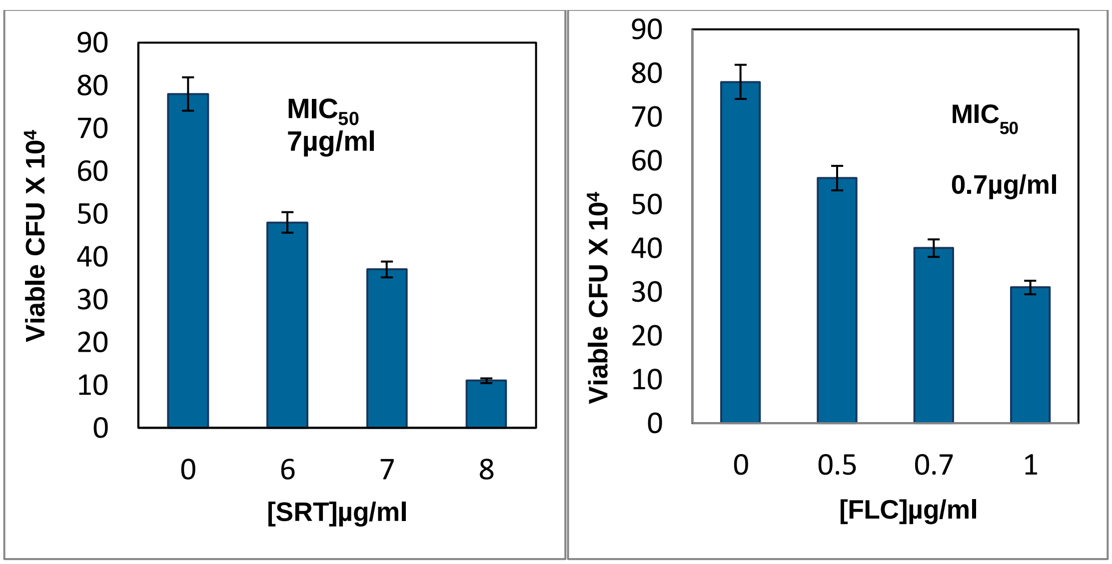

Figure III-2 Fig.3.2. Fungicidal effect of SRT and FLC. MIC$_{50}$ calculated to be 7 µg/ml SRT and 0.7 µg/ml FLC after 12 h incubation at 150 rpm agitation and at 37°C.

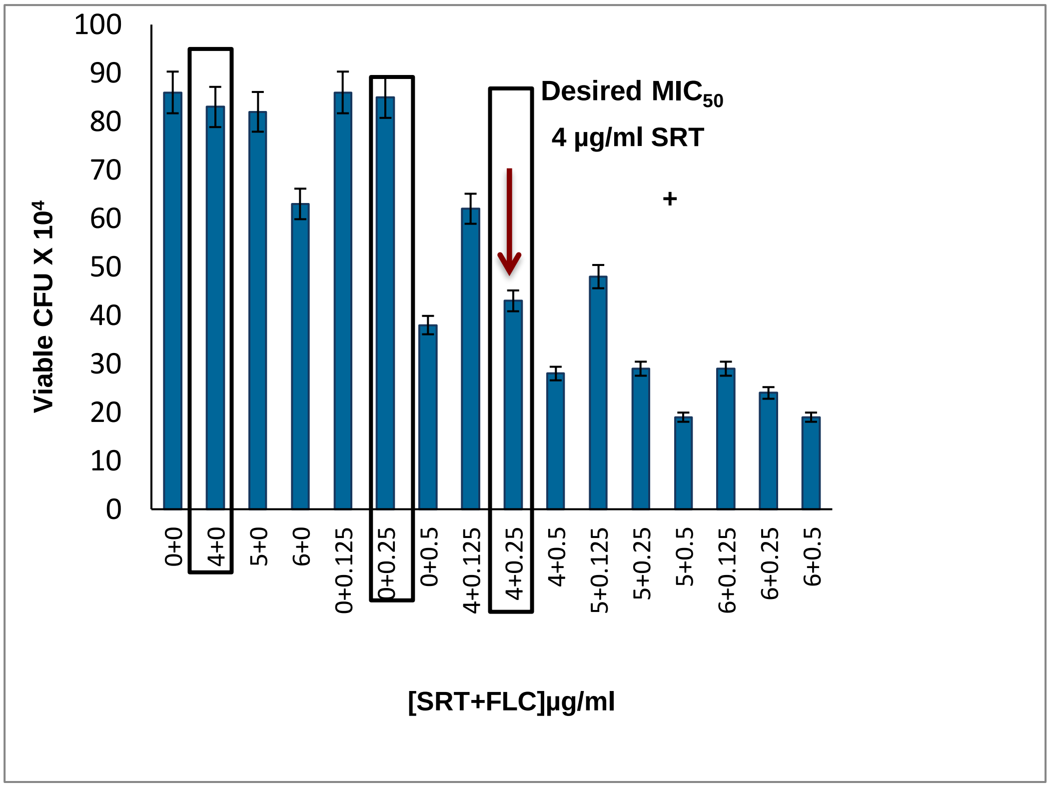

Figure III-3 Fungicidal effect of drug combinations. MIC_{50} calculated to be 4 µg/ml SRT and 0.25 µg/ml FLC when added together after 12 h incubation at 150 rpm agitation and at 37°C.

RNA-seq

C. neoformans H99 was treated for 4h which was used as approximately one generation time in RPMI 1640 media with 7 μg/ml SRT, 0.7 μg/ml FLC, or 4 μg/ml SRT and 0.25 μg/ml FLC in combination, and DMSO as vehicle control. Genome-wide transcriptomics on *C. neoformans* cells using different drug concentrations revealed that drug treatments resulted in substantial changes in the gene expression profiles of this pathogenic yeast.

To present an overall picture of the altered genetic landscape, Venn-diagrams are constructed to combine all the three treatments (SRT, FLC and SRT+FLC) compared to the vehicle control using fold change ≥ 2 with a significance cut off of adjusted p-value or padj ≤0.05 (Supplementary Tables 1 and 2). Fig. 3.4 and Fig. 3.5 shows the Venn diagrams for up-regulated and down-regulated gene sets respectively.

Notably gene CNAG_01953, a potential MFS transporter is shared by both upregulated SRT and SRT+FLC (SF) groups but not in FLC treatment. These are detailed in SRT RNA seq section later. Many ergosterol biosynthesis pathway genes including *ERG11, ERG10*, *ERG2*, *ERG130*, *ERG4*, *ERG5* and *ERG25*, are shared by upregulated sets of FLC and SF treatments but not in SRT, indicating a FLC specific response. The transcripts upregulated by all treatments induce common targets such as *ERG3* and *SRE1* genes in common. These are discussed in detail below in the FLC RNA-seq section. Most of the genes in the Venn diagram for down-regulated genes encode unspecified products or are annotated as hypothetical protein coding genes.

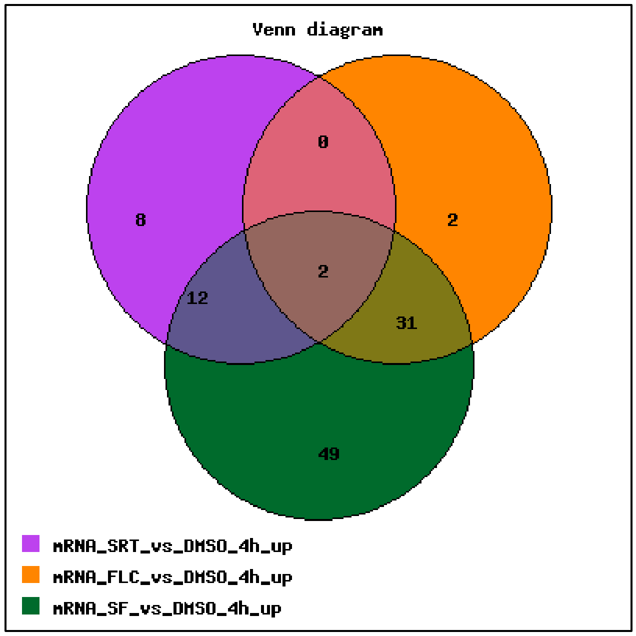

Figure III-4 Venn-diagram showing transcripts up-regulated by different treatments based on RNA-seq.

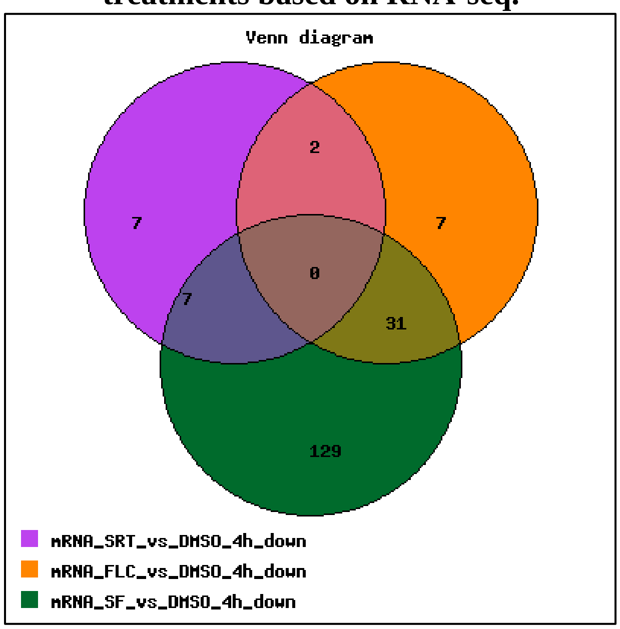

Figure III-5 Venn-diagram showing transcripts down-regulated by different treatments based on RNA-seq.

GENES UP-REGULATED BY FLC IN RNA-seq

1085 genes identified by RNA-seq are significantly up-regulated in *C. neoformans* after 4h incubation with 0.7 μg/ml FLC compared to DMSO treated cells at a significance cutoff of padj (adjusted p-value) ≤ 0.05 padj (Supplementary Table 3). Out of these 1085 genes, 155 genes exhibit a fold change of 1.5 or greater. The top 25 differentially up-regulated genes from this list is shown in Table 3.1. The ergosterol biosynthesis pathway genes makes the majority of the list and is consistent with Erg11 being a well-established drug target for FLC in previous scientific literature including genome-wide transcriptomic studies [4, 19, 20, 118, 119]. The transcript encoding Sre1 (sterol regulatory-element binding protein 1), a master regulator of the biosynthesis of ergosterol, is also induced by FLC.

Ergosterol biosynthesis genes

Ergosterol is an important membrane component of fungi involved in the maintenance of cell integrity, fluidity and permeability [19, 118, 120-125]. Azole antifungals such as FLC is known to abrogate ergosterol biosynthesis by preventing the enzyme Erg11 (lanosterol 14α-demethylase), a member of the hemoprotein cytochrome P450 protein family, by direct interaction with the iron in the heme group of the enzyme [124, 125]. This results in depletion of the pool of ergosterol and accumulation of sterol precursors that can be methylated and can induce structural destabilization of the membrane and subsequently inhibit cell proliferation [118, 120, 122]. In presence of azoles, cells utilize the alternate pathway leading to accumulation of the fungistatic compound 14 α methylERGosta 8-24 (28) dienol as shown in Fig. 3.6 [119, 125].

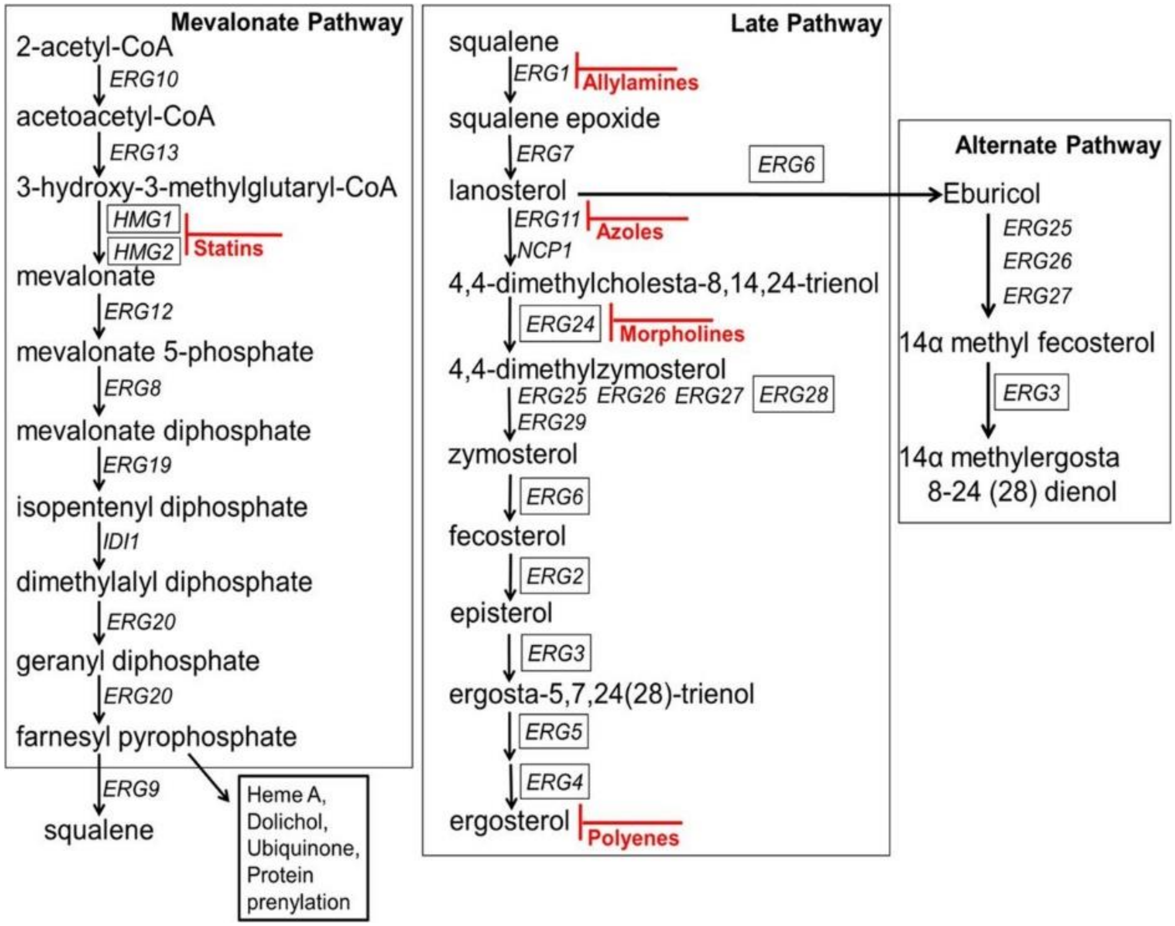

Figure III-6 Ergosterol biosynthetic pathway. Essential genes are boxed and antifungals are denoted with red text font [reproduced with permission from [119].

Ergosterol biosynthesis is an essential and complex pathway and expression of the genes are strictly controlled by transcription factors that can bind to sterol responsive element or SREs in the respective promoter region, eliciting transactivation. In fungi Sre1 and Upc2 function as two such sterol regulators. Homologs of *SRE1* are found from human to fungi indicating its pivotal role in maintaining ergosterol homeostasis, oxygen sensing and adapting to hypoxic conditions [125-140]. The up-regulation of *ERG* biosynthetic genes and *SRE1* after FLC treatment is therefore crucial to the cellular response to FLC.

Cells potentially resist drug inhibition by ramping up the production of Erg11 protein. The *C. neoformans* genes involved in the Ergosterol biosynthesis pathway that are upregulated after FLC treatment are listed in Table 3.2.

Gene Ontology

Functional characterization of the total 1085 up-regulated transcripts using Gene Ontology (GO) enrichment shows impact encompassing various cellular pathways [117]. Binding to ions, proteins and DNA are the major processes identified in the Molecular Function branch and cell membranes and membranes of organelles are highly represented categories in the Cellular Component and Biological Process branches of the GO enrichment shows the induction of general cell regulation to stimuli (Supplementary Table 4). The top 10 GO categories based solely on the most represented genes with p-value <0.01 for each of the branches of enrichment are shown in three different pie charts in Fig 3.7.

Gene ID	**Product (Janbon annotation)**	**Gene Name or Symbol**	**FLC 4h Log_2 (Fold Change)**	**FLC padj**
CNAG_01737	methylsterol monooxygenase	ERG25	2.43	0.00
CNAG_04804	hypothetical protein	SRE1	2.27	0.00
CNAG_04675	hypothetical protein	N/A	1.96	0.00
CNAG_00519	lathosterol oxidase	ERG3	1.84	0.00
CNAG_01862	hexose transporter	N/A	1.80	0.00
CNAG_00854	C-8 sterol isomerase	ERG2	1.75	0.00
CNAG_02896	hydroxymethylglutaryl-CoA synthase	ERG130	1.66	0.00

Table 3.1. continued

Gene ID	Product (Janbon annotation)	Gene Name or Symbol	FLC 4h Log2 (Fold Change)	FLC padj
CNAG_02918	acetyl-CoA C-acetyltransferase	ERG10	1.64	0.00
CNAG_12865	ncRNA	N/A	1.54	0.03
CNAG_06644	C-22 sterol desaturase	ERG5	1.49	0.00
CNAG_03746	hypothetical protein	N/A	1.48	0.00
CNAG_05305	hypothetical protein	N/A	1.44	0.01
CNAG_02830	delta24(24(1))-sterol reductase	ERG4	1.44	0.00
CNAG_07316	hydroxyacid-oxoacid transhydrogenase	N/A	1.41	0.00
CNAG_01653	cytokine inducing-glycoprotein	CIG1	1.41	0.02
CNAG_07912	hypothetical protein	N/A	1.38	0.00
CNAG_12901	ncRNA	N/A	1.35	0.00
CNAG_05607	cytoplasmic protein	N/A	1.33	0.00
CNAG_04869	carboxylesterase	PNB1	1.32	0.00
CNAG_00040	cytochrome P450, family 51 (sterol 14-demethylase)	ERG11	1.30	0.00
CNAG_07845	hypothetical protein, variant 1	N/A	1.29	0.00
CNAG_06323	L-fucose permease	N/A	1.27	0.00
CNAG_01803	hypothetical protein	N/A	1.27	0.00
CNAG_07540	hypothetical protein	N/A	1.23	0.00
CNAG_07784	hypothetical protein	N/A	1.21	0.00

Table 3.1. Transcripts up-regulated by FLC in *C. neoformans* based on RNa-seq.

Top differentially up-regulated *C. neoformans* genes after 4 h incubation with 0.7 μg/ml FLC identified by RNA-seq. Significance cutoff: padj (adjusted p-value) ≤ 0.05.

Gene ID	Product (Janbon annotation)	Gene Name or Symbol	FLC 4h Log_2 (Fold Change)	FLC padj	SRT 4h Log_2 (Fold Change)	SRT padj	SRT+FLC 4h Log_2 (Fold Change)	SRT+FLC padj
CNAG_02918	Acetyl-CoA C-acetyltransferase	ERG10	1.64	0.00	0.74	0.00	1.41	0.00
CNAG_03311	3-hydroxy-3-methylglutaryl-CoA (HMG-CoA) synthase	ERG13	0.73	0.00	0.20	0.09	0.51	0.00
CNAG_02896	3-hydroxy-3-methylglutaryl-CoA (HMG-CoA) synthase	ERG130	1.66	0.00	0.54	0.00	1.31	0.00
CNAG_06534	hydroxymethylglutaryl-CoA reductase (NADPH)	HMG1	0.80	0.00	0.51	0.00	0.79	0.00
CNAG_06535	hydroxymethylglutaryl-CoA reductase (NADPH)	HMG2	-0.52	0.00	-0.14	0.44	-0.60	0.00
CNAG_06001	phosphomevalonate kinase	ERG8	0.47	0.00	0.10	0.49	0.46	0.00
CNAG_05125	Diphosphomevalonate decarboxylase	ERG19/ MVD1	0.53	0.00	0.27	0.03	0.59	0.00
CNAG_00265	isopentenyl-diphosphate delta-isomerase	IDI1	-0.41	0.01	-0.18	0.28	-0.38	0.00
CNAG_02084	farnesyl diphosphate synthase	ERG20	0.67	0.00	0.60	0.00	0.81	0.00
CNAG_07510	farnesyl-diphosphate farnesyltransferase	ERG9	0.30	0.00	0.14	0.16	0.25	0.00

Table 3.2. continued

Gene ID	Product (Janbon annotation)	Gene Name or Symbol	FLC 4h Log2 (Fold Change)	FLC padj	SRT 4h Log2 (Fold Change)	SRT padj	SRT+FLC 4h Log2 (Fold Change)	SRT+FLC padj
CNAG_06829	Squalene monooxygenase	ERG1	0.92	0.00	0.44	0.00	0.90	0.00
CNAG_01129	lanosterol synthase	ERG7	0.97	0.00	0.30	0.01	0.89	0.00
CNAG_00040	cytochrome P450, family 51 (sterol 14-demethylase)	ERG11	1.30	0.00	0.59	0.00	1.09	0.00
CNAG_00117	c-14 sterol reductase	ERG24	0.85	0.00	0.19	0.03	0.60	0.00
CNAG_01737	C-4 methyl sterol oxidase, putative	ERG25	2.43	0.00	0.89	0.00	2.16	0.00
CNAG_04605	C-3 sterol dehydrogenase	ERG26	0.31	0.03	0.01	0.97	0.29	0.03
CNAG_07437	3-keto sterol reductase	ERG27	-0.24	0.23	-0.12	0.59	-0.09	0.63
CNAG_03009	putative ER membrane protein	ERG28	-0.13	0.34	-0.05	0.74	-0.24	0.03
CNAG_03819	sterol 24-C-methyltransferase	ERG6	1.20	0.00	0.42	0.00	0.99	0.00
CNAG_00854	C-8 sterol isomerase	ERG2	1.75	0.00	0.54	0.00	1.45	0.00
CNAG_00519	lathosterol oxidase	ERG3	1.84	0.00	1.10	0.00	1.96	0.00
CNAG_06644	C-22 sterol desaturase	ERG5	1.49	0.00	0.81	0.00	1.43	0.00
CNAG_02830	delta24(24(1))-sterol reductase	ERG4	1.44	0.00	0.74	0.00	1.32	0.00
CNAG_04804	hypothetical protein	SRE1	2.27	0.00	1.01	0.00	2.30	0.00

Table 3.2. continued

Gene ID	Product (Janbon annotation)	Gene Name or Symbol	FLC 4h Log2 (Fold Change)	FLC padj	SRT 4h Log2 (Fold Change)	SRT padj	SRT+FLC 4h Log2 (Fold Change)	SRT+ FLC padj
CNAG_01003	NADPH-ferrihemoprotein reductase	NCP1	0.69	0.00	0.23	0.06	0.61	0.00

Table 3.2. FLC up-regulates transcript levels of Ergosterol biosynthesis genes in *C. neoformans* based on RNA-seq. *C. neoformans* genes involved in the Ergosterol biosynthesis pathway and its regulation, after 4 h incubation with 0.7 μg/ml FLC identified by RNA-seq. Genes are ordered according to their sequence of action in the biosynthetic pathway. Corresponding gene expression changes after 4 h incubation with 7 μg/ml SRT and the combination of 4 μg/ml SRT+0.25 μg/ml FLC, provided for comparison. Significance cutoff: padj (adjusted p-value) ≤ 0.05; non-significant padj values are highlighted red.

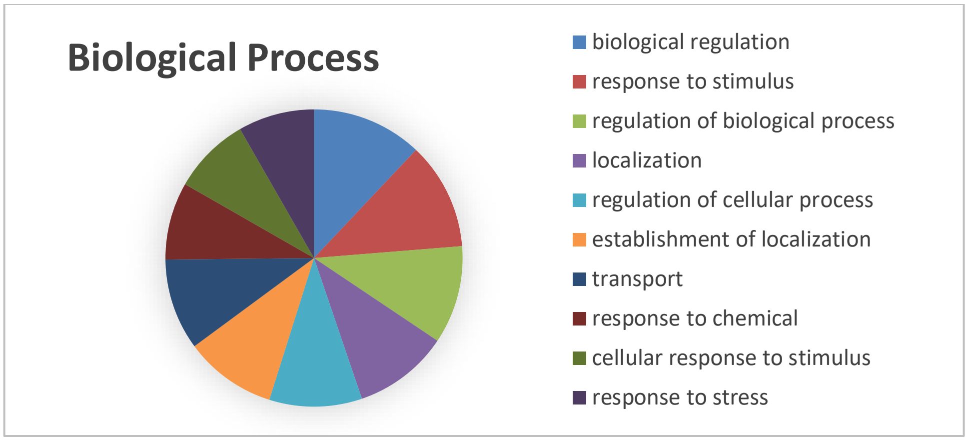
Biological Process
biological regulation
response to stimulus
regulation of biological process
localization
regulation of cellular process
establishment of localization
transport
response to chemical
cellular response to stimulus
response to stress

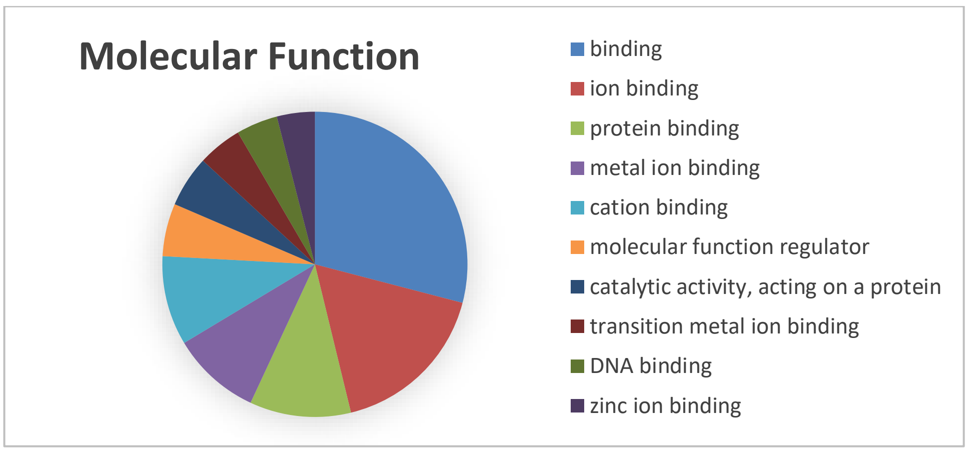
Molecular Function
binding
ion binding
protein binding
metal ion binding
cation binding
molecular function regulator
catalytic activity, acting on a protein
transition metal ion binding
DNA binding
zinc ion binding

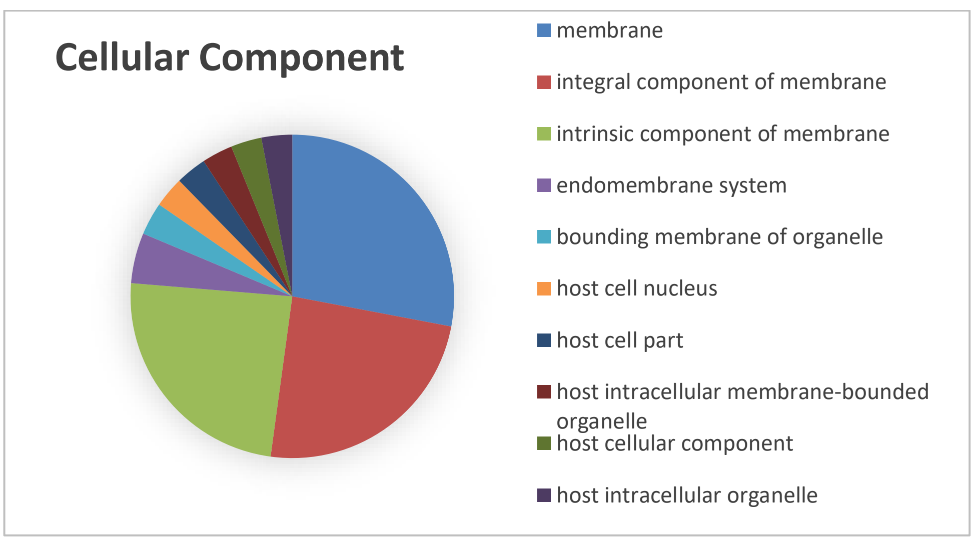
Cellular Component
membrane
integral component of membrane
intrinsic component of membrane
endomembrane system
bounding membrane of organelle
host cell nucleus
host cell part
host intracellular membrane-bounded organelle
host cellular component
host intracellular organelle

Figure III-7 Functional enrichment of up-regulated transcripts by FLC in *C. neoformans* based on RNA-seq. Three Gene Ontology (GO) enrichments namely Biological Process, Molecular Function and Cellular Component are generated for the *C. neoformans* genes up-regulated after FLC treatment, using resources from FungiDB. The top 10 GO categories based solely on the most represented genes with p-value <0.01 for each of the branches of enrichment are shown in three different pie charts.

GENES DOWN-REGULATED BY FLC IN RNAseq

1048 genes identified by RNA-seq are significantly down-regulated in *C. neoformans* after 4h incubation with 0.7 μg/ml FLC compared to DMSO treated cells at a significance cutoff of padj (adjusted p-value) ≤ 0.05 (Supplementary Table 5). Out of these 1048 genes, 243 have a repression of 1.5 fold or greater and 42 genes are more than 2 fold repressed. Table 3.3 shows the top 25 repressed genes showing a repression of 2 fold or greater. In-depth inspection of these genes, revealed the following observations:

Ribosomal genes

112 genes encoding ribosomal proteins or subunits of ribonucleoprotein complexes were down-regulated. 41 of these genes were specifically downregulated by FLC. Genes are considered FLC specific if they are significantly differentially expressed after FLC as well as SRT+FLC treatment but are not significantly altered by SRT treatment. Down-regulation of ribosomal genes by FLC has not been reported in *C. neoformans* before. In a proteomics study on *C. gatti* using FLC at concentrations 20 times greater than what we have used, reported a decrease in most ribosomal proteins. Table 3.4 shows the top

20 ribosomal and ribonucleoprotein genes down-regulated by FLC. However most of the significantly down-regulated genes in this list exhibit a less than 1.5 fold repression.

Translation machinery

Sixteen genes encoding products associated with the term translation including initiation factors were identified (Table 3.5). Again this observation in addition to the ribosomal genes, provides evidence to support translational inhibition as one of the antifungal mechanisms of FLC. However, most of the genes in this list exhibit a less than 1.5 fold repression.

Gene Ontology

In the GO enrichment analysis (Supplementary Table 6), both the Biological processes and Cellular component branches shows a multi-pathway impact of FLC whereas the Molecular function branch showed involvement with ribosomes and RNA binding. The top 10 GO categories based solely on the most represented genes with p-value <0.01 for each of the branches of enrichment are shown in three different pie charts in Fig 3.8.

Gene ID	Product (Janbon annotation)	Gene Name or Symbol	FLC 4h Log_2 (Fold Change)	FLC padj
CNAG_12380	ncRNA	N/A	-3.42	0.03
CNAG_00315	HHE domain-containing protein	N/A	-2.16	0.00
CNAG_12847	ncRNA	N/A	-1.91	0.02
CNAG_03226	succinate dehydrogenase [ubiquinone] iron-sulfur subunit, mitochondrial	N/A	-1.74	0.00
CNAG_12264	ncRNA	N/A	-1.74	0.01
CNAG_03666	acyl-CoA dehydrogenase	N/A	-1.72	0.01
CNAG_12050	ncRNA	N/A	-1.66	0.00
CNAG_12430	ncRNA	N/A	-1.44	0.02
CNAG_12211	ncRNA	N/A	-1.42	0.05
CNAG_12347	ncRNA	N/A	-1.42	0.00
CNAG_07911	streptomycin biosynthesis protein StrI	N/A	-1.42	0.00
CNAG_06723	succinate dehydrogenase (ubiquinone) membrane anchor subunit	N/A	-1.28	0.00
CNAG_06623	inositol oxygenase	N/A	-1.25	0.00
CNAG_12967	ncRNA	N/A	-1.23	0.00
CNAG_00462	electron-transferring-flavoprotein dehydrogenase	N/A	-1.23	0.01
CNAG_05041	NADH-ubiquinone oxidoreductase subunit 8	N/A	-1.22	0.00
CNAG_04905	tRNA (uracil-5-)-methyltransferase	N/A	-1.22	0.00
CNAG_12073	ncRNA	N/A	-1.21	0.00
CNAG_01138	cytochrome c peroxidase, mitochondrial	CCP1	-1.20	0.01
CNAG_01846	flavoprotein	N/A	-1.20	0.00
CNAG_00716	cytochrome c	N/A	-1.18	0.00

Table 3.3. continued

Gene ID	Product (Janbon annotation)	Gene Name or Symbol	FLC 4h Log2 (Fold Change)	FLC padj
CNAG_12845	ncRNA	N/A	-1.14	0.00
CNAG_01500	taurine dioxygenase	N/A	-1.13	0.01
CNAG_06050	UDP-glucose 4-epimerase, variant	UGE2	-1.13	0.00

Table 3.3. Transcripts down-regulated by FLC in *C. neoformans* based on RNA-seq. Differentially down-regulated *C. neoformans* genes after 4 h incubation with 0.7 μg/ml FLC identified by RNA-seq. Only top 25 repressed genes showing a fold of repression of 2 times or higher are represented. Significance cutoff: padj (adjusted p-value) ≤ 0.05.

Gene ID	Product (Janbon annotation)	FLC 4h Log_2 (Fold Change)	FLC padj	SRT 4h Log_2 (Fold Change)	SRT padj	SRT+FLC 4h Log_2 (Fold Change)	SRT+FLC padj
CNAG_04072	60S ribosome subunit biogenesis protein nip7	-0.95	0.00	-0.73	0.00	-1.30	0.00
CNAG_07864	U3 small nucleolar ribonucleoprotein IMP3	-0.73	0.00	-0.52	0.00	-1.24	0.00
CNAG_00819	small subunit ribosomal protein S30	-0.62	0.04	-0.58	0.07	-1.09	0.00
CNAG_06127	ribosome biogenesis protein NSA2	-0.62	0.00	-0.46	0.00	-0.95	0.00
CNAG_02382	ribosome biogenesis protein BRX1	-0.58	0.00	-0.30	0.02	-0.80	0.00
CNAG_05762	large subunit acidic ribosomal protein P2	-0.57	0.01	-0.56	0.01	-0.88	0.00
CNAG_06318	ribosome biogenesis protein YTM1	-0.57	0.00	-0.28	0.13	-0.66	0.00
CNAG_02378	H/ACA ribonucleoprotein complex subunit 2	-0.56	0.00	-0.42	0.00	-0.80	0.00
CNAG_01432	ribosome assembly protein 4	-0.55	0.00	-0.28	0.06	-0.70	0.00
CNAG_02454	H/ACA ribonucleoprotein complex non-core subunit NAF1	-0.53	0.00	-0.33	0.02	-0.78	0.00
CNAG_06535	ribosome biogenesis protein UTP30	-0.52	0.00	-0.14	0.44	-0.60	0.00
CNAG_01198	small nuclear ribonucleoprotein F	-0.52	0.00	-0.61	0.00	-0.93	0.00

Table 3.4. continued

Gene ID	Product (Janbon annotation)	FLC 4h Log2 (Fold Change)	FLC padj	SRT 4h Log2 (Fold Change)	SRT padj	SRT+FLC 4h Log2 (Fold Change)	SRT+FLC padj
CNAG_01455	large subunit ribosomal protein L39	-0.52	0.01	-0.54	0.00	-1.00	0.00
CNAG_01437	ribosomal RNA assembly protein	-0.51	0.00	-0.33	0.01	-0.64	0.00
CNAG_01187	ribosome production factor 2	-0.51	0.00	-0.28	0.06	-0.69	0.00
CNAG_01049	H/ACA ribonucleoprotein complex subunit 3	-0.50	0.00	-0.40	0.01	-0.88	0.00
CNAG_06847	small subunit ribosomal protein S28	-0.50	0.01	-0.26	0.23	-0.75	0.00
CNAG_04830	large subunit ribosomal protein L33	-0.50	0.01	-0.23	0.32	-0.70	0.00
CNAG_00771	large subunit ribosomal protein L29	-0.49	0.00	-0.47	0.01	-0.85	0.00

Table 3.4. FLC down-regulates transcript levels of ribosomal genes in *C. neoformans* based on RNA-seq. Differentially down-regulated *C. neoformans* ribosomal genes after 4 h incubation with 0.7 μg/ml FLC identified by RNA-seq. Corresponding gene expression changes after 4 h incubation with 7 μg/ml SRT and the combination of 4 μg/ml SRT+0.25 μg/ml FLC, provided for comparison. Significance cutoff: padj (adjusted p-value) ≤ 0.05; non-significant padj values are highlighted red.

Gene ID	Product (Janbon annotation)	FLC 4h Log_2 (Fold Change)	FLC padj	SRT 4h Log_2 (Fold Change)	SRT padj	SRT+FLC 4h Log_2 (Fold Change)	SRT+FLC padj
CNAG_06865	translation machinery-associated protein 16	-0.68	0.00	-0.47	0.01	-0.86	0.00
CNAG_05455	translation initiation factor eIF-1A	-0.58	0.00	-0.52	0.00	-0.91	0.00
CNAG_03263	translation elongation factor Tu	-0.39	0.00	-0.19	0.16	-0.45	0.00
CNAG_02656	translation machinery-associated protein 20	-0.36	0.01	-0.33	0.02	-0.57	0.00
CNAG_04628	translation initiation factor 6	-0.33	0.01	-0.26	0.04	-0.56	0.00
CNAG_01111	translation initiation factor 3 subunit K	-0.33	0.01	-0.17	0.20	-0.43	0.00
CNAG_01833	translation initiation factor 4E	-0.32	0.02	-0.07	0.69	-0.38	0.00
CNAG_02128	translation initiation factor 3 subunit J	-0.30	0.00	-0.39	0.00	-0.58	0.00
CNAG_01428	translation initiation factor 5A	-0.29	0.03	-0.23	0.10	-0.51	0.00
CNAG_07778	translation initiation factor 2 subunit 1	-0.29	0.00	-0.14	0.11	-0.38	0.00
CNAG_05366	translation initiation factor 2A	-0.29	0.00	-0.10	0.33	-0.22	0.01

Table 3.5. continued

Gene ID	Product (Janbon annotation)	FLC 4h Log2 (Fold Change)	FLC padj	SRT 4h Log2 (Fold Change)	SRT padj	SRT+FLC 4h Log2 (Fold Change)	SRT+FLC padj
CNAG_02657	translation initiation factor 3 subunit G	-0.28	0.02	-0.25	0.04	-0.43	0.00
CNAG_06563	translation initiation factor 3 subunit F	-0.27	0.04	-0.14	0.32	-0.29	0.01
CNAG_04054	translation initiation factor SUI1	-0.26	0.00	-0.24	0.01	-0.43	0.00
CNAG_02482	translation machinery-associated protein 22	-0.26	0.01	-0.17	0.15	-0.40	0.00
CNAG_00602	translation initiation factor 3 subunit I	-0.20	0.03	-0.09	0.39	-0.24	0.00

Table 3.5. FLC down-regulates transcript levels of genes related to the translation machinery in *C. neoformans* based on RNA-seq. Differentially down-regulated *C. neoformans* genes related to the translation machinery including initiation factors, after 4 h incubation with 0.7 μg/ml FLC identified by RNA-seq. Corresponding gene expression changes after 4 h incubation with 7 μg/ml SRT and the combination of 4 μg/ml SRT+0.25 μg/ml FLC, provided for comparison. Significance cutoff: padj (adjusted p-value) ≤ 0.05.

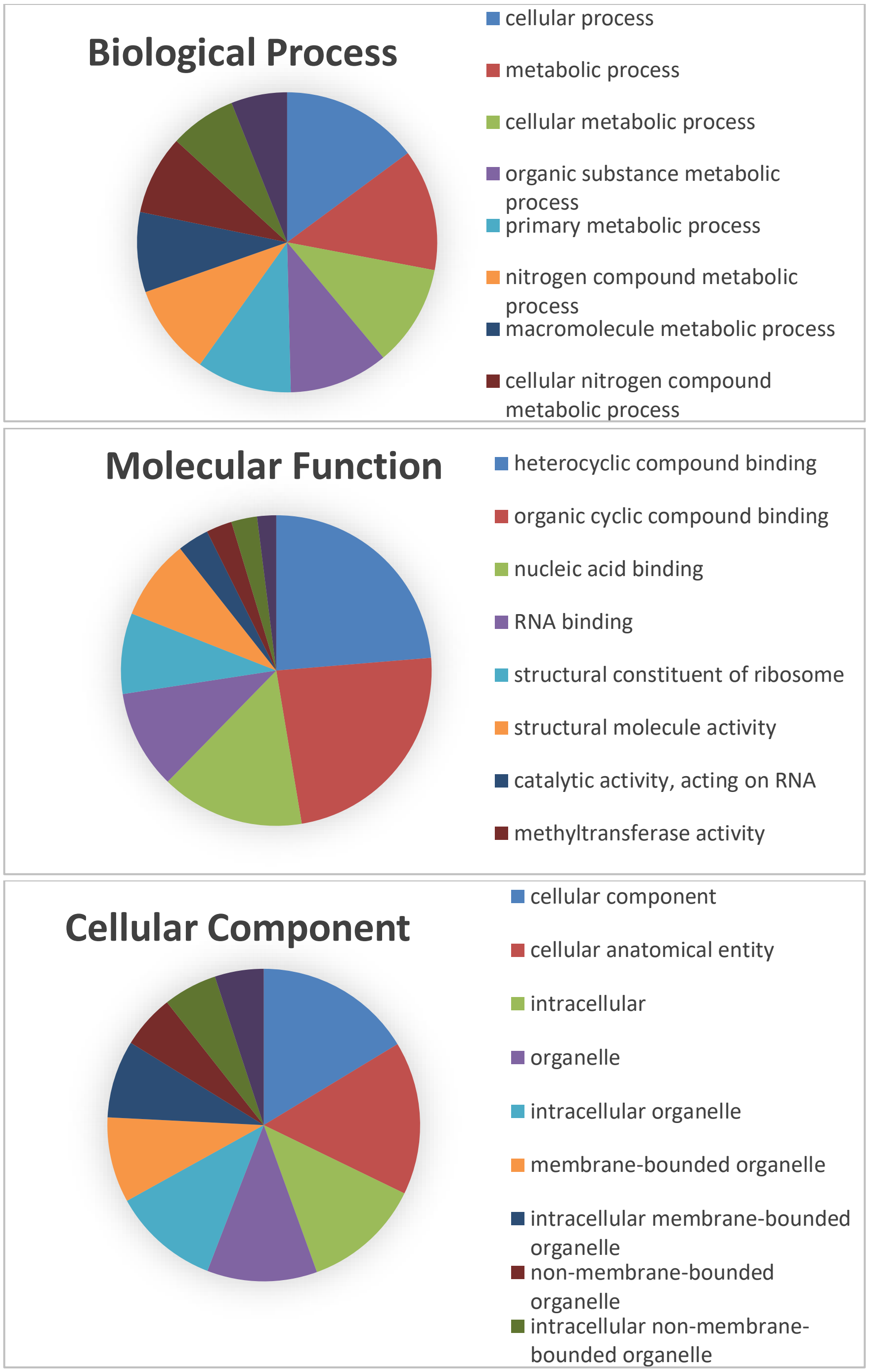

Figure III-8 Functional enrichment of down-regulated transcripts by FLC in *C. neoformans* based on RNAseq. Three Gene Ontology (GO) enrichments namely Biological Process, Molecular Function and Cellular Component are generated for the *C. neoformans* genes down-regulated after FLC treatment, using resources from FungiDB.

The top 10 GO categories based solely on the most represented genes with p-value <0.01 for each of the branches of enrichment are shown in three different pie charts.

GENES UP-REGULATED BY SRT IN RNAseq

871 genes were identified by RNA-seq are significantly up-regulated in *C. neoformans* after 4h incubation with 7 μg/ml SRT compared to vehicle (DMSO) treated cells at a significance cutoff of padj (adjusted p-value) ≤ 0.05 (Supplementary Table 7). Table 3.6 shows the top 25 differentially up-regulated genes from this list. Out of these 871 genes, 307 were SRT specific. However the magnitudes of changes in gene expression are not always high. 89 genes out of the 871 total genes and 43 of the 307 SRT specific genes exhibit a fold change of 1.5 or higher. Noteworthy genes in this list include the putative MFS (Major facilitator Superfamily) transporter (CNAG_01953), *FZC46* (CNAG_03115), a putative transcription factor with fungal Zn(2)-Cys(6) binuclear cluster DNA binding domain shared with *UPC2*, *ERG 3* (CNAG_00519) and *SRE1* (CNAG_04804), the latter two being widely studied in the antifungal interactions and stress responses [124, 125, 134, 135, 138, 141]. In-depth inspection of these 871 genes, revealed the following details:

Membrane related

72 genes are found to be annotated as membrane proteins/transporters or as genes containing MFS domain were up-regulated and 31 genes out of them were SRT specific.

21 genes out of the total and 13 out of the potentially SRT specific genes exhibited a fold change of 1.5 or higher (Table 3.7). *CNAG_01953* gene is the most induced gene in this list of membrane proteins. Although this gene is annotated as a hypothetical protein, it possesses MFS like domain and therefore likely functions as a transporter. It was in fact the most induced gene amongst all genes up-regulated by SRT and was specifically induced by SRT.

Kinase related

50 genes found to be annotated as kinases were up-regulated by SRT and 22 of them were SRT specific. However, most of the genes in this list exhibit a lower than1.5 fold change. The top 20 representative genes from the list is shown in Table 3.8

Thus SRT appears to create a distinct genetic landscape, which is different from that of FLC.

ss

Transcription related

22 genes found to be associated with transcription were up-regulated by SRT and 10 of these were SRT specific (Table 3.9). However, most of these genes exhibit a less than 1.5 fold change.

Ergosterol biosynthesis genes

SRT treatment also significantly upregulates more than half of the genes involved in the ergosterol biosynthesis pathway, thus revealing a common branch of action with FLC

(Table 3.2) in addition to the distinct response generated by SRT from the rest of the differential gene expression data.

Gene Ontology

Functional characterization of the total 871 SRT up-regulated transcripts using Gene Ontology (GO) enrichment shows a more general and widespread impact on various cellular pathways [117]. Categories for transcription factors and intracellular membrane are highly enriched in molecular function and cellular component branches of GO terms respectively. In the search for GO terms in biological processes, transport is the only notable category that is identified (Supplementary Table 8). The top 10 GO categories based solely on the most represented genes with p-value <0.0.1 for each of the branches of enrichment are shown in three different pie charts in Fig 3.9.

Gene ID	Product (Janbon annotation)	Gene Name or Symbol	SRT 4h Log_2 (Fold Change)	SRT padj
CNAG_01953	hypothetical protein	N/A	5.42	0.00
CNAG_13035	ncRNA	N/A	4.28	0.00
CNAG_03764	integral membrane protein	N/A	3.88	0.00
CNAG_03115	hypothetical protein	FZC46	2.16	0.00
CNAG_03733	hypothetical protein	N/A	1.98	0.00
CNAG_03732	integral membrane protein	N/A	1.93	0.00
CNAG_04988	Gly-Xaa carboxypeptidase	N/A	1.81	0.00
CNAG_03199	FAD dependent oxidoreductase	N/A	1.56	0.00
CNAG_04546	multidrug transporter	LPI10	1.30	0.00
CNAG_06890	membrane transporter	N/A	1.26	0.00
CNAG_04819	hypothetical protein	N/A	1.24	0.00
CNAG_00728	dityrosine transporter	N/A	1.23	0.00
CNAG_04818	hypothetical protein	N/A	1.20	0.00
CNAG_02299	hypothetical protein	N/A	1.19	0.00
CNAG_01076	4-aminobutyrate aminotransferase	N/A	1.15	0.00
CNAG_06346	hypothetical protein	BLP1	1.15	0.00
CNAG_12679	ncRNA	N/A	1.13	0.02
CNAG_00519	lathosterol oxidase	ERG3	1.10	0.00
CNAG_06009	cyclohydrolase	N/A	1.09	0.00
CNAG_01231	agmatinase	N/A	1.06	0.00
CNAG_01118	AAT family amino acid transporter	N/A	1.06	0.02
CNAG_04804	hypothetical protein	SRE1	1.01	0.00
CNAG_04675	hypothetical protein	N/A	0.96	0.04
CNAG_00079	hypothetical protein	N/A	0.96	0.00
CNAG_01865	hypothetical protein	N/A	0.95	0.00

Table 3.6. Transcripts up-regulated by SRT in *C. neoformans* based on RNA-seq.

Top differentially up-regulated *C. neoformans* genes after 4 h incubation with 7 μg/ml SRT identified by RNA-seq. Significance cutoff: padj (adjusted p-value) ≤ 0.05.

Gene ID	Product (Janbon annotation)	Pfam domain	SRT 4h Log_2 (Fold Change)	SRT padj	FLC 4h Log_2 (Fold Change)	FLC padj	SRT+FLC 4h Log_2 (Fold Change)	SRT+ FLC padj
CNAG_01953	hypothetical protein	MFS_1,MFS_1_like	5.42	0.00	0.32	0.04	4.44	0.00
CNAG_03764	integral membrane protein	PQ-loop	3.88	0.00	-0.16	0.57	2.05	0.00
CNAG_03732	integral membrane protein	PQ-loop	1.93	0.00	0.27	0.05	1.05	0.00
CNAG_04546	multidrug transporter	MFS_1	1.30	0.00	0.95	0.00	1.78	0.00
CNAG_06890	membrane transporter	MFS_1	1.26	0.00	-0.12	0.67	0.90	0.00
CNAG_00728	dityrosine transporter	MFS_1,Sugar_tr	1.23	0.00	0.19	0.40	1.18	0.00
CNAG_04818	hypothetical protein	MFS_1	1.20	0.00	-0.03	0.92	0.55	0.00
CNAG_02299	hypothetical protein	MFS_1,MFS_1_like,OATP	1.19	0.00	-0.04	0.78	0.62	0.00
CNAG_01118	AAT family amino acid transporter	AA_permease,AA_permease_2	1.06	0.02	0.25	0.63	1.05	0.01
CNAG_02777	phosphate:H symporter	Sugar_tr, MFS_1	0.87	0.01	-0.15	0.71	0.15	0.64
CNAG_04947	high-affinity nicotinic acid transporter	MFS_1	0.78	0.05	0.36	0.43	0.91	0.01

Table 3.7. continued

Gene ID	Product (Janbon annotation)	Pfam domain	SRT 4h Log2 (Fold Change)	SRT padj	FLC 4h Log2 (Fold Change)	FLC padj	SRT+FLC 4h Log2 (Fold Change)	SRT+FLC padj
CNAG_03215	hypothetical protein	MFS_1,Sugar_tr	0.76	0.00	0.13	0.61	0.67	0.00
CNAG_04758	amt family ammonium transporter	Ammonium_transp	0.75	0.00	0.47	0.02	1.09	0.00
CNAG_06323	L-fucose permease	MFS_1	0.70	0.00	1.27	0.00	1.50	0.00
CNAG_02039	integral membrane protein	EamA	0.67	0.02	0.36	0.26	1.27	0.00
CNAG_07449	amino acid transporter	AA_permease,AA_permease_2	0.65	0.01	0.36	0.15	0.98	0.00
CNAG_03838	hypothetical protein	MFS_1,Sugar_tr	0.64	0.00	0.18	0.45	0.77	0.00
CNAG_01208	high-affinity cell membrane calcium channel protein	Ion_trans	0.63	0.00	0.25	0.12	0.44	0.00
CNAG_05377	MFS transporter, SP family, solute carrier family 2 (myo-inositol transporter), member 13	Sugar_tr, MFS_1	0.62	0.04	0.42	0.18	0.90	0.00
CNAG_06776	membrane protein	MFS_1,Sugar_tr,UNC-93	0.61	0.01	0.55	0.02	1.11	0.00

Table 3.7. SRT up-regulates transcript levels of membrane proteins and transporters in *C. neoformans* based on RNA-seq. Differentially up-regulated *C. neoformans* genes having 1.5 fold change or greater, related to membrane proteins/transporters or genes containing MFS (Major facilitator Superfamily) domain after 4 h incubation with 7 μg/ml SRT identified by RNA-seq. Corresponding gene expression changes after 4 h incubation with 0.7 μg/ml FLC and the combination of 4 μg/ml SRT+0.25 μg/ml FLC are provided for comparison. Significance cutoff: padj (adjusted p-value) ≤ 0.05; non-significant padj values are highlighted red.

Gene ID	Product (Janbon annotation)	SRT 4h Log_2 (Fold Change)	SRT padj	FLC 4h Log_2 (Fold Change)	FLC padj	SRT+FLC 4h Log_2 (Fold Change)	SRT+FLC padj
CNAG_06568	RAN protein kinase	0.85	0.00	0.94	0.00	1.57	0.00
CNAG_01061	serine/threonine protein kinase	0.72	0.00	0.68	0.00	1.22	0.00
CNAG_03369	Wee protein kinase	0.51	0.00	0.19	0.25	0.43	0.00
CNAG_05558	CAMK/CAMKL/Kin4 protein kinase	0.51	0.00	0.22	0.19	0.45	0.00
CNAG_01209	1-phosphatidylinositol-3-phosphate 5-kinase	0.46	0.00	0.35	0.03	0.56	0.00
CNAG_05771	serine/threonine-protein kinase TEL1, variant	0.45	0.02	0.44	0.01	0.64	0.00
CNAG_02028	CMGC/SRPK protein kinase	0.45	0.00	0.19	0.22	0.50	0.00
CNAG_06642	Atypical/PIKK/FRAP protein kinase	0.45	0.00	0.42	0.00	0.60	0.00
CNAG_04040	AGC/RSK protein kinase	0.44	0.00	0.36	0.00	0.77	0.00

Table 3.8. continued

Gene ID	Product (Janbon annotation)	SRT 4h Log2 (Fold Change)	SRT padj	FLC 4h Log2 (Fold Change)	FLC padj	SRT+FLC 4h Log2 (Fold Change)	SRT+FLC padj
CNAG_03893	MAP kinase phosphatase	0.44	0.00	0.21	0.18	0.32	0.01
CNAG_03024	AGC protein kinase	0.43	0.01	0.66	0.00	0.84	0.00
CNAG_01905	serine/threonine protein kinase	0.43	0.01	0.48	0.00	0.67	0.00
CNAG_07377	transformation/transcription domain-associated protein	0.43	0.01	0.27	0.10	0.43	0.00
CNAG_05005	ULK/ULK protein kinase	0.42	0.00	0.54	0.00	0.63	0.00
CNAG_00405	STE/STE20/YSK protein kinase	0.41	0.00	0.53	0.00	0.75	0.00
CNAG_04433	CMGC/DYRK/DYRK2 protein kinase	0.41	0.01	0.51	0.00	0.68	0.00
CNAG_02541	cyclin-dependent protein kinase inhibitor	0.39	0.01	0.20	0.17	0.36	0.00
CNAG_04335	phosphatidylinositol 4-kinase	0.38	0.01	0.38	0.01	0.53	0.00
CNAG_05386	glutamate 5-kinase, variant	0.38	0.00	0.29	0.02	0.66	0.00
CNAG_04282	CMGC/MAPK protein kinase	0.37	0.05	0.35	0.06	0.36	0.03

Table 3.8. SRT up-regulates transcript levels of kinase genes in *C. neoformans* based on RNA-seq. Top 20 differentially up-regulated *C. neoformans* kinase genes after 4 h incubation with 7 μg/ml SRT identified by RNA-seq. Corresponding gene

expression changes after 4 h incubation with 0.7 µg/ml FLC and the combination of 4 µg/ml SRT+0.25 µg/ml FLC are provided for comparison. Significance cutoff: padj (adjusted p-value) ≤ 0.05; non-significant padj values are highlighted red.

Gene ID	**Product (Janbon annotation)**	**SRT 4h Log_2 (Fold Change)**	**SRT padj**	**FLC 4h Log_2 (Fold Change)**	**FLC padj**	**SRT+FLC 4h Log_2 (Fold Change)**	**SRT+FLC padj**
CNAG_03115	hypothetical protein	2.16	0.00	-0.29	0.05	1.66	0.00
CNAG_05290	transcription initiation protein SPT3	0.83	0.00	0.12	0.54	0.56	0.00
CNAG_06425	fungal specific transcription factor	0.60	0.00	0.50	0.00	1.10	0.00
CNAG_00068	specific RNA polymerase II transcription factor	0.58	0.00	0.40	0.00	0.85	0.00
CNAG_00883	transcription factor	0.57	0.00	0.44	0.02	0.82	0.00
CNAG_05431	pH-response transcription factor pacC/RIM101	0.52	0.00	1.09	0.00	1.35	0.00
CNAG_05420	RNA polymerase II transcription factor	0.48	0.00	0.43	0.00	0.72	0.00
CNAG_07435	transcription activator	0.40	0.02	0.71	0.00	0.99	0.00
CNAG_03423	transcriptional activator	0.39	0.01	0.38	0.01	0.57	0.00
CNAG_03859	transcriptional regulator Medusa	0.38	0.00	0.15	0.19	0.15	0.12
CNAG_01292	pol II transcription elongation factor	0.36	0.01	0.23	0.10	0.39	0.00
CNAG_03273	transcription initiation factor TFIID subunit 2	0.36	0.02	0.40	0.01	0.48	0.00
CNAG_03625	RNA polymerase I-specific transcription initiation factor RRN7	0.36	0.02	0.15	0.37	0.49	0.00

Table3.9. continued

Gene ID	Product (Janbon annotation)	SRT 4h Log2 (Fold Change)	SRT padj	FLC 4h Log2 (Fold Change)	FLC padj	SRT+FLC 4h Log2 (Fold Change)	SRT+FLC padj
CNAG_07724	ligand-regulated transcription factor	0.35	0.01	0.39	0.00	0.67	0.00
CNAG_02936	CCR4-NOT transcription complex subunit 1	0.34	0.04	0.27	0.10	0.45	0.00
CNAG_01902	general transcriptional repressor	0.33	0.02	0.31	0.03	0.46	0.00
CNAG_00027	transcriptional activator	0.31	0.02	0.25	0.06	0.47	0.00
CNAG_03190	glucose-repressible alcohol dehydrogenase transcriptional effector	0.27	0.03	0.30	0.01	0.46	0.00
CNAG_07924	RNA polymerase II transcription factor	0.27	0.02	0.29	0.01	0.44	0.00
CNAG_06465	transcription regulator	0.25	0.05	0.11	0.44	0.25	0.02
CNAG_06635	CCR4-NOT transcription complex subunit 3	0.24	0.05	0.11	0.40	0.25	0.02
CNAG_04641	general transcription factor 3C polypeptide 3 (transcription factor C subunit 4)	0.24	0.04	0.15	0.22	0.30	0.00
CNAG_05222	transcriptional regulator Nrg1	0.23	0.02	0.20	0.05	0.28	0.00

Table 3.9. SRT up-regulates genes related to transcription in *C. neoformans* based on RNA-seq. Differentially up-regulated *C. neoformans* genes related to transcription after 4 h incubation with 7 µg/ml SRT identified by RNA-seq. Corresponding gene expression changes after 4 h incubation with 0.7 µg/ml FLC and the combination of 4 µg/ml SRT+0.25 µg/ml FLC, provided for comparison. Significance cutoff: padj (adjusted p-value) ≤ 0.05; non-significant padj values are highlighted red.

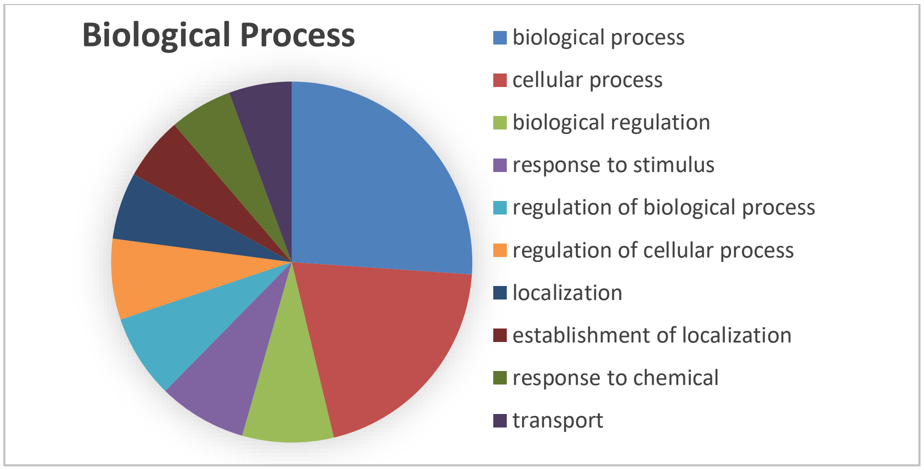
Biological Process
biological process
cellular process
biological regulation
response to stimulus
regulation of biological process
regulation of cellular process
localization
establishment of localization
response to chemical
transport

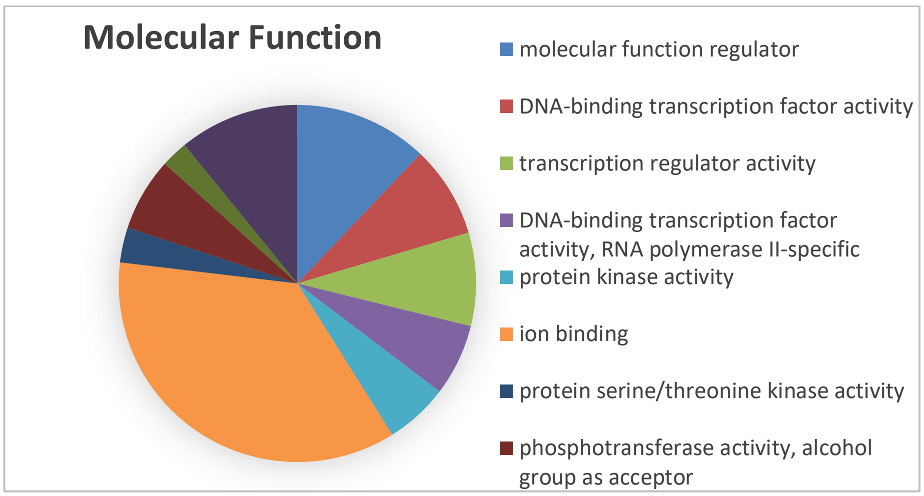
Molecular Function
molecular function regulator
DNA-binding transcription factor activity
transcription regulator activity
DNA-binding transcription factor activity, RNA polymerase II-specific
protein kinase activity
ion binding
protein serine/threonine kinase activity
phosphotransferase activity, alcohol group as acceptor

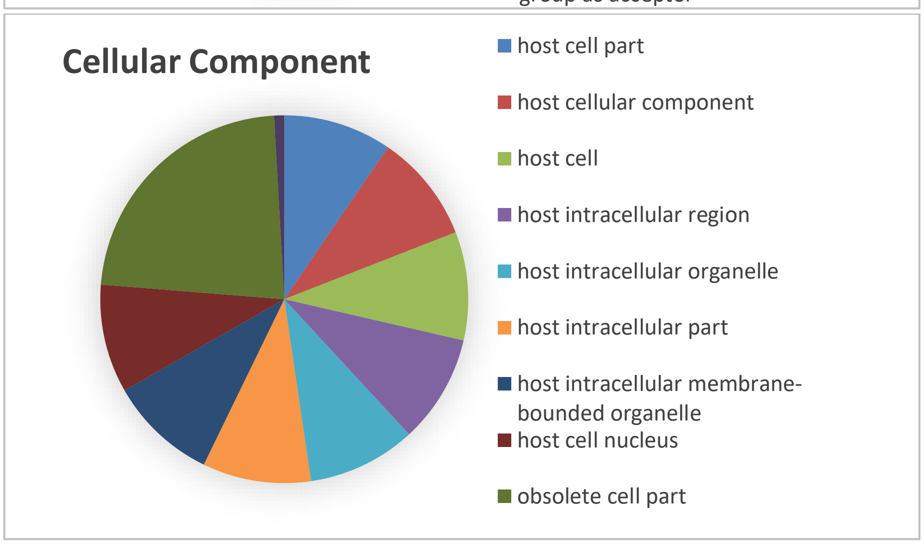
Cellular Component
host cell part
host cellular component
host cell
host intracellular region
host intracellular organelle
host intracellular part
host intracellular membrane-bounded organelle
host cell nucleus
obsolete cell part

Figure III-9 Functional enrichment of up-regulated transcripts by SRT in *C. neoformans* based on RNA-seq. Three Gene Ontology (GO) enrichments namely Biological Process, Molecular Function and Cellular Component are generated for the *C. neoformans* genes up-regulated after SRT treatment, using resources from FungiDB. The top 10 GO categories based solely on the most represented genes with p-value <0.01 for each of the branches of enrichment are shown in three different pie charts.

GENES DOWN-REGULATED BY SRT IN RNAseq

852 genes identified by RNA-seq are significantly down-regulated in *C. neoformans* after 4h incubation with 7 μg/ml SRT as compared to vehicle (DMSO) treated cells at a significance cutoff of padj (adjusted p-value) ≤ 0.05 (Supplementary Table 9). Table 3.10 shows the top 25 repressed genes showing a fold of repression of 1.85 times or more. Out of these 852 genes, only 161 were repressed 1.5 fold or more.In-depth inspection of these 852 genes, revealed the following details:

Ribosomal genes

77 genes encoding ribosomal proteins or subunits of ribonucleoprotein complexes were identified and of which 8 were SRT specific. Table 3.11 shows the top 25 repressed genes in this section. Most of these genes exhibit a less than 1.5 fold of repression.

Translation machinery

7 genes encoding products associated with the term translation including initiation factors were identified (Table 3.12). Most of these genes exhibit a lower than 1.5 fold of repression.

Non-coding RNA or (ncRNA) genes

216 non-coding RNA genes are identified and 98 of which seem to be SRT specific. 107 genes out of the total and 48 were SRT specific genes exhibit a fold repression of 1.5 or higher as shown in Table 3.13. FLC also down-regulates many ncRNA genes as shown in the table indicating a similar pattern of cryptococcal responses to SRT and FLC.

Gene Ontology

Functional characterization of the total 852 down-regulated transcripts using Gene Ontology (GO) enrichment shows a general impact after SRT treatment [117]. Categories for ribosome constituent, RNA binding and transporter activity are highly enriched in molecular function branch, cellular organelles and ribosome are highly enriched in cellular component branch, and various metabolic pathways are enriched in biological process branch of GO terms respectively (Supplementary Table 10). These results indicate SRT can be involved in repressing ribosome biogenesis and inhibit translation, which is consistent with the results reported in the literature [4, 66] . The top 10 GO categories based solely on the most represented genes with p-value <0.01 for each of the branch of enrichment are shown in three different pie charts in Fig 3.10.

Gene ID	product (Janbon annotation)	Gene Name or Symbol	SRT 4h Log_2 (Fold Change)	SRT padj
CNAG_12264	ncRNA	N/A	-1.46	0.03
CNAG_12277	ncRNA	N/A	-1.45	0.00
CNAG_12557	ncRNA	N/A	-1.44	0.00
CNAG_13068	ncRNA	N/A	-1.39	0.03
CNAG_13050	ncRNA	N/A	-1.13	0.02
CNAG_07896	hypothetical protein	N/A	-1.12	0.01
CNAG_13156	ncRNA	N/A	-1.10	0.02
CNAG_12737	ncRNA	N/A	-1.10	0.04
CNAG_03759	conidiation-specific protein 6	N/A	-1.10	0.00
CNAG_12128	ncRNA	N/A	-1.07	0.01
CNAG_12028	ncRNA	N/A	-1.07	0.00
CNAG_12022	ncRNA	N/A	-1.06	0.00
CNAG_12938	ncRNA	N/A	-1.05	0.03
CNAG_12464	ncRNA	N/A	-1.03	0.03
CNAG_12239	ncRNA	N/A	-1.01	0.00
CNAG_12864	ncRNA	N/A	-1.01	0.01
CNAG_12021	ncRNA	N/A	-0.98	0.00
CNAG_04793	hypothetical protein	N/A	-0.98	0.00
CNAG_13183	ncRNA	N/A	-0.97	0.01
CNAG_12289	ncRNA	N/A	-0.94	0.00
CNAG_12967	ncRNA	N/A	-0.93	0.00
CNAG_12261	ncRNA	N/A	-0.92	0.00
CNAG_12485	ncRNA	N/A	-0.92	0.04
CNAG_12845	ncRNA	N/A	-0.91	0.00
CNAG_12176	ncRNA	N/A	-0.90	0.00

Table 3.10. Transcripts down-regulated by SRT in *C. neoformans* based on RNA-seq. Differentially down-regulated *C. neoformans* genes after 4 h incubation with 7

µg/ml SRT identified by RNA-seq. Top 25 repressed genes showing a fold of repression of 1.85 times or higher are represented. Significance cutoff: padj (adjusted p-value) ≤ 0.05.

Gene ID	Product (Janbon annotation)	SRT 4h Log_2 (Fold Change)	SRT padj	FLC 4h Log_2 (Fold Change)	FLC padj	SRT+FLC 4h Log_2 (Fold Change)	SRT+FLC padj
CNAG_04072	60S ribosome subunit biogenesis protein nip7	-0.73	0.00	-0.95	0.00	-1.30	0.00
CNAG_05232	large subunit ribosomal protein L8	-0.62	0.04	-0.43	0.16	-0.68	0.01
CNAG_01198	small nuclear ribonucleoprotein F	-0.61	0.00	-0.52	0.00	-0.93	0.00
CNAG_04884	large subunit ribosomal protein L44	-0.58	0.00	-0.48	0.00	-0.85	0.00
CNAG_03015	large subunit ribosomal protein L37-A	-0.57	0.05	-0.50	0.09	-0.89	0.00
CNAG_05762	large subunit acidic ribosomal protein P2	-0.56	0.01	-0.57	0.01	-0.88	0.00
CNAG_01455	large subunit ribosomal protein L39	-0.54	0.00	-0.52	0.01	-1.00	0.00
CNAG_04011	large subunit ribosomal protein L37a	-0.54	0.00	-0.45	0.01	-0.92	0.00
CNAG_07864	U3 small nucleolar ribonucleoprotein IMP3	-0.52	0.00	-0.73	0.00	-1.24	0.00
CNAG_05525	small subunit ribosomal protein S26	-0.51	0.00	-0.37	0.02	-0.69	0.00
CNAG_00232	large subunit ribosomal protein L30e	-0.51	0.00	-0.44	0.01	-0.90	0.00

Table 3.11. continued

Gene ID	Product (Janbon annotation)	SRT 4h Log2 (Fold Change)	SRT padj	FLC 4h Log2 (Fold Change)	FLC padj	SRT+FLC 4h Log2 (Fold Change)	SRT+FLC padj
CNAG_01300	small subunit ribosomal protein S21e	-0.49	0.00	-0.46	0.00	-0.86	0.00
CNAG_03221	large subunit ribosomal protein L29	-0.49	0.00	-0.38	0.00	-0.79	0.00
CNAG_01976	large subunit ribosomal protein L23	-0.49	0.00	-0.42	0.00	-0.76	0.00
CNAG_03000	small subunit ribosomal protein S19e	-0.48	0.00	-0.43	0.00	-0.72	0.00
CNAG_05831	endoribonuclease	-0.47	0.01	-0.27	0.15	-0.66	0.00
CNAG_00771	large subunit ribosomal protein L29	-0.47	0.01	-0.49	0.00	-0.85	0.00
CNAG_06127	ribosome biogenesis protein NSA2	-0.46	0.00	-0.62	0.00	-0.95	0.00
CNAG_03747	large subunit ribosomal protein L27Ae	-0.44	0.00	-0.38	0.01	-0.66	0.00

Table 3.11. **SRT down-regulates transcript levels of ribosomal genes in *C. neoformans* based on RNA-seq** Differentially down-regulated *C. neoformans* ribosomal genes after 4 h incubation with 7 μg/ml SRT identified by RNA-seq. Corresponding gene expression changes after 4 h incubation with 0.7 μg/ml FLC and the combination of 4 μg/ml SRT+0.25 μg/ml FLC, provided for comparison.

Significance cutoff: padj (adjusted p-value) ≤ 0.05; non-significant padj values are highlighted red.

Gene ID	Product (Janbon annotation)	SRT 4h Log_2 (Fold Change)	SRT padj	FLC 4h Log_2 (Fold Change)	FLC padj	SRT+FLC 4h Log_2 (Fold Change)	SRT+FLC padj
CNAG_05455	translation initiation factor eIF-1A	-0.52	0.00	-0.58	0.00	-0.91	0.00
CNAG_06865	translation machinery-associated protein 16	-0.47	0.01	-0.68	0.00	-0.86	0.00
CNAG_02128	translation initiation factor 3 subunit J	-0.39	0.00	-0.30	0.00	-0.58	0.00
CNAG_02656	translation machinery-associated protein 20	-0.33	0.02	-0.36	0.01	-0.57	0.00
CNAG_04628	translation initiation factor 6	-0.26	0.04	-0.33	0.01	-0.56	0.00
CNAG_02657	translation initiation factor 3 subunit G	-0.25	0.04	-0.28	0.02	-0.43	0.00
CNAG_04054	translation initiation factor SUI1	-0.24	0.01	-0.26	0.00	-0.43	0.00

Table 3.12. SRT down-regulates transcript levels of genes related to the translation machinery in *C. neoformans* based on RNA-seq. Differentially down-regulated *C. neoformans* genes related to the translation machinery including initiation factors, after 4 h incubation with 7 μg/ml SRT identified by RNA-seq. Corresponding gene expression changes after 4 h incubation with 0.7 μg/ml FLC and the combination of 4 μg/ml SRT+0.25 μg/ml FLC, provided for comparison. Significance cutoff: padj (adjusted p-value) ≤ 0.05.

Gene ID	Product (Janbon annotation)	SRT 4h Log_2 (Fold Change)	SRT padj	FLC 4h Log_2 (Fold Change)	FLC padj	SRT+FLC 4h Log_2 (Fold Change)	SRT+FLC padj
CNAG_12264	ncRNA	-1.46	0.03	-1.74	0.01	-1.23	0.03
CNAG_12277	ncRNA	-1.45	0.00	-0.09	0.86	-0.26	0.48
CNAG_12557	ncRNA	-1.44	0.00	-0.64	0.08	-1.77	0.00
CNAG_13068	ncRNA	-1.39	0.03	-0.21	0.78	-0.82	0.12
CNAG_13050	ncRNA	-1.13	0.02	-0.46	0.33	-0.71	0.08
CNAG_13156	ncRNA	-1.10	0.02	-1.00	0.03	-0.56	0.18
CNAG_12737	ncRNA	-1.10	0.04	-0.94	0.08	-0.53	0.26
CNAG_12128	ncRNA	-1.07	0.01	-0.66	0.09	-1.35	0.00
CNAG_12028	ncRNA	-1.07	0.00	-0.82	0.02	-0.99	0.00
CNAG_12022	ncRNA	-1.06	0.00	-0.85	0.02	-1.22	0.00
CNAG_12938	ncRNA	-1.05	0.03	-0.30	0.57	-1.32	0.00
CNAG_12464	ncRNA	-1.03	0.03	-0.27	0.61	-0.66	0.11
CNAG_12239	ncRNA	-1.01	0.00	-0.52	0.12	-1.05	0.00
CNAG_12864	ncRNA	-1.01	0.01	-0.46	0.22	-1.01	0.00
CNAG_12021	ncRNA	-0.98	0.00	-0.51	0.08	-1.49	0.00
CNAG_13183	ncRNA	-0.97	0.01	-0.94	0.01	-0.66	0.05
CNAG_12289	ncRNA	-0.94	0.00	-0.44	0.14	-1.16	0.00
CNAG_12967	ncRNA	-0.93	0.00	-1.23	0.00	-1.04	0.00
CNAG_12261	ncRNA	-0.92	0.00	-0.57	0.08	-1.39	0.00
CNAG_12485	ncRNA	-0.92	0.04	-0.85	0.05	-0.61	0.11
CNAG_12845	ncRNA	-0.91	0.00	-1.14	0.00	-1.20	0.00
CNAG_12176	ncRNA	-0.90	0.00	-0.80	0.00	-1.76	0.00

Table 3.13. continued

Gene ID	Product (Janbon annotation)	SRT 4h Log2 (Fold Change)	SRT padj	FLC 4h Log2 (Fold Change)	FLC padj	SRT+FLC 4h Log2 (Fold Change)	SRT+FLC padj
CNAG_12919	ncRNA	-0.89	0.00	-0.60	0.01	-0.89	0.00
CNAG_12160	ncRNA	-0.89	0.02	-0.22	0.60	-0.86	0.01
CNAG_13200	ncRNA	-0.88	0.00	-0.57	0.00	-1.52	0.00
CNAG_13165	ncRNA	-0.88	0.00	-0.70	0.02	-0.57	0.03
CNAG_12303	ncRNA	-0.87	0.03	-0.13	0.79	0.35	0.30
CNAG_12386	ncRNA	-0.87	0.00	-0.93	0.00	-1.86	0.00
CNAG_12216	ncRNA	-0.86	0.03	-0.76	0.05	-1.18	0.00
CNAG_12165	ncRNA	-0.85	0.01	-0.22	0.54	-1.51	0.00
CNAG_12844	ncRNA	-0.85	0.02	-0.36	0.33	-0.71	0.02
CNAG_13148	ncRNA	-0.84	0.04	-0.87	0.03	-1.44	0.00
CNAG_13088	ncRNA	-0.84	0.02	-0.31	0.41	-0.71	0.02
CNAG_12685	ncRNA	-0.83	0.02	-0.57	0.12	-0.76	0.02
CNAG_12315	ncRNA	-0.83	0.00	-0.49	0.02	-1.21	0.00

Table 3.13. SRT down-regulates transcript levels of non-coding RNA or ncRNA genes in *C. neoformans* based on RNA-seq. Differentially down-regulated *C. neoformans* ncRNA genes after 4 h incubation with 7 μg/ml SRT identified by RNA-seq. Corresponding gene expression changes after 4 h incubation with 0.7 μg/ml FLC and the combination of 4 μg/ml SRT+0.25 μg/ml FLC, provided for comparison. Significance cutoff: padj (adjusted p-value) ≤ 0.05; non-significant padj values are highlighted red.

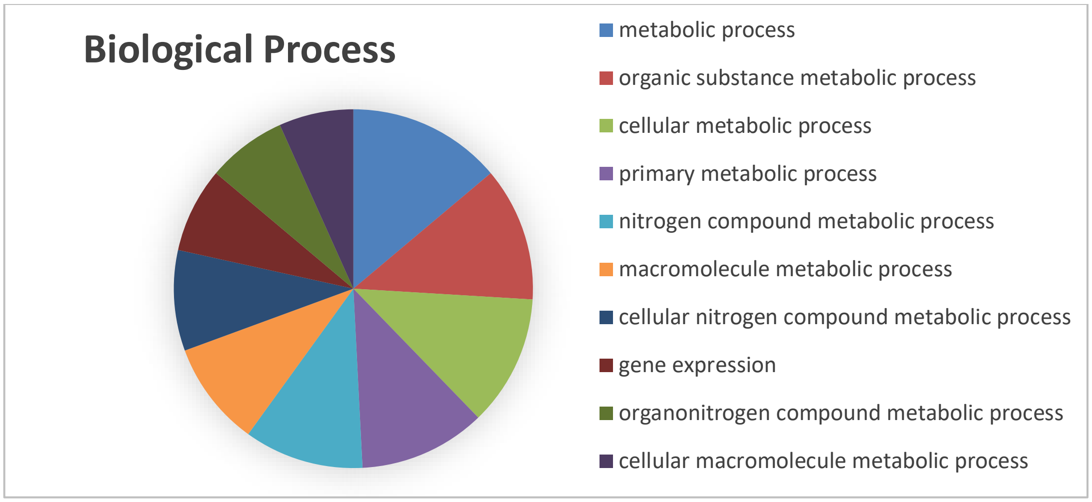

Biological Process
metabolic process
organic substance metabolic process
cellular metabolic process
primary metabolic process
nitrogen compound metabolic process
macromolecule metabolic process
cellular nitrogen compound metabolic process
gene expression
organonitrogen compound metabolic process
cellular macromolecule metabolic process

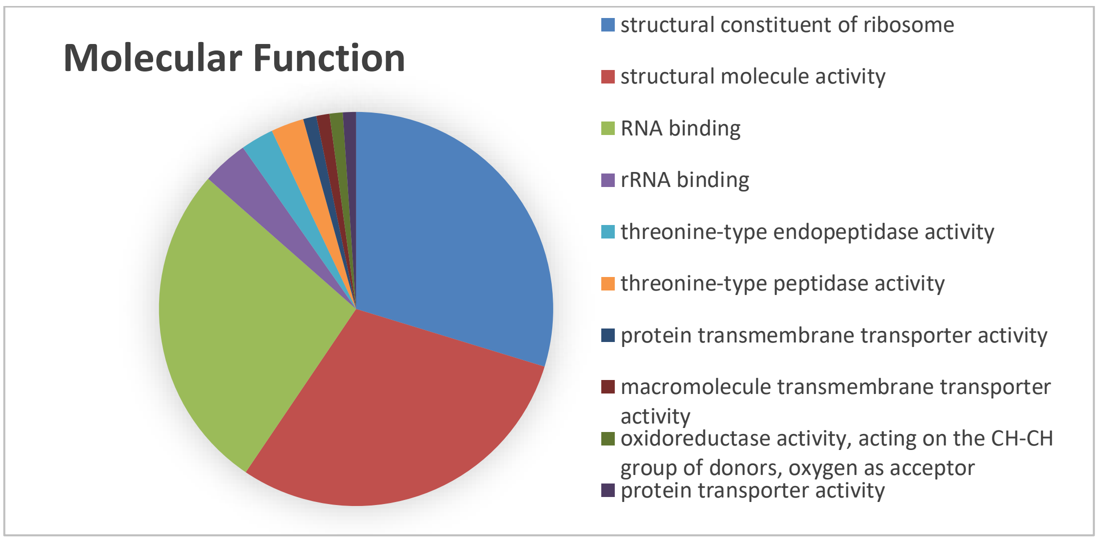

Molecular Function
structural constituent of ribosome
structural molecule activity
RNA binding
rRNA binding
threonine-type endopeptidase activity
threonine-type peptidase activity
protein transmembrane transporter activity
macromolecule transmembrane transporter activity
oxidoreductase activity, acting on the CH-CH group of donors, oxygen as acceptor
protein transporter activity

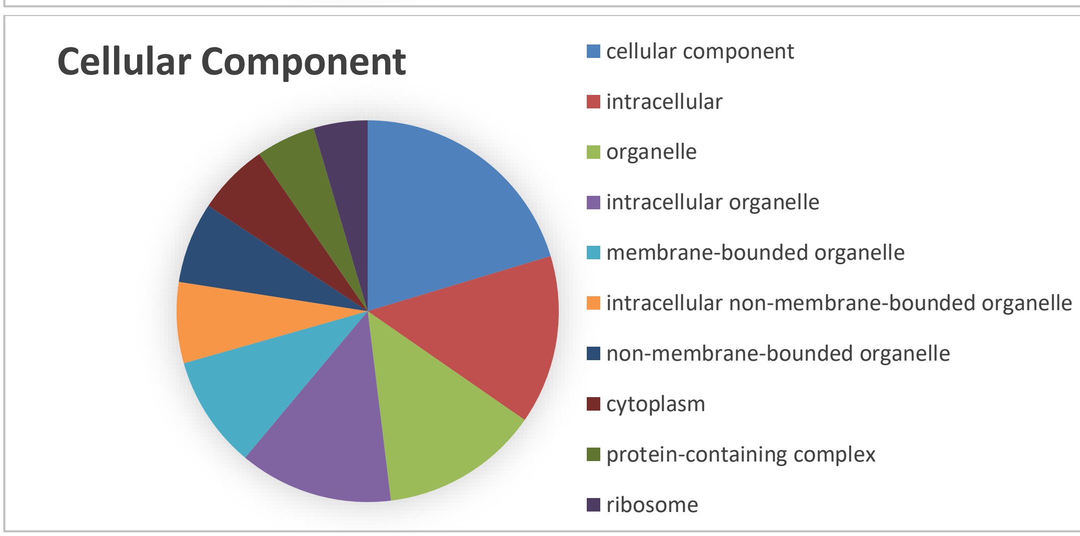

Cellular Component
cellular component
intracellular
organelle
intracellular organelle
membrane-bounded organelle
intracellular non-membrane-bounded organelle
non-membrane-bounded organelle
cytoplasm
protein-containing complex
ribosome

Figure III-10 . Functional enrichment of down-regulated transcripts by SRT in *C. neoformans* based on RNA-seq. Three Gene Ontology (GO) enrichments namely Biological Process, Molecular Function and Cellular Component are generated for the *C. neoformans* genes down-regulated after SRT treatment, using resources from FungiDB. The top 10 GO categories based solely on the most represented genes with p-value <0.01 for each of the branches of enrichment are shown in three different pie charts.

GENES UP-REGULATED BY SRT+FLC IN RNAseq

2063 genes identified by RNA-seq are significantly up-regulated in *C. neoformans* after 4h incubation with the combination of 4 μg/ml SRT+0.25 μg/ml FLC compared to DMSO treated cells at a significance cutoff of padj (adjusted p-value) ≤ 0.05 (Supplementary Table 11). This is almost one fourth of all genes present in *C. neoformans* and indicates on the greater range of impact of the drug combination each at a lower concentration than observed when each is used alone at higher concentrations. This indicates the synergy in the drug treatments and is consistent with the potentiating effect of SRT on FLC activity [4].

498 genes out of the total exhibit a fold change of 1.5 or higher. Interestingly 701 genes out of the 2063, were exclusively regulated by SRT+FLC i.e, they are significantly upregulated by SRT+FLC combination but are not altered significantly by either drug alone. Table 3.14 shows the top 25 differentially up-regulated genes from this list of 701 genes.

Many hypothetical proteins are encoded by genes uniquely induced by the drug combination, indicating possible important functions of these genes whose functions are not established.

Membrane related

130 genes found to be annotated as membrane proteins/transporters or as genes containing MFS (Major facilitator Superfamily) domain were upregulated (Supplementary Table 11). Among those, 43 genes exhibit a fold change of 1.5 or higher

and 37 genes of the total were uniquely up-regulated by the combination drug treatment and not by individual drug treatment. The top 20 genes from this list of 130 genes are shown in Table 3.15. Gene *CNAG_01953*, the potential MFS transporter, is the most induced gene as with SRT treatment alone.

Kinase related

50 genes found to be annotated as kinases were upregulated and 25 of them were uniquely specific to the combination of SRT+FLC SRT (Supplementary Table 11). However, most of the genes except the op 16, in this list exhibit a lower than1.5 fold change. The top 25 representative genes from the list are shown in Table 3.16.

Transcription related

50 genes found to be associated with transcription were upregulated and 20 of them seem to be uniquely specific to SRT+FLC combination (Supplementary Table 11). However, most of the genes in this list exhibit a lower than 1.5 fold change. The top 25 representative genes from the list are shown in Table 3.17.

Ergosterol biosynthesis genes

SRT+FLC treatment significantly upregulates most genes involved in the Ergosterol biosynthesis pathway (Table 3.2)

Gene Ontology

Functional characterization of the 2063 up-regulated transcripts using Gene Ontology (GO) enrichment shows categories for ionic or ribonucleotide binding are highly enriched in molecular function and intracellular membranes and organelles in the cellular component branches of GO terms respectively [117] (Supplementary Table 12). In the search for GO terms in biological processes, no specific regulation is highlighted. The top 10 GO categories based solely on the most represented genes with p-value <0.01 for each of the branch of enrichment are shown in three different pie charts in Fig 3.11

Gene ID	**Product (Janbon annotation)**	**SRT+FLC 4h Log_2 (Fold Change)**	**SRT+FLC padj**	**SRT 4h Log_2 (Fold Change)**	**SRT padj**	**FLC 4h Log_2 (Fold Change)**	**FLC padj**
CNAG_06207	hypothetical protein	0.93	0.00	0.32	0.10	0.29	0.12
CNAG_05397	hypothetical protein	0.90	0.00	0.02	0.94	0.33	0.20
CNAG_02066	hypothetical protein	0.88	0.00	-0.05	0.85	0.34	0.11
CNAG_12197	ncRNA	0.80	0.00	0.25	0.21	0.26	0.19
CNAG_07421	hypothetical protein	0.79	0.00	0.02	0.94	0.30	0.18
CNAG_04875	hypothetical protein	0.73	0.00	0.37	0.08	0.29	0.17
CNAG_04178	hypothetical protein	0.73	0.00	0.34	0.09	0.18	0.39

Table 3.14 continued

Gene ID	**Product (Janbon annotation)**	**SRT+FLC 4h Log2 (Fold Change)**	**SRT+FLC padj**	**SRT 4h Log2 (Fold Change)**	**SRT padj**	**FLC 4h Log2 (Fold Change)**	**FLC padj**
CNAG_12767	ncRNA	0.72	0.00	0.21	0.33	0.28	0.19
CNAG_00889	hypothetical protein	0.69	0.00	0.19	0.37	0.21	0.32
CNAG_13067	ncRNA	0.64	0.00	0.06	0.78	0.19	0.30
CNAG_03976	hypothetical protein	0.61	0.00	0.22	0.22	0.31	0.07

CNAG_00976	carbamoyl-phosphate synthase, small subunit	0.61	0.00	0.27	0.06	0.20	0.17
CNAG_03834	C4-hydroxylase	0.56	0.00	0.15	0.30	0.23	0.09
CNAG_01009	hypothetical protein, variant	0.54	0.00	0.25	0.10	0.26	0.09
CNAG_06265	high-affinity nicotinic acid transporter	0.54	0.00	0.22	0.14	0.17	0.28
CNAG_03017	transcription initiation factor TFIIF subunit alpha	0.54	0.00	0.18	0.25	0.23	0.12
CNAG_00028	high-affinity nicotinic acid transporter	0.53	0.00	0.25	0.08	0.24	0.08
CNAG_05520	hypothetical protein	0.53	0.00	0.14	0.38	0.13	0.41
CNAG_03003	chromatin structure-remodeling complex subunit SFH1	0.52	0.00	0.17	0.24	0.22	0.10
CNAG_00337	hypothetical protein	0.47	0.00	0.20	0.13	0.21	0.11
CNAG_00514	hypothetical protein	0.46	0.00	0.13	0.33	0.22	0.08
CNAG_03265	hypothetical protein	0.45	0.00	0.19	0.10	0.21	0.06
CNAG_03815	hypothetical protein	0.40	0.00	0.19	0.08	0.16	0.14
CNAG_04221	6-phosphofructo-2-kinase/fructose-2, 6-bisphosphatase	0.37	0.00	0.11	0.29	0.16	0.09
CNAG_00354	vacuolar protein 8	0.30	0.00	0.14	0.11	0.14	0.10

Table 3.14. SRT+FLC combination treatment up-regulates transcript levels of a unique set of genes in *C. neoformans* based on RNA-seq. Differentially up-regulated *C. neoformans* genes after 4 h incubation with of 4 μg/ml SRT+0.25 μg/ml FLC identified by RNA-seq which are not differentially expressed at significant levels by either treatment of SRT or FLC alone. Corresponding gene expression changes after 4 h

incubation with 7 μg/ml SRT and 0.7 μg/ml FLC, provided for comparison. Significance cutoff: padj (adjusted p-value) ≤ 0.05; non-significant padj values are highlighted red.

Gene ID	**Product (Janbon annotation)**	**Pfam domain**	**SRT+FLC 4h Log_2 (Fold Change)**	**SRT+ FLC padj**	**SRT 4h Log_2 (Fold Change)**	**SRT padj**	**FLC 4h Log_2 (Fold Change)**	**FLC padj**
CNAG_01953	hypothetical protein	MFS_1,MFS_1_like	4.44	0.00	5.42	0.00	0.32	0.04
CNAG_03764	integral membrane protein	PQ-loop	2.05	0.00	3.88	0.00	-0.16	0.57
CNAG_04546	multidrug transporter	MFS_1	1.78	0.00	1.30	0.00	0.95	0.00
CNAG_06323	L-fucose permease	MFS_1	1.50	0.00	0.70	0.00	1.27	0.00
CNAG_04253	transmembrane protein	SNARE_assoc	1.29	0.00	0.48	0.00	1.14	0.00
CNAG_02039	integral membrane protein	EamA	1.27	0.00	0.67	0.02	0.36	0.26
CNAG_01862	hexose transporter	Sugar_tr,MFS_1	1.25	0.00	0.37	0.47	1.80	0.00
CNAG_05075	solute carrier family 20 (sodium-dependent phosphate transporter)	PHO4	1.21	0.04	1.20	0.07	1.09	0.10

Table 3.15. continued

Gene ID	**Product (Janbon annotation)**	**Pfam domain**	**SRT+FLC 4h Log2 (Fold Change)**	**SRT+ FLC padj**	**SRT 4h Log2 (Fold Change)**	**SRT padj**	**FLC 4h Log2 (Fold Change)**	**FLC padj**

CNAG_00728	dityrosine transporter	MFS_1,Sugar_tr	1.18	0.00	1.23	0.00	0.19	0.40
CNAG_05345	amino acid transporter	AA_permease,AA_permease_2	1.17	0.02	0.41	0.58	0.34	0.66
CNAG_06776	membrane protein	MFS_1,Sugar_tr,UNC-93	1.11	0.00	0.61	0.01	0.55	0.02
CNAG_04758	amt family ammonium transporter	Ammonium_transp	1.09	0.00	0.75	0.00	0.47	0.02
CNAG_03732	integral membrane protein	PQ-loop	1.05	0.00	1.93	0.00	0.27	0.05
CNAG_01118	AAT family amino acid transporter	AA_permease,AA_permease_2	1.05	0.01	1.06	0.02	0.25	0.63
CNAG_00869	ATP-binding cassette transporter	ABC2_membrane,PDR_CDR,ABC_tran,ABC_trans_N,AAA_25	1.04	0.00	0.50	0.00	1.06	0.00
CNAG_05718	multidrug resistance protein fnx1	MFS_1,TRI12	1.01	0.00	0.48	0.00	0.64	0.00
CNAG_07449	amino acid transporter	AA_permease,AA_permease_2	0.98	0.00	0.65	0.01	0.36	0.15

Table 3.15. continued

Gene ID	**Product (Janbon annotation)**	**Pfam domain**	**SRT+FLC 4h Log2 (Fold Change)**	**SRT+ FLC padj**	**SRT 4h Log2 (Fold Change)**	**SRT padj**	**FLC 4h Log2 (Fold Change)**	**FLC padj**

CNAG_04947	high-affinity nicotinic acid transporter	MFS_1	0.91	0.01	0.78	0.05	0.36	0.43
CNAG_06890	membrane transporter	MFS_1	0.90	0.00	1.26	0.00	-0.12	0.67
CNAG_05377	MFS transporter, SP family, solute carrier family 2 (myo-inositol transporter), member 13	Sugar_tr,MFS_1	0.90	0.00	0.62	0.04	0.42	0.18

Table 3.15. SRT+FLC up-regulates transcript levels of membrane proteins and transporters in *C. neoformans* based on RNAseq. Top 20 differentially up-regulated *C. neoformans* genes having fold change of 1.87 or above i.e, $\log_2$ values ≥ 0.9, related to membrane proteins/transporters or genes containing MFS (Major facilitator Superfamily) domain after 4 h incubation with the combination of 4 μg/ml SRT+0.25 μg/ml FLC identified by RNA-seq. Corresponding gene expression changes after 4 h incubation with 0.7 μg/ml FLC and 7 μg/ml SRT, provided for comparison. Significance cutoff: padj (adjusted p-value) ≤ 0.05; non-significant padj values are highlighted red.

Gene ID	Product (Janbon annotation)	SRT+FLC 4h $\log_2$ (Fold Change)	SRT+FLC padj	SRT 4h $\log_2$ (Fold Change)	SRT padj	FLC 4h $\log_2$ (Fold Change)	FLC padj
CNAG_06568	RAN protein kinase	1.57	0.00	0.85	0.00	0.94	0.00
CNAG_01061	serine/threonine protein kinase	1.22	0.00	0.72	0.00	0.68	0.00
CNAG_03024	AGC protein kinase	0.84	0.00	0.43	0.01	0.66	0.00

CNAG_00396	AGC/PKA protein kinase	0.77	0.00	0.29	0.00	0.76	0.00
CNAG_04040	AGC/RSK protein kinase	0.77	0.00	0.44	0.00	0.36	0.00
CNAG_00405	STE/STE20/YSK protein kinase	0.75	0.00	0.41	0.00	0.53	0.00
CNAG_04433	CMGC/DYRK/DYRK2 protein kinase	0.68	0.00	0.41	0.01	0.51	0.00
CNAG_01905	serine/threonine protein kinase	0.67	0.00	0.43	0.01	0.48	0.00
CNAG_05386	glutamate 5-kinase, variant	0.66	0.00	0.38	0.00	0.29	0.02
CNAG_03843	NAK protein kinase	0.66	0.00	0.29	0.02	0.39	0.00
CNAG_06490	CAMK/CAMKL protein kinase	0.64	0.00	0.34	0.06	0.45	0.01
CNAG_05771	serine/threonine-protein kinase TEL1, variant	0.64	0.00	0.45	0.02	0.44	0.01
CNAG_05005	ULK/ULK protein kinase	0.63	0.00	0.42	0.00	0.54	0.00
CNAG_06642	Atypical/PIKK/FRAP protein kinase	0.60	0.00	0.45	0.00	0.42	0.00
CNAG_03670	IRE protein kinase	0.59	0.00	0.29	0.03	0.32	0.01
CNAG_04408	choline kinase	0.58	0.00	0.17	0.22	0.29	0.02
CNAG_00388	1-phosphatidylinositol-4-phosphate 5-kinase	0.56	0.00	0.30	0.02	0.30	0.02
CNAG_04347	aspartate kinase	0.56	0.00	0.31	0.00	0.20	0.07
CNAG_01209	1-phosphatidylinositol-3-phosphate 5-kinase	0.56	0.00	0.46	0.00	0.35	0.03
CNAG_06086	CMGC/CDK/CDK8 protein kinase	0.53	0.00	0.35	0.03	0.22	0.20
CNAG_04335	phosphatidylinositol 4-kinase	0.53	0.00	0.38	0.01	0.38	0.01
CNAG_06193	CMGC/RCK protein kinase	0.52	0.00	0.36	0.02	0.30	0.05
CNAG_05063	STE/STE11/SSK protein kinase	0.51	0.00	0.29	0.03	0.31	0.02

Table 316. continued

Gene ID	Product (Janbon annotation)	SRT+FLC 4h Log2 (Fold Change)	SRT+FLC padj	SRT 4h Log2 (Fold Change)	SRT padj	FLC 4h Log2 (Fold Change)	FLC padj

CNAG_02233	serine/threonine-protein kinase ATR	0.51	0.00	0.32	0.01	0.28	0.02
CNAG_06174	PEK/GCN2 protein kinase	0.50	0.00	0.36	0.00	0.28	0.02

Table 3.16. SRT+FLC up-regulates transcript levels of kinase genes in *C. neoformans* based on RNAseq. Top 25 differentially up-regulated *C. neoformans* kinase genes after 4 h incubation with the combination of 4 μg/ml SRT+0.25 μg/ml FLC identified by RNA-seq. Corresponding gene expression changes after 4 h incubation with 0.7 μg/ml FLC and 7 μg/ml SRT, provided for comparison. Significance cutoff: padj (adjusted p-value) ≤ 0.05; non-significant padj values are highlighted red.

Gene ID	Product (Janbon annotation)	SRT+FLC 4h Log_2 (Fold Change)	SRT+FLC padj	SRT 4h Log_2 (Fold Change)	SRT padj	FLC 4h Log_2 (Fold Change)	FLC padj
CNAG_03115	hypothetical protein	1.66	0.00	2.16	0.00	-0.29	0.05
CNAG_05431	pH-response transcription factor pacC/RIM101	1.35	0.00	0.52	0.00	1.09	0.00

CNAG_06425	fungal specific transcription factor	1.10	0.00	0.60	0.00	0.50	0.00
CNAG_07435	transcription activator	0.99	0.00	0.40	0.02	0.71	0.00
CNAG_00068	specific RNA polymerase II transcription factor	0.85	0.00	0.58	0.00	0.40	0.00
CNAG_00883	transcription factor	0.82	0.00	0.57	0.00	0.44	0.02
CNAG_05420	RNA polymerase II transcription factor	0.72	0.00	0.48	0.00	0.43	0.00
CNAG_07724	ligand-regulated transcription factor	0.67	0.00	0.35	0.01	0.39	0.00
CNAG_00627	specific transcriptional repressor	0.61	0.00	0.12	0.61	0.28	0.17
CNAG_04398	specific RNA polymerase II transcription factor	0.60	0.00	0.27	0.07	0.38	0.01
CNAG_03423	transcriptional activator	0.57	0.00	0.39	0.01	0.38	0.01
CNAG_05290	transcription initiation protein SPT3	0.56	0.00	0.83	0.00	0.12	0.54
CNAG_03017	transcription initiation factor TFIIF subunit alpha	0.54	0.00	0.18	0.25	0.23	0.12
CNAG_04345	specific RNA polymerase II transcription factor	0.50	0.00	0.30	0.06	0.21	0.22
CNAG_03625	RNA polymerase I-specific transcription initiation factor RRN7	0.49	0.00	0.36	0.02	0.15	0.37
CNAG_07680	transcriptional activator HAP5	0.49	0.00	0.16	0.28	0.17	0.24

Table3.17.continued

Gene ID	Product (Janbon annotation)	SRT+FLC 4h Log2 (Fold Change)	SRT+FLC padj	SRT 4h Log2 (Fold Change)	SRT padj	FLC 4h Log2 (Fold Change)	FLC padj

CNAG_03273	transcription initiation factor TFIID subunit 2	0.48	0.00	0.36	0.02	0.40	0.01
CNAG_00027	transcriptional activator	0.47	0.00	0.31	0.02	0.25	0.06
CNAG_01902	general transcriptional repressor	0.46	0.00	0.33	0.02	0.31	0.03
CNAG_03190	glucose-repressible alcohol dehydrogenase transcriptional effector	0.46	0.00	0.27	0.03	0.30	0.01
CNAG_02936	CCR4-NOT transcription complex subunit 1	0.45	0.00	0.34	0.04	0.27	0.10
CNAG_03851	general transcription factor 3C polypeptide 5 (transcription factor C subunit 1)	0.45	0.00	0.27	0.08	0.14	0.42
CNAG_04674	transcriptional adapter 3	0.45	0.01	0.12	0.59	0.30	0.13
CNAG_07924	RNA polymerase II transcription factor	0.44	0.00	0.27	0.02	0.29	0.01
CNAG_00777	CCR4-NOT transcriptional complex subunit CAF120	0.43	0.00	0.28	0.08	0.29	0.06
CNAG_05622	specific transcriptional repressor	0.43	0.00	0.23	0.14	0.34	0.02

Table 3.17. SRT+FLC up-regulates genes related to transcription in *C. neoformans* based on RNAseq. Top 25 differentially up-regulated *C. neoformans* genes related to transcription after 4 h incubation with the combination of 4 µg/ml SRT+0.25 µg/ml FLC identified by RNA-seq. Corresponding gene expression changes after 4 h incubation with 0.7 µg/ml FLC and 7 µg/ml SRT, provided for comparison. Significance cutoff: padj (adjusted p-value) ≤ 0.05; non-significant padj values are highlighted red.

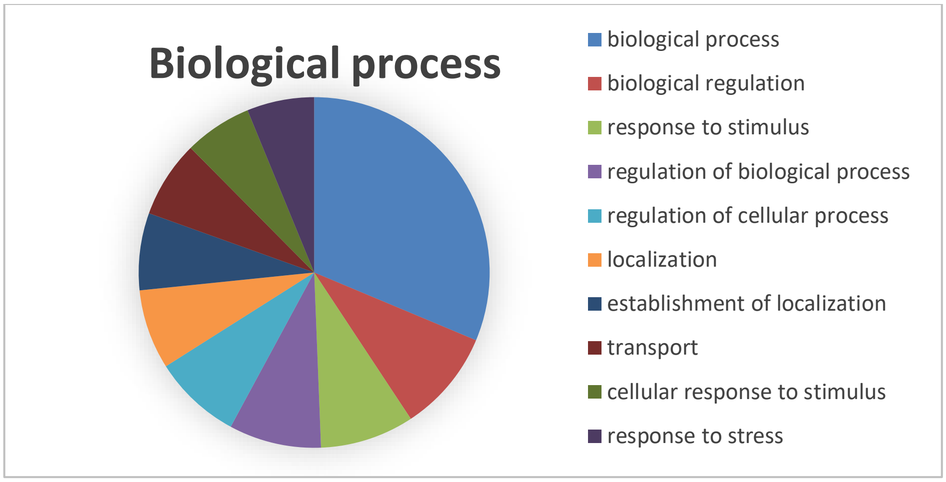
Biological process
biological process
biological regulation
response to stimulus
regulation of biological process
regulation of cellular process
localization
establishment of localization
transport
cellular response to stimulus
response to stress

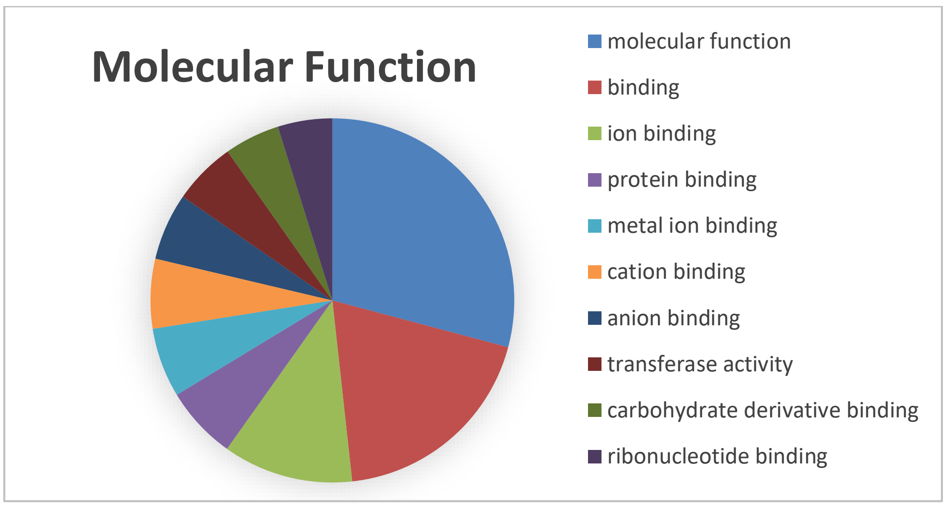
Molecular Function
molecular function
binding
ion binding
protein binding
metal ion binding
cation binding
anion binding
transferase activity
carbohydrate derivative binding
ribonucleotide binding

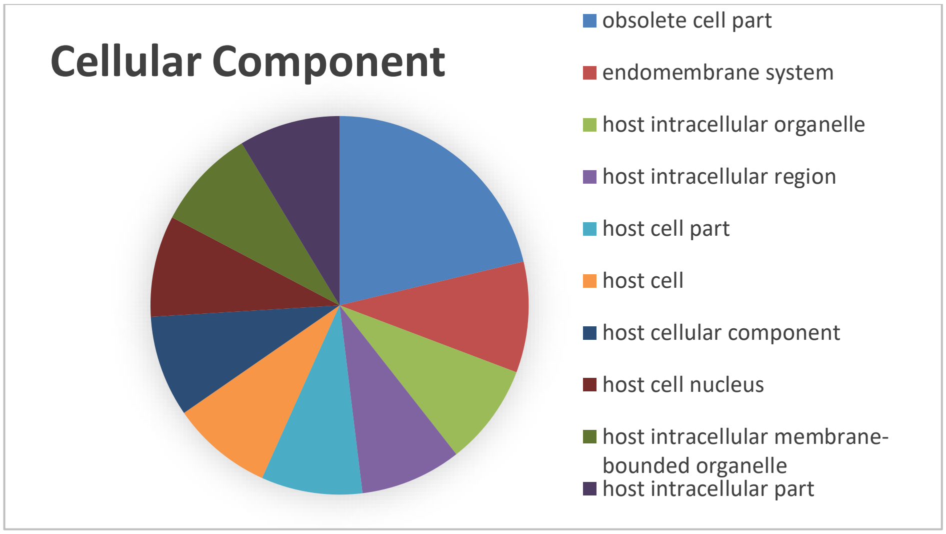

Figure III-11 Functional enrichment of up-regulated transcripts by SRT+FLC combination in *C. neoformans* based on RNAseq Three Gene Ontology (GO) enrichments namely Biological Process, Molecular Function and Cellular Component are generated for the *C. neoformans* genes down-regulated after SRT treatment, using resources from FungiDB. The top 10 GO categories based solely on the most represented genes with p-value <0.0.1 for each of the branches of enrichment are shown in three different pie charts.

GENES DOWN-REGULATED BY SRT+FLC IN RNA-seq

Similar to the up-regulated set, a huge number of genes are also repressed by the drug combination, indicating yet again the depth of the synergistic impact of combining the drugs even at lower concentrations than when used alone. 2081 genes identified by RNA-seq are significantly down-regulated in *C. neoformans* after 4h incubation with the combination of 4 µg/ml SRT+0.25 µg/ml FLC compared to DMSO treated cells at a significance cutoff of padj (adjusted p-value) ≤ 0.05 (Supplementary Table 13). Out of these 2081 genes, 882 were repressed1.5 fold or more. Among these 185 have more than 2 fold repression. Also 740 genes out of the total are specifically repressed by the drug combination but not by either of the drugs alone. Table 3.18 shows the top 25 repressed genes showing a fold of repression of more than 2 fold. In-depth inspection of these 2081 genes, revealed the following details:

Ribosomal genes

158 genes encoding ribosomal proteins or subunits of ribonucleoprotein complexes were identified and 32 of which were solely specific to the combination drug treatment (Supplementary Table 13). Also 68 of the total 158 genes in this list exhibit a higher than 1.5 fold of repression. Table 3.19 shows the top 20 repressed genes in this section.

Translation machinery

Seventeen genes encoding products associated with the term translation including initiation factors were identified as shown in Table 3.20. Again this observation in addition to the ribosomal genes, indicates a common pathway i.e. translation, being influenced by both drugs independently and in combination. Most of these genes exhibit a lower than 1.5 fold repression.

Non-coding RNA (ncRNA) genes

461 non-coding RNA genes are identified and 195 of which were specific to the combination of drugs only (Supplementary Table 13). Top 30 such repressed genes are represented in Table 3.21.

Gene Ontology

Functional characterization of the total 2081 down-regulated transcripts using Gene Ontology (GO) enrichment shows categories for ribosomal structure, RNA and ribonucleoside binding are highly enriched in molecular function and intracellular membranes and organelles in the cellular component branches of GO terms respectively [117] (Supplementary Table 14). In the search for GO terms in biological processes, no specific regulation is highlighted. The top 10 GO categories based solely on the most represented genes with p-value <0.01 for each of the branches of enrichment are shown in three different pie charts in Fig 3.12.

Gene ID	Product (Janbon annotation)	Gene Name or Symbol	SRT+FLC 4h Log_2 (Fold Change)	SRT+FLC padj	SRT 4h Log_2 (Fold Change)	SRT padj	FLC 4h Log_2 (Fold Change)	FLC padj
CNAG_00315	HHE domain-containing protein	N/A	-3.12	0.00	-0.68	0.14	-2.16	0.00
CNAG_07934	hypothetical protein	N/A	-3.04	0.03	-0.18	NA	-0.41	0.76
CNAG_12380	ncRNA	N/A	-2.61	0.03	-0.19	NA	-3.42	0.03
CNAG_12196	ncRNA	N/A	-2.13	0.00	-0.61	0.00	-1.00	0.00
CNAG_13160	ncRNA	N/A	-2.02	0.02	-0.04	NA	-0.67	0.47
CNAG_02899	hypothetical protein	N/A	-2.02	0.00	-0.49	0.01	-1.12	0.00
CNAG_12559	ncRNA	N/A	-2.00	0.00	-0.74	NA	-1.17	0.09
CNAG_06623	inositol oxygenase	N/A	-1.88	0.00	-0.48	0.00	-1.25	0.00
CNAG_12386	ncRNA	N/A	-1.86	0.00	-0.87	0.00	-0.93	0.00
CNAG_12512	ncRNA	N/A	-1.84	0.01	-0.33	NA	-0.60	0.45
CNAG_12563	ncRNA	N/A	-1.81	0.02	-0.87	NA	-0.86	0.34
CNAG_13071	ncRNA	N/A	-1.79	0.00	-0.46	0.15	-1.03	0.00
CNAG_12557	ncRNA	N/A	-1.77	0.00	-1.44	0.00	-0.64	0.08
CNAG_12847	ncRNA	N/A	-1.76	0.01	-0.21	NA	-1.91	0.02
CNAG_12176	ncRNA	N/A	-1.76	0.00	-0.90	0.00	-0.80	0.00
CNAG_12759	ncRNA	N/A	-1.74	0.05	-1.12	NA	-0.86	0.41

CNAG_06052	galactose-1-phosphate uridylyltransferase	GAL7	-1.72	0.00	-0.30	0.15	-1.11	0.00
CNAG_12211	ncRNA	N/A	-1.70	0.01	-1.19	NA	-1.42	0.05
CNAG_01846	flavoprotein	N/A	-1.68	0.00	-0.50	0.21	-1.20	0.00
CNAG_12347	ncRNA	N/A	-1.67	0.00	-0.78	0.12	-1.42	0.00
CNAG_06518	no prediction	N/A	-1.65	0.00	-0.87	0.01	-0.88	0.01

Table 3.18 continued

Gene ID	Product (Janbon annotation)	Gene Name or Symbol	SRT+FLC 4h Log2 (Fold Change)	SRT+FLC padj	SRT 4h Log2 (Fold Change)	SRT padj	FLC 4h Log2 (Fold Change)	FLC padj
CNAG_07894	hypothetical protein	N/A	-1.65	0.02	-0.54	NA	-0.59	0.46
CNAG_07733	no prediction	N/A	-1.63	0.00	-0.69	0.00	-0.71	0.00
CNAG_03107	hypothetical protein	N/A	-1.63	0.02	-0.19	NA	-1.23	0.11
CNAG_08017	hypothetical protein	N/A	-1.61	0.01	-0.31	NA	-1.09	0.10

Table 3.18. Transcripts down-regulated by SRT+FLC in *C. neoformans* based on RNAseq. Differentially down-regulated *C. neoformans* genes after 4 h incubation with 4 h incubation with the combination of 4 µg/ml SRT+0.25 µg/ml FLC identified by RNA-seq. Only top 25 repressed genes showing a fold of repression of more than 2 fold are represented. Significance cutoff: padj (adjusted p-value) ≤ 0.05.

Gene ID	Product (Janbon annotation)	SRT+FLC 4h Log_2 (Fold Change)	SRT+FLC padj	SRT 4h Log_2 (Fold Change)	SRT padj	FLC 4h Log_2 (Fold Change)	FLC padj
CNAG_04072	60S ribosome subunit biogenesis protein nip7	-1.30	0.00	-0.73	0.00	-0.95	0.00

CNAG_07864	U3 small nucleolar ribonucleoprotein IMP3	-1.24	0.00	-0.52	0.00	-0.73	0.00
CNAG_00819	small subunit ribosomal protein S30	-1.09	0.00	-0.58	0.07	-0.62	0.04
CNAG_01455	large subunit ribosomal protein L39	-1.00	0.00	-0.54	0.00	-0.52	0.01

Table 3.19. continued

Gene ID	**Product (Janbon annotation)**	**SRT+FLC 4h Log2 (Fold Change)**	**SRT+FLC padj**	**SRT 4h Log2 (Fold Change)**	**SRT padj**	**FLC 4h Log2 (Fold Change)**	**FLC padj**
CNAG_06127	ribosome biogenesis protein NSA2	-0.95	0.00	-0.46	0.00	-0.62	0.00
CNAG_01198	small nuclear ribonucleoprotein F	-0.93	0.00	-0.61	0.00	-0.52	0.00
CNAG_04011	large subunit ribosomal protein L37a	-0.92	0.00	-0.54	0.00	-0.45	0.01
CNAG_00232	large subunit ribosomal protein L30e	-0.90	0.00	-0.51	0.00	-0.44	0.01
CNAG_03015	large subunit ribosomal protein L37-A	-0.89	0.00	-0.57	0.05	-0.50	0.09
CNAG_01049	H/ACA ribonucleoprotein complex subunit 3	-0.88	0.00	-0.40	0.01	-0.50	0.00
CNAG_05762	large subunit acidic ribosomal protein P2	-0.88	0.00	-0.56	0.01	-0.57	0.01
CNAG_01300	small subunit ribosomal protein S21e	-0.86	0.00	-0.49	0.00	-0.46	0.00
CNAG_04884	large subunit ribosomal protein L44	-0.85	0.00	-0.58	0.00	-0.48	0.00
CNAG_00771	large subunit ribosomal protein L29	-0.85	0.00	-0.47	0.01	-0.49	0.00

CNAG_02811	small subunit ribosomal protein S29	-0.81	0.00	-0.43	0.00	-0.43	0.00
CNAG_00779	large subunit ribosomal protein L27e	-0.81	0.00	-0.42	0.00	-0.48	0.00
CNAG_02382	ribosome biogenesis protein BRX1	-0.80	0.00	-0.30	0.02	-0.58	0.00

Table 3.19. continued

Gene ID	Product (Janbon annotation)	SRT+FLC 4h Log2 (Fold Change)	SRT+FLC padj	SRT 4h Log2 (Fold Change)	SRT padj	FLC 4h Log2 (Fold Change)	FLC padj
CNAG_02378	H/ACA ribonucleoprotein complex subunit 2	-0.80	0.00	-0.42	0.00	-0.56	0.00
CNAG_03221	large subunit ribosomal protein L29	-0.79	0.00	-0.49	0.00	-0.38	0.00
CNAG_02754	small subunit ribosomal protein S12e	-0.79	0.00	-0.52	0.07	-0.49	0.08

Table 3.19. SRT+FLC down-regulates transcript levels of ribosomal genes in *C. neoformans* based on RNAseq. Differentially down-regulated *C. neoformans* ribosomal genes after 4 h incubation with the combination of 4 μg/ml SRT+0.25 μg/ml FLC identified by RNA-seq. Only top 20 repressed genes showing a fold of repression of more than 1.5 fold are represented. Significance cutoff: padj (adjusted p-value) ≤ 0.05; non-significant padj values are highlighted red.

Gene ID	Product (Janbon annotation)	SRT+FLC 4h Log_2	SRT+FLC padj	SRT 4h Log_2	SRT padj	FLC 4h Log_2	FLC padj

		(Fold Change)		(Fold Change)		(Fold Change)	
CNAG_05455	translation initiation factor eIF-1A	-0.91	0.00	-0.52	0.00	-0.58	0.00
CNAG_06865	translation machinery-associated protein 16	-0.86	0.00	-0.47	0.01	-0.68	0.00
CNAG_02128	translation initiation factor 3 subunit J	-0.58	0.00	-0.39	0.00	-0.30	0.00

Table 3.20. continued

Gene ID	Product (Janbon annotation)	SRT+FLC 4h Log2 (Fold Change)	SRT+FLC padj	SRT 4h Log2 (Fold Change)	SRT padj	FLC 4h Log2 (Fold Change)	FLC padj
CNAG_02656	translation machinery-associated protein 20	-0.57	0.00	-0.33	0.02	-0.36	0.01
CNAG_04628	translation initiation factor 6	-0.56	0.00	-0.26	0.04	-0.33	0.01
CNAG_01428	translation initiation factor 5A	-0.51	0.00	-0.23	0.10	-0.29	0.03
CNAG_03263	translation elongation factor Tu	-0.45	0.00	-0.19	0.16	-0.39	0.00
CNAG_02657	translation initiation factor 3 subunit G	-0.43	0.00	-0.25	0.04	-0.28	0.02
CNAG_01111	translation initiation factor 3 subunit K	-0.43	0.00	-0.17	0.20	-0.33	0.01
CNAG_04054	translation initiation factor SUI1	-0.43	0.00	-0.24	0.01	-0.26	0.00
CNAG_02482	translation machinery-associated protein 22	-0.40	0.00	-0.17	0.15	-0.26	0.01
CNAG_01833	translation initiation factor 4E	-0.38	0.00	-0.07	0.69	-0.32	0.02

CNAG_07778	translation initiation factor 2 subunit 1	-0.38	0.00	-0.14	0.11	-0.29	0.00
CNAG_06563	translation initiation factor 3 subunit F	-0.29	0.01	-0.14	0.32	-0.27	0.04
CNAG_00602	translation initiation factor 3 subunit I	-0.24	0.00	-0.09	0.39	-0.20	0.03
CNAG_00509	translation initiation factor 3 subunit M	-0.23	0.03	-0.18	0.18	-0.22	0.08
CNAG_05366	translation initiation factor 2A	-0.22	0.01	-0.10	0.33	-0.29	0.00

Table 3.20. SRT+FLC down-regulates transcript levels of genes related to the translation machinery in *C. neoformans* based on RNAseq. Differentially down-regulated *C. neoformans* genes related to the translation machinery including initiation factors, after 4 h incubation with the combination of 4 µg/ml SRT+0.25 µg/ml FLC identified by RNA-seq. Corresponding gene expression changes after 4 h incubation with 0.7 µg/ml FLC and 7 µg/ml SRT, provided for comparison. Significance cutoff: padj (adjusted p-value) ≤ 0.05; non-significant padj values are highlighted red.

Gene ID	Product (Janbon annotation)	SRT+FLC 4h Log_2 (Fold Change)	SRT+FLC padj	SRT 4h Log_2 (Fold Change)	SRT padj	FLC 4h Log_2 (Fold Change)	FLC padj
CNAG_13160	ncRNA	-2.02	0.02	-0.04	NA	-0.67	0.47
CNAG_12559	ncRNA	-2.00	0.00	-0.74	NA	-1.17	0.09
CNAG_12512	ncRNA	-1.84	0.01	-0.33	NA	-0.60	0.45
CNAG_12563	ncRNA	-1.81	0.02	-0.87	NA	-0.86	0.34
CNAG_12759	ncRNA	-1.74	0.05	-1.12	NA	-0.86	0.41
CNAG_13086	ncRNA	-1.59	0.00	-0.74	NA	-0.77	0.20

CNAG_12650	ncRNA	-1.58	0.04	-0.36	NA	-0.77	0.39
CNAG_12699	ncRNA	-1.56	0.00	-0.18	0.81	-0.84	0.17
CNAG_12622	ncRNA	-1.53	0.00	-1.30	NA	-0.94	0.11
CNAG_12460	ncRNA	-1.53	0.01	-0.42	0.56	0.03	0.98
CNAG_12850	ncRNA	-1.45	0.02	-0.24	NA	-1.10	0.13
CNAG_12950	ncRNA	-1.45	0.01	-0.48	NA	-0.69	0.30
CNAG_12287	ncRNA	-1.39	0.00	-0.58	0.08	-0.60	0.06
CNAG_13020	ncRNA	-1.36	0.04	-0.32	NA	-1.19	0.12
CNAG_12589	ncRNA	-1.32	0.00	-0.21	0.69	-0.63	0.18
CNAG_12468	ncRNA	-1.24	0.02	-0.48	0.48	-0.65	0.32

Table 3.21. continued

Gene ID	**Product (Janbon annotation)**	**SRT+FLC 4h Log2 (Fold Change)**	**SRT+FLC padj**	**SRT 4h Log2 (Fold Change)**	**SRT padj**	**FLC 4h Log2 (Fold Change)**	**FLC padj**
CNAG_12110	ncRNA	-1.23	0.01	-0.24	0.71	-0.42	0.49
CNAG_12436	ncRNA	-1.22	0.01	-0.77	0.14	-0.50	0.36
CNAG_13176	ncRNA	-1.17	0.02	-1.09	0.07	-0.81	0.17
CNAG_12509	ncRNA	-1.17	0.04	-0.64	NA	-0.19	0.80
CNAG_13180	ncRNA	-1.12	0.00	-0.45	0.27	-0.62	0.11
CNAG_12669	ncRNA	-1.11	0.00	-0.65	0.13	-0.62	0.15
CNAG_12972	ncRNA	-1.09	0.00	-0.22	0.50	-0.50	0.08
CNAG_12043	ncRNA	-1.08	0.04	-0.63	0.32	-0.79	0.20
CNAG_13185	ncRNA	-1.07	0.03	-0.35	0.57	-0.34	0.59
CNAG_13128	ncRNA	-1.07	0.00	-0.46	0.25	-0.50	0.21
CNAG_13070	ncRNA	-1.06	0.00	-0.64	0.06	-0.37	0.31
CNAG_12070	ncRNA	-1.06	0.01	-0.79	0.10	-0.21	0.72
CNAG_12783	ncRNA	-1.04	0.00	-0.61	0.08	-0.28	0.45
CNAG_12683	ncRNA	-1.03	0.01	-0.41	0.41	-0.61	0.20

Table 3.21. SRT+FLC down-regulates transcript levels of of non-coding RNA or ncRNA genes in *C. neoformans* based on RNAseq. Differentially down-regulated *C. neoformans* genes after 4 h incubation with 4 h incubation with the combination of 4 µg/ml SRT+0.25 µg/ml FLC identified by RNA-seq. Only top 30 repressed genes showing a fold of repression of more than 2 fold are represented. Significance cutoff: padj (adjusted p-value) ≤ 0.05.

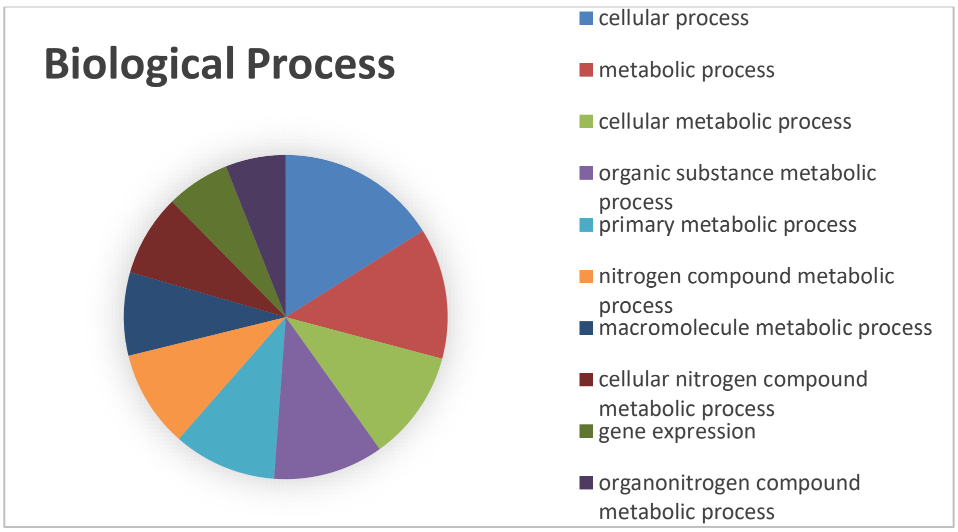

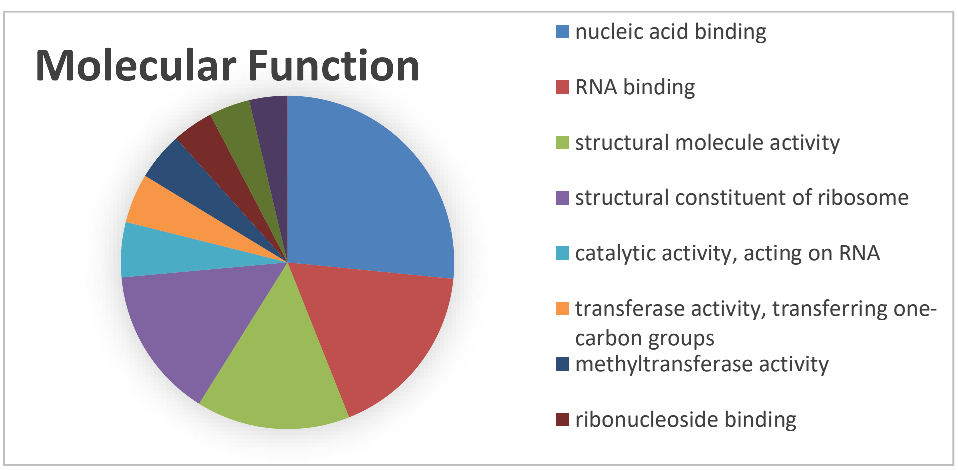

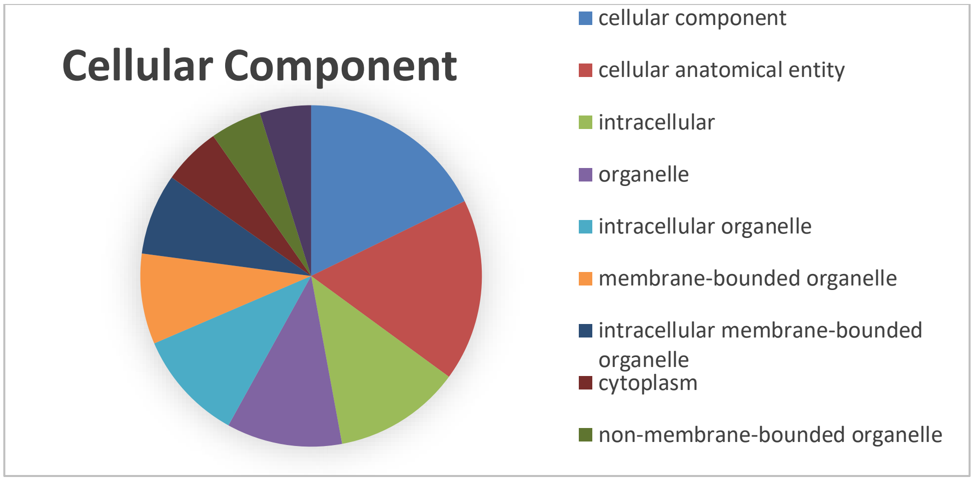

Figure III-12 Functional enrichment of down-regulated transcripts by SRT+FLC combination in *C. neoformans* based on RNAseq. Three Gene Ontology (GO) enrichments namely Biological Process, Molecular Function and Cellular Component are generated for the *C. neoformans* genes down-regulated after SRT treatment, using resources from FungiDB. The top 10 GO categories based solely on the most represented genes with p-value <0.0.1 for each of the branches of enrichment are shown in three different pie charts.

RIBOSOME PROFILING

Since sertraline is known to influence translation, it was of interest to identify transcript levels of genes undergoing the process of translation [4, 66]. Ribo-seq or ribosome profiling is utilized, in order to obtain a snapshot of ribosome occupied mRNAs or in other words ribosomal footprints, leading to the determination of the translational status of these genes. Therefore ribo-seq was performed on *C. neoformans* treated with 7 μg/ml SRT, 0.7 μg/ml FLC, or 4 μg/ml SRT and 0.25 μg/ml FLC in combination, and DMSO as vehicle control for each of the time points of 1,2 and 4 h using the protocol mentioned in the Material and Methods chapter as adapted from [116] . The time course is chosen to capture translational landscape at earlier generation time points considering 4h as the approximate doubling time. Thus 1/4th or 1 h, half or 2h and one generation or 4h were selected respectively. The cells used were independently grown in the above conditions and do not belong to the same matched sample from which the 4h RNA-seq was performed. Nevertheless, the ribo-seq provides a basic conceptual translational information. When compared to the unmatched RNA-seq we can identify some consistent pattern of gene expression manifested under respective drug treatments but cannot distinguish if more reads in ribo-seq correspond to more steady state transcripts available for ribosome loading or if transcripts are getting differentially translated. The analyses on the 4h experimental samples of ribo-seq are discussed before other time points. As a whole ribo-seq analysis yielded much lower read counts overall and the numbers of differentially expressed genes are considerably lower across all the treatments.

Genes up-regulated by FLC in ribo-seq

68 genes identified by ribo-seq were significantly up-regulated in *C. neoformans* after 4h incubation with 0.7 μg/ml FLC compared to DMSO treated cells at a significance cutoff of padj (adjusted p-value) ≤ 0.05 padj (Supplementary Table 15). Out of these, 51 genes exhibit a 1.5 fold change or greater. By relaxing the significance stringency to padj ≤ 0.1, we could identify 92 genes and of which 63 had a 1.5 fold change or greater. Many genes of the ergosterol biosynthetic pathway including the established FLC target gene *ERG11* and *SRE1* were significantly induced under these conditions (Table 3.22). Most of the *ERG* genes that were induced at higher fold change in RNA-seq maintained a similar trend in the ribo-seq data. The heatmap in Fig 3.13 demonstrates the ergosterol biosynthetic pathway gene expression levels identified in both RNA-seq and ribo-seq at 4h drug treatments. Thus, consistent with the literature, FLC targets *ERG* genes as supported by our RNA-seq and ribo-seq results.

Gene ID	**Product (Janbon annotation)**	**Gene Name or Symbol**	**FLC 4h Log2 (Fold Change)**	**FLC 4h padj**	**SRT 4h Log2 (Fold Change)**	**SRT 4h padj**	**SRT+FLC 4h Log2 (Fold Change)**	**SRT+ FLC 4h padj**
CNAG_02918	Acetyl-CoA C-acetyltransferase	ERG10	2.09	0.00	1.19	0.00	0.66	0.02

CNAG_03311	3-hydroxy-3-methylglutaryl-CoA (HMG-CoA) synthase	ERG13	1.24	0.00	0.42	0.09	0.12	0.80
CNAG_02896	3-hydroxy-3-methylglutaryl-CoA (HMG-CoA) synthase	ERG130	2.49	0.00	1.38	0.00	1.11	0.00
CNAG_06534	hydroxymethylglutaryl-CoA reductase (NADPH)	HMG1	1.08	0.00	0.26	0.52	-0.16	0.76
CNAG_06535	hydroxymethylglutaryl-CoA reductase (NADPH)	HMG2	0.32	0.62	-0.26	0.72	0.38	0.53
CNAG_06001	phosphomevalonate kinase	ERG8	0.69	0.36	0.18	0.88	0.27	NA
CNAG_05125	Diphosphomevalonate decarboxylase	ERG19/MVD1	0.36	0.44	0.17	0.79	0.31	0.57
CNAG_00265	isopentenyl-diphosphate delta-isomerase	IDI1	0.29	0.55	0.28	0.57	0.37	0.43
CNAG_02084	farnesyl diphosphate synthase	ERG20	0.88	0.00	0.70	0.00	0.69	0.00
CNAG_07510	farnesyl-diphosphate farnesyltransferase	ERG9	0.43	0.13	0.12	0.81	0.08	0.89
CNAG_06829	Squalene monooxygenase	ERG1	0.58	0.17	0.06	0.94	0.10	0.91
CNAG_01129	lanosterol synthase	ERG7	1.07	0.00	0.72	0.07	0.47	0.44

Table 3.22. continued

Gene ID	**Product (Janbon annotation)**	**Gene Name or Symbol**	**FLC 4h Log2 (Fold Change)**	**FLC 4h padj**	**SRT 4h Log2 (Fold Change)**	**SRT 4h padj**	**SRT+FLC 4h Log2 (Fold Change)**	**SRT+ FLC 4h padj**

CNAG_00040	cytochrome P450, family 51 (sterol 14-demethylase)	ERG11	1.36	0.00	0.46	0.10	0.51	0.08
CNAG_00117	c-14 sterol reductase	ERG24	0.83	0.00	-0.01	0.99	0.07	0.93
CNAG_01737	C-4 methyl sterol oxidase, putative	ERG25	2.05	0.00	0.68	0.00	1.26	0.00
CNAG_04605	C-3 sterol dehydrogenase	ERG26	0.55	0.05	0.08	0.89	0.26	0.58
CNAG_07437	3-keto sterol reductase	ERG27	-0.99	NA	-0.32	0.75	-0.25	NA
CNAG_03009	putative ER membrane protein	ERG28	-0.44	0.58	-0.24	0.80	-0.02	NA
CNAG_03819	sterol 24-C-methyltransferase	ERG6	1.39	0.00	0.38	0.17	0.93	0.00
CNAG_00854	C-8 sterol isomerase	ERG2	1.94	0.00	0.62	0.05	0.57	0.15
CNAG_00519	lathosterol oxidase	ERG3	2.75	0.00	1.55	0.00	1.40	0.00
CNAG_06644	C-22 sterol desaturase	ERG5	1.83	0.00	0.72	0.00	0.72	0.00
CNAG_02830	delta24(24(1))-sterol reductase	ERG4	1.65	0.00	0.57	0.01	0.74	0.00
CNAG_04804	hypothetical protein	SRE1	2.97	0.00	1.15	0.00	1.17	0.01
CNAG_01003	NADPH-ferrihemoprotein reductase	NCP1	0.82	0.00	0.35	0.29	-0.05	0.95

Table 3.22. FLC up-regulates ergosterol biosynthesis genes in *C. neoformans* based on ribo-seq. *C. neoformans* genes involved in the ergosterol biosynthesis pathway and its regulation, after 4 h incubation with 0.7 μg/ml FLC identified by ribo-seq. Genes are ordered according to their sequence of action in the biosynthetic pathway. Corresponding gene expression changes after 4 h incubation with 7 μg/ml SRT and the

combination of 4 μg/ml SRT+0.25 μg/ml FLC, provided for comparison. Significance cutoff: padj (adjusted p-value) ≤ 0.05; non-significant padj values are highlighted red.

Gene ID	Product (Janbon annotation)	Gene Name or Symbol	RNAseq 4h Log_2 (Fold Change)			Riboseq 4h Log2 (Fold Change)		
			FLC	SRT	SRT + FLC	FLC	SRT	SRT + FLC
CNAG_02918	Acetyl-CoA C-acetyltransferase	ERG10						
CNAG_03311	3-hydroxy-3-methylglutaryl-CoA (HMG-CoA) synthase	ERG13						
CNAG_02896	3-hydroxy-3-methylglutaryl-CoA (HMG-CoA) synthase	ERG130						
CNAG_06534	hydroxymethylglutaryl-CoA reductase (NADPH)	HMG1						
CNAG_06535	hydroxymethylglutaryl-CoA reductase (NADPH)	HMG2						
CNAG_06001	phosphomevalonate kinase	ERG8						
CNAG_05125	Diphosphomevalonate decarboxylase	ERG19						
CNAG_00265	isopentenyl-diphosphate delta-isomerase	IDI1						
CNAG_02084	farnesyl diphosphate synthase	ERG20						
CNAG_07510	farnesyl-diphosphate farnesyltransferase	ERG9						
CNAG_06829	Squalene monooxygenase	ERG1						
CNAG_01129	lanosterol synthase	ERG7						

Fig. 3.13. continued

	RNAseq 4h Log_2 (Fold Change)	Riboseq 4h Log2 (Fold Change)

Gene ID	Product (Janbon annotation)	Gene Name or Symbol	FLC	SRT	SRT + FLC	FLC	SRT	SRT + FLC
CNAG_00040	cytochrome P450, family 51 (sterol 14-demethylase)	ERG11						
CNAG_00117	c-14 sterol reductase	ERG24						
CNAG_01737	C-4 methyl sterol oxidase, putative	ERG25						
CNAG_04605	C-3 sterol dehydrogenase	ERG26						
CNAG_07437	3-keto sterol reductase	ERG27						
CNAG_03009	putative ER membrane protein	ERG28						
CNAG_03819	sterol 24-C-methyltransferase	ERG6						
CNAG_00854	C-8 sterol isomerase	ERG2						
CNAG_00519	lathosterol oxidase	ERG3						
CNAG_06644	C-22 sterol desaturase	ERG5						
CNAG_02830	delta24(24(1))-sterol reductase	ERG4						
CNAG_04804	hypothetical protein	SRE1						
CNAG_01003	NADPH-ferrihemoprotein reductase	NCP1						

Fig 3.13. Heatmap of ergosterol biosynthetic pathway gene expression in *C. neoformans* identified by RNA-seq and ribo-seq. Genes are ordered according to their sequence of action in the biosynthetic pathway. Color scale represent log2 fold changes for genes after different drug treatments, with padj (adjusted p-value) < 0.05 as significance cutoff. Color bar on top right provides the range of log2 fold values corresponding to the colors. Non-significant values are left white and not color coded.

Genes down-regulated by FLC in ribo-seq

37 genes identified by ribo-seq were significantly up-regulated in *C. neoformans* after 4h incubation with 0.7 μg/ml FLC compared to DMSO treated cells at a significance cutoff of padj (adjusted p-value) ≤ 0.05 padj (Supplementary Table 16). Out of these, 30 genes exhibit a 1.5 fold repression or greater. By relaxing the significance stringency to padj ≤ 0.1, we could identify 51 genes and of which 37 had a 1.5 fold change or greater. Few ribosomal subunit genes were identified in this list which was a class of genes that were highly repressed by FLC treatment in the 4h RNA-seq analyses. However, there were no appreciable overlap with the genes identified by RNA-seq under similar conditions. The overall lower numbers of significant genes that were identified by ribo-seq compared to RNA-seq and the fact that these sequencing libraries were generated under similar growth conditions but from separate cell cultures, could be a possible explanation for these results.

Genes up-regulated by SRT in ribo-seq

92 genes identified by ribo-seq were significantly up-regulated in *C. neoformans* after 4h incubation with 7 μg/ml SRT compared to DMSO treated cells at a significance cutoff of padj (adjusted p-value) ≤ 0.05 padj (Supplementary Table 17). Out of these, 68 genes exhibit a 1.5 fold change or greater. Top 25 differentially expressed genes from this list of 68 are illustrated in Table 3.23. By relaxing the significance stringency to padj ≤ 0.1, we could identify 120 genes and of which 87 showed a 1.5 fold change or greater. Several *ERG* genes including *ERG3, ERG130, ERG10, ERG5, ERG20, ERG25, ERG2* and *ERG4* were identified to be induced at a significance cutoff of padj ≤ 0.05. Few genes encoding membrane protein and transporters and kinases were found to be

overlapping with the RNA-seq data from SRT treatment. Though the overlaps between genes upregulated by SRT in ribo-seq compared to RNA-seq are not huge due to reasons discussed earlier, but some expression patterns were appreciably well-maintained. For example, gene *CNAG_01953*, the putative MFS transporter and *FZC46* (CNAG_03115), the gene containing the *UPC2* transcription factor domain, mentioned earlier in the RNA-seq section also presents as the most induced gene in the riboseq data for 4h SRT treatment. Other membrane proteins induced by SRT in both ribo-seq and RNA-seq include genes *CNAG_03732*, *CNAG_03764* and *CNAG_02299*, the latter though not annotated but has sequence similarity with *CNAG_01953* and is a potential paralog. Also genes related to ergosterol biosynthesis such as *ERG3*, *ERG10*, *ERG13*, *ERG20*, *ERG25*, *ERG4* and *SRE1* were induced in both ribo-seq and RNA-seq data for SRT treatment. However, for ergosterol biosynthetic genes, SRT exerts partial influence or to a lesser extent compared to FLC because not all *ERG* genes altered by FLC were identified to be differentially expressed by SRT at the significance cutoffs used. Additionally, the membrane related genes that were SRT specific targets are distinct and not common between the set of genes targeted by SRT and FLC.

Gene ID	**Product**	**Gene Name**	**SRT 4h Log2**	**SRT 4h padj**	**FLC 4h Log2**	**FLC 4h padj**	**SRT+FLC 4h Log2**	**SRT+FLC 4h padj**

		or symbol	(Fold Change)		(Fold Change)		(Fold Change)	
CNAG_01953	**hypothetical protein**	N/A	5.97	0.00	-1.13	0.38	5.20	0.00
CNAG_05075	solute carrier family 20 (sodium-dependent phosphate transporter)	N/A	4.60	0.01	5.72	0.00	5.98	0.00
CNAG_03764	**integral membrane protein**	N/A	4.53	0.00	-2.40	NA	2.14	NA
CNAG_06817	NCS2 family nucleobase:cation symporter-2	UAP1	4.14	0.00	1.68	0.13	-0.12	0.97
CNAG_04632	uracil permease	N/A	3.79	0.00	1.76	0.18	1.04	0.53
CNAG_03732	**integral membrane protein**	N/A	3.64	0.00	0.20	0.92	1.59	0.09
CNAG_07448	urea transporter	DUR3	2.22	0.04	1.63	0.20	-0.67	0.70
CNAG_02777	**phosphate:H symporter**	**PHO84**	2.12	0.00	1.83	0.00	0.80	0.20
CNAG_02768	hypothetical protein	N/A	2.08	0.00	0.10	0.96	1.52	NA
CNAG_02225	glucan 1%2C3-beta-glucosidase	EXG104	2.00	0.05	3.01	NA	1.57	NA
CNAG_03115	**hypothetical protein**	**FZC46**	1.84	0.00	-0.01	0.99	0.76	0.32
CNAG_01865	hypothetical protein	N/A	1.71	0.00	0.78	NA	0.53	NA
CNAG_00519	**lathosterol oxidase**	**ERG3**	1.55	0.00	2.75	0.00	1.40	0.00
CNAG_02299	**hypothetical protein**	N/A	1.53	0.00	0.11	0.92	0.85	0.12
CNAG_04186	hypothetical protein	N/A	1.52	0.03	1.14	NA	0.20	NA
CNAG_01946	allantoate permease	N/A	1.40	0.03	-0.65	0.57	-1.25	NA
CNAG_02896	**hydroxymethylglutaryl-CoA synthase**	**ERG130**	1.38	0.00	2.49	0.00	1.11	0.00
CNAG_04730	hypothetical protein	GPR4	1.36	0.05	1.03	0.25	0.74	NA
CNAG_03007	hypothetical protein	N/A	1.32	0.04	-0.73	0.46	-0.90	0.37

Table 3.23. continued

Gene ID	Product	Gene Name or symbol	SRT 4h Log2 (Fold Change)	SRT 4h padj	FLC 4h Log2 (Fold Change)	FLC 4h padj	SRT+FLC 4h Log2 (Fold Change)	SRT+FLC 4h padj
CNAG_03114	hypothetical protein	N/A	1.29	0.00	0.54	0.34	1.13	0.00
CNAG_05411	endoglucanase	LPI9	1.24	0.00	0.39	0.58	0.55	0.40
CNAG_03347	ATP-dependent Clp protease ATP-binding subunit ClpB	N/A	1.24	0.00	0.55	0.20	-0.31	0.66
CNAG_05913	alpha-glucosidase	N/A	1.22	0.01	0.08	NA	-1.15	NA
CNAG_02852	4-aminobutyrate transaminase	N/A	1.21	0.00	0.11	0.92	1.20	0.01
CNAG_07745	alcohol dehydrogenase%2C propanol-preferring	MPD1	1.21	0.00	0.39	0.63	0.85	0.14

Table 3.23. SRT up-regulates transcript levels of genes in *C. neoformans* based on ribo-seq. *C. neoformans* genes identified by ribo-seq after 4 h incubation with 7 μg/ml SRT. Corresponding gene expression changes after 4 h incubation with 0.7 μg/ml FLC and the combination of 4 μg/ml SRT+0.25 μg/ml FLC, provided for comparison. Genes that were also upregulated by SRT in RNA-seq are bolded. Significance cutoff: padj (adjusted p-value) ≤ 0.05.

Genes down-regulated by SRT in ribo-seq

57 genes identified by ribo-seq were significantly up-regulated in *C. neoformans* after 4h incubation with 7 μg/ml SRT compared to DMSO treated cells at a significance cutoff of padj (adjusted p-value) ≤ 0.05 padj (Supplementary Table 18). Out of these, 42 genes

exhibit a 1.5 fold repression or greater. By relaxing the significance stringency to padj ≤ 0.1, we could identify 96 genes and of which 65 had a 1.5 fold change or greater. Two ribosomal subunit genes were identified in this list which was a class of genes that were highly repressed by SRT treatment in the 4h RNA-seq analyses. However, there were no appreciable overlap with most of the genes identified by the respective RNA-seq data.

Genes up-regulated by SRT+FLC in ribo-seq

93 genes identified by ribo-seq were significantly up-regulated in *C. neoformans* after 4h incubation with the combination of 4 μg/ml SRT+0.25 μg/ml FLC compared to DMSO treated cells at a significance cutoff of padj (adjusted p-value) ≤ 0.05 (Supplementary Table 19). Out of these, 71 genes exhibit a 1.5 fold change or greater. By relaxing the significance stringency to padj ≤ 0.1, we could identify 129 genes and of which 91 showed a 1.5 fold change or greater. Several *ERG* genes, membrane proteins and metabolic enzymes were induced. Comparing with the RNAseq data on SRT+FLC treatment, genes from the ergosterol related pathway such as *SRE1*, *ERG3*, *ERG25* and *ERG130* and membrane protein encoding genes *CNAG_01953* and *CNAG_03732* overlap with the ribo-seq data.

Some of these genes are shared by individual drug treatments identified by ribo-seq, hinting at genes that could be drug specific targets. Table 3.24 illustrates the set of induced genes identified by ribo-seq that are shared between FLC and SRT+FLC treatment. As expected from the analyses so far, *ERG* genes are mostly represented in this list. Most of these *ERG* genes are also significantly upregulated by SRT ribo-seq treatment showing a concerted mechanism of drug activity with common target genes. However, genes such as *ERG6*, genes encoding cytochrome b5 reductase, histone H3 and metallo-beta-lactamase were specific to FLC from this data. Similarly, up-regulated genes shared between SRT and SRT+FLC treatments in the ribo-seq data are shown in Table 3.25. This list includes gene *CNAG_01953*, genes encoding NAD synthase and trehalose synthase which were SRT specific.

Another important information that was extracted from Supplementary table 19 was those genes that are uniquely upregulated by SRT+FLC from the ribo-seq data and are not significantly altered by either drug when used alone. Out of 61 genes unique to SRT+FLC at a significance cutoff padj ≤ 0.05, 46 are induced at 1.5 fold change or greater. Table 3.26 illustrates top 25 candidates from the list of genes uniquely regulated by SRT+FLC treatment.

Gene ID	**Product**	**Gene Name or Symbol**	**SRT+FLC 4h Log2 (Fold Change)**	**SRT+FLC 4h padj**	**FLC 4h Log2 (Fold Change)**	**FLC 4h padj**	**SRT 4h Log2 (Fold Change)**	**SRT 4h padj**
CNAG_05075	solute carrier family 20 (sodium-dependent phosphate transporter)	N/A	5.98	0.00	5.72	0.00	4.60	0.01
CNAG_00519	lathosterol oxidase	ERG3	1.40	0.00	2.75	0.00	1.55	0.00
CNAG_01669	metallo-beta-lactamase	N/A	1.27	0.04	1.29	0.02	0.90	0.16
CNAG_01737	methylsterol monooxygenase	ERG25	1.26	0.00	2.05	0.00	0.68	0.00

Table 3.24. continued

Gene ID	Product	Gene Name or Symbol	SRT+FLC 4h Log2 (Fold Change)	SRT+FLC 4h padj	FLC 4h Log2 (Fold Change)	FLC 4h padj	SRT 4h Log2 (Fold Change)	SRT 4h padj
CNAG_04804	hypothetical protein	SRE1	1.17	0.01	2.97	0.00	1.15	0.00
CNAG_02896	hydroxymethylglutaryl-CoA synthase	ERG130	1.11	0.00	2.49	0.00	1.38	0.00
CNAG_03819	sterol 24-C-methyltransferase	ERG6	0.93	0.00	1.39	0.00	0.38	0.17
CNAG_05462	cytochrome b5 reductase	N/A	0.88	0.00	0.65	0.00	0.04	0.95
CNAG_06745	histone H3	H3	0.77	0.03	0.84	0.01	0.41	0.42
CNAG_02830	delta24(24(1))-sterol reductase	ERG4	0.74	0.00	1.65	0.00	0.57	0.01
CNAG_06644	C-22 sterol desaturase	ERG5	0.72	0.00	1.83	0.00	0.72	0.00
CNAG_05847	thioredoxin reductase	TRR1	0.69	0.00	1.08	0.00	0.95	0.00
CNAG_02084	farnesyl diphosphate synthase	ERG20	0.69	0.00	0.88	0.00	0.70	0.00
CNAG_02918	acetyl-CoA C-acetyltransferase	ERG10	0.66	0.02	2.09	0.00	1.19	0.00
CNAG_06377	solute carrier family 25 (mitochondrial phosphate transporter)%2C member 3	N/A	0.55	0.00	0.31	0.01	0.26	0.05
CNAG_03677	hypothetical protein	N/A	0.54	0.02	0.52	0.01	0.24	0.48
CNAG_03358	phosphoglycerate kinase	N/A	0.40	0.04	0.39	0.05	0.32	0.13

Table 3.24. ***C. neoformans*** **transcripts upregulated by both SRT+FLC and FLC based on ribo-seq.** Differentially up-regulated *C. neoformans* genes shared between 4h treatments with 0.7 μg/ml FLC and with the combination of 4 μg/ml SRT+0.25 μg/ml FLC identified by ribo-seq. Corresponding gene expression changes after 4h incubation with 7 μg/ml SRT provided for comparison. Significance cutoff: padj (adjusted p-value) ≤ 0.05; non-significant padj values are highlighted red.

Gene ID	Product	Gene Name or Symbol	SRT+FLC 4h Log2 (Fold Change)	SRT+FLC 4h padj	SRT 4h Log2 (Fold Change)	SRT 4h padj	FLC 4h Log2 (Fold Change)	FLC 4h padj
CNAG_05075	solute carrier family 20 (sodium-dependent phosphate transporter)	N/A	5.98	0.00	4.60	0.01	5.72	0.00
CNAG_01953	hypothetical protein	N/A	5.20	0.00	5.97	0.00	-1.13	0.38
CNAG_01949	chlorophyll synthesis pathway protein BchC	N/A	1.50	0.00	1.15	0.01	-2.20	0.00
CNAG_00519	lathosterol oxidase	ERG3	1.40	0.00	1.55	0.00	2.75	0.00
CNAG_01737	methylsterol monooxygenase	ERG25	1.26	0.00	0.68	0.00	2.05	0.00
CNAG_02852	4-aminobutyrate transaminase	N/A	1.20	0.01	1.21	0.00	0.11	0.92
CNAG_04804	hypothetical protein	SRE1	1.17	0.01	1.15	0.00	2.97	0.00
CNAG_03114	hypothetical protein	N/A	1.13	0.00	1.29	0.00	0.54	0.34
CNAG_02896	hydroxymethylglutaryl-CoA synthase	ERG130	1.11	0.00	1.38	0.00	2.49	0.00
CNAG_04269	leucyl aminopeptidase	N/A	0.85	0.04	0.88	0.01	0.60	0.19
CNAG_01912	NAD synthetase	N/A	0.85	0.00	0.88	0.00	0.10	0.87
CNAG_03113	trehalose synthase	N/A	0.75	0.02	0.94	0.00	0.41	0.36
CNAG_02830	delta24(24(1))-sterol reductase	ERG4	0.74	0.00	0.57	0.01	1.65	0.00
CNAG_03486	peptidyl-prolyl cis-trans isomerase B	N/A	0.73	0.00	0.49	0.04	0.28	0.39
CNAG_06644	C-22 sterol desaturase	ERG5	0.72	0.00	0.72	0.00	1.83	0.00

Table 3.25. continued

Gene ID	Product	Gene Name or Symbol	SRT+FLC 4h Log2 (Fold Change)	SRT+FLC 4h padj	SRT 4h Log2 (Fold Change)	SRT 4h padj	FLC 4h Log2 (Fold Change)	FLC 4h padj
CNAG_02084	farnesyl diphosphate synthase	ERG20	0.69	0.00	0.70	0.00	0.88	0.00
CNAG_02918	acetyl-CoA C-acetyltransferase	ERG10	0.66	0.02	1.19	0.00	2.09	0.00
CNAG_07851	isocitrate dehydrogenase%2C NAD-dependent	N/A	0.62	0.02	0.76	0.00	0.15	0.78
CNAG_01019	superoxide dismutase [Cu-Zn]	SOD1	0.61	0.00	0.52	0.00	-0.02	0.96
CNAG_06377	solute carrier family 25 (mitochondrial phosphate transporter)%2C member 3	N/A	0.55	0.00	0.26	0.05	0.31	0.01
CNAG_03225	malate dehydrogenase%2C NAD-dependent	N/A	0.51	0.01	0.54	0.00	0.37	0.12
CNAG_01984	transaldolase	TAL1	0.41	0.00	0.56	0.00	0.25	0.14
CNAG_03765	trehalose-phosphatase	TPS2	0.39	0.04	0.44	0.01	0.30	0.15

Table 3.25. ***C. neoformans* transcripts upregulated by both SRT+FLC and SRT based on ribo-seq.** Differentially up-regulated *C. neoformans* genes shared between 4h treatments with 7 µg/ml SRT and with the combination of 4 µg/ml SRT+0.25 µg/ml FLC identified by ribo-seq. Corresponding gene expression changes after 4h incubation

with 0.7 μg/ml FLC provided for comparison. Significance cutoff: padj (adjusted p-value) ≤ 0.05; non-significant padj values are highlighted red.

Gene ID	**Product**	**Gene Name**	**SRT+FLC 4h Log2 (Fold Change)**	**SRT+FLC 4h padj**	**SRT 4h Log2 (Fold Change)**	**SRT 4h padj**	**FLC 4h Log2 (Fold Change)**	**FLC 4h padj**
CNAG_03759	conidiation-specific protein 6	N/A	2.26	0.01	0.67	0.69	-1.32	0.32
CNAG_03002	hypothetical protein	N/A	2.08	0.03	1.38	0.27	1.38	0.26
CNAG_01743	hypothetical protein	N/A	2.03	0.00	0.76	0.20	-0.02	0.99
CNAG_01272	hypothetical protein	N/A	1.85	0.00	-0.12	0.87	-0.65	0.10
CNAG_03492	hypothetical protein	N/A	1.72	0.00	0.28	0.81	-0.33	0.76
CNAG_04206	hypothetical protein	N/A	1.72	0.00	0.59	0.34	0.11	0.92
CNAG_01093	hypothetical protein	N/A	1.46	0.01	-0.20	0.88	-0.72	0.39
CNAG_00485	hypothetical protein	N/A	1.40	0.00	0.11	0.92	0.32	0.73
CNAG_01446	hypothetical protein	HSP12	1.36	0.00	0.15	0.90	0.13	0.91
CNAG_05458	endo-1%2C3(4)-beta-glucanase	N/A	1.26	0.00	0.64	0.22	0.68	0.19
CNAG_06576	allergen	CAR1	1.21	0.00	-0.05	0.96	-0.05	0.96
CNAG_06347	hypothetical protein	BLP2	1.20	0.00	-0.24	0.43	0.12	0.77
CNAG_05994	multidrug transporter	N/A	1.20	0.01	0.04	0.97	0.31	0.76
CNAG_01751	hypothetical protein	N/A	1.14	0.02	0.80	0.17	0.63	0.36
CNAG_02226	hypothetical protein	N/A	1.14	0.05	0.35	0.72	0.24	0.84
CNAG_03566	hypothetical protein	N/A	1.14	0.01	0.02	0.98	0.00	1.00
CNAG_06346	hypothetical protein	BLP1	1.13	0.01	-0.03	0.97	-0.62	0.30
CNAG_00057	fructose-1%2C6-bisphosphatase I	FPP1	1.11	0.00	0.31	0.55	0.63	0.07
CNAG_01348	cyanate hydratase	N/A	1.08	0.00	0.21	0.74	0.47	0.26
CNAG_00605	cytoplasmic protein	N/A	1.08	0.00	0.18	0.78	0.18	0.78

Table 3.26. continued

Gene ID	Product	Gene Name	SRT+FLC 4h Log2 (Fold Change)	SRT+FLC 4h padj	SRT 4h Log2 (Fold Change)	SRT 4h padj	FLC 4h Log2 (Fold Change)	FLC 4h padj
CNAG_02925	d-arabinitol 2-dehydrogenase	N/A	1.05	0.04	-0.10	0.93	0.20	0.85
CNAG_02422	hypothetical protein	N/A	1.03	0.05	0.05	0.97	-0.42	0.63
CNAG_07519	hypothetical protein	N/A	0.98	0.00	0.31	0.38	0.35	0.31
CNAG_01558	chlorophyll synthesis pathway protein BchC	N/A	0.97	0.00	0.33	0.53	-0.17	0.79
CNAG_06759	dehydrogenase	LPI1	0.95	0.02	-0.02	0.98	-0.49	0.43

Table 3.26. SRT+FLC combination treatment up-regulates transcript levels of a unique set of genes in *C. neoformans* based on ribo-seq. Top 25 representative genes up-regulated in *C. neoformans* after 4 h incubation with of 4 µg/ml SRT+0.25 µg/ml FLC identified by ribo-seq which are not differentially expressed at significant levels by either treatment of SRT or FLC alone. Corresponding gene expression changes after 4h incubation with 7 µg/ml SRT and 0.7 µg/ml FLC, provided for comparison. Significance cutoff: padj (adjusted p-value) ≤ 0.05; non-significant padj values are highlighted red.

Genes down-regulated by SRT+FLC in ribo-seq

45 genes identified by ribo-seq were significantly up-regulated in *C. neoformans* after 4h with the combination of 4 µg/ml SRT+0.25 µg/ml FLC compared to DMSO treated cells at a significance cutoff of padj (adjusted p-value) ≤ 0.05 (Supplementary Table 20). Out

of these, 41 genes exhibit a 1.5 fold repression or greater. By relaxing the significance stringency to padj ≤ 0.1, we could identify 72 genes and of which 60 had a 1.5 fold change or greater. When compared to 4h RNA-seq data for SRT+FLC treatment, no significant overlap was identified.

Interestingly, several genes were recognized to be uniquely down-regulated by SRT+FLC and were not significantly altered by either drug when used alone (Supplementary Table 20). Out of 35 genes unique to SRT+FLC at a significance cutoff padj ≤ 0.05, 33 are induced at 1.5 fold change or greater. Table 3.27 illustrates top 25 candidates from the list of genes uniquely regulated at the level of translation by SRT+FLC combination.

Gene ID	**Product**	**Gene Name or Symbol**	**SRT+FLC 4h Log2 (Fold Change)**	**SRT+FLC 4h padj**	**SRT 4h Log2 (Fold Change)**	**SRT 4h padj**	**FLC 4h Log2 (Fold Change)**	**FLC 4h padj**
CNAG_04245	chitinase	CHI22	-2.92	0.00	-0.19	0.78	0.09	0.91
CNAG_04183	hypothetical protein	N/A	-2.40	0.00	-0.16	0.84	0.04	0.96
CNAG_06205	hypothetical protein	BLP3	-2.03	0.00	0.00	1.00	0.12	0.89
CNAG_13008	#N/A	N/A	-2.00	0.03	-1.49	0.09	-0.02	0.99
CNAG_00311	3-hydroxyisobutyryl-CoA hydrolase	N/A	-1.95	0.01	-0.64	0.66	-0.46	0.77
CNAG_00442	cyclin	N/A	-1.69	0.00	0.14	0.88	0.25	0.76
CNAG_03716	hypothetical protein	BLP6	-1.67	0.02	0.12	0.91	0.73	0.20
CNAG_02850	glucan endo-1%2C3-alpha-glucosidase agn1	N/A	-1.56	0.00	-0.04	0.94	0.26	0.46
CNAG_01907	PLK/PLK1 protein kinase	N/A	-1.43	0.00	-0.32	0.60	-0.18	0.81

Table 3.27. continued

Gene ID	Product	Gene Name or Symbol	SRT+FLC 4h Log2 (Fold Change)	SRT+FLC 4h padj	SRT 4h Log2 (Fold Change)	SRT 4h padj	FLC 4h Log2 (Fold Change)	FLC 4h padj
CNAG_06104	hypothetical protein	N/A	-1.36	0.01	-0.34	0.62	-0.27	0.73
CNAG_07463	separase	N/A	-1.26	0.00	-0.19	0.75	0.11	0.88
CNAG_05522	hypothetical protein	N/A	-1.21	0.01	-0.51	0.34	-0.13	0.88
CNAG_04149	nuclear pore complex protein Nup107	N/A	-1.19	0.01	-0.25	0.68	-0.29	0.63
CNAG_03715	hypothetical protein	N/A	-1.19	0.04	-0.04	0.97	0.05	0.96
CNAG_04788	hypothetical protein	N/A	-1.13	0.03	-0.24	0.75	-0.12	0.90
CNAG_04227	hypothetical protein	N/A	-1.07	0.01	-0.35	0.53	0.04	0.96
CNAG_01938	CAMK/CAMKL/Kin1 protein kinase	KIN1	-1.04	0.01	-0.06	0.92	-0.18	0.76
CNAG_05724	hypothetical protein	N/A	-1.00	0.03	-0.44	0.35	-0.55	0.23
CNAG_00250	hypothetical protein	N/A	-0.96	0.02	0.02	0.98	0.45	0.27
CNAG_04224	carboxy-terminal domain RNA polymerase II polypeptide A small phosphatase	PSR1	-0.94	0.03	-0.61	0.10	-0.56	0.20
CNAG_00919	carboxypeptidase D	N/A	-0.92	0.04	0.51	0.34	0.41	0.49
CNAG_01334	hypothetical protein	N/A	-0.91	0.01	-0.38	0.32	0.01	0.98
CNAG_06487	chitin synthase	CHS6	-0.88	0.02	-0.03	0.97	-0.02	0.97
CNAG_02675	CAMK/CAMKL/GIN4 protein kinase	HSL101	-0.85	0.00	0.05	0.92	0.01	0.99

Table 3.27. SRT+FLC combination treatment down-regulates transcript levels of a unique set of genes in *C. neoformans* based on ribo-seq. Top 25 representative genes udown-regulated in *C. neoformans* after 4 h incubation with of 4 µg/ml SRT+0.25 µg/ml

FLC identified by ribo-seq which are not differentially expressed at significant levels by either treatment of SRT or FLC alone. Corresponding gene expression changes after 4h incubation with 7 μg/ml SRT and 0.7 μg/ml FLC, provided for comparison. Significance cutoff: padj (adjusted p-value) ≤ 0.05; non-significant padj values are highlighted red.

Venn-diagrams based on drug treatment

To present an overall picture of the altered gene expression, Venn diagrams are used to have a compact understanding of the complex data comprising of different drug treatments at different time points. Venn-diagrams are constructed to combine all the three time points for each treatment of SRT, FLC and SRT+FLC. Every set is comprised of the differentially expressed genes based on ribo-seq reads from a specific treatment at a specific time point, as compared to the respective DMSO control. Genes in each list are extracted with the following parameters: log fold change Threshold = 0, p-value < 0.01, padj < 0.1 as a significance cut off, to be able to identify greater gene candidates with altered expression based on riboseq.

FLC treatment time course

After riboseq on *C. neoformans* treated with FLC for 1hr, 2h and 4h it was observed from the venn-diagram (Fig. 3.14. A) that genes upregulated in 1h were over two fold more than those identified in 2h and about 10 fold more than 4h treatment (Supplementary Table 21). Therefore, with time FLC response narrows down and much less overlapping genes are shared between 4h and the earlier time points. Induction of most of the *Erg* genes were found to ensue from 2h through 4h FLC treatments. *Erg10* and *Erg13* were included in the list of genes shared between all three FLC treatment time points (Table 3.28). *Erg10* and *Erg13* act at the beginning of the pathway and hence the consistent upregulation of these genes indicate impact of FLC to curb ergosterol biosynthesis at earlier steps of the pathway.

Down-regulated genes identified by riboseq FLC treatment time course, revealed a greater abundance of differentially expressed genes observed for 1hr and gradually decreasing numbers were obtained with increasing time (Supplementary Table 22). Several genes were shared in the overlapping time point sets (Fig. 3.14. B) and interestingly every pair of overlap includes ribosomal proteins or ribosomal biogenesis genes. Table 3.29 represents down-regulated genes shared by all riboseq FLC time points and includes genes encoding ribosomal proteins L10-like and L37a.

A B

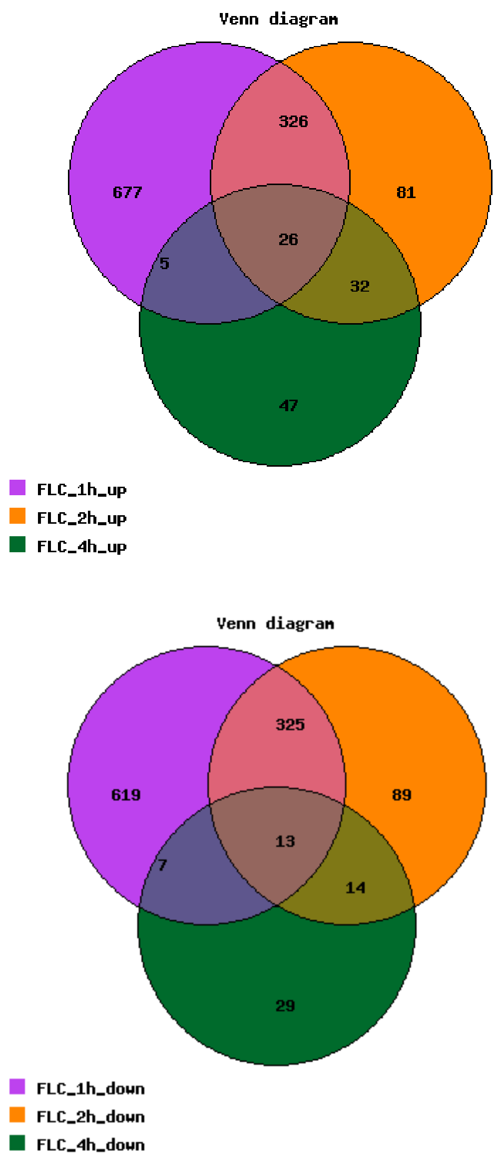

Figure III-13 Venn-diagram showing A, upregulated and B, down-regulated genes in FLC treatments at different time points based on riboseq.

Gene ID	Product Description	Gene Name or Symbol
CNAG_02918	Acetyl-CoA C-acetyltransferase	ERG10
CNAG_03311	hydroxymethylglutaryl-CoA synthase	ERG13

CNAG_00176	glutamate carboxypeptidase	N/A
CNAG_00990	F-type H -transporting ATPase subunit H, variant	N/A
CNAG_01239	Chitin deacetylase	CDA3
CNAG_02752	Short-chain dehydrogenase	N/A
CNAG_03072	enolase	N/A
CNAG_03358	Phosphoglycerate kinase	N/A
CNAG_04735	extracellular elastinolytic metalloproteinase	MEP1
CNAG_04869	para-nitrobenzyl esterase	PNB1

Table 3.28. continued

Gene ID	**Product Description**	**Gene Name or Symbol**
CNAG_06534	hydroxymethylglutaryl-CoA reductase (NADPH)	HMG1
CNAG_06628	aldehyde dehydrogenase (NAD)	N/A
CNAG_06666	starch phosphorylase	N/A
CNAG_00730	ATP-binding cassette transporter	AFR1
CNAG_00895	solute carrier family 39 (zinc transporter), member 1/2/3	ZIP1
CNAG_01023	cohesin complex subunit SCC1	N/A
CNAG_01060	hypothetical protein	N/A
CNAG_02300	hypothetical protein	N/A
CNAG_02777	phosphate:H symporter, variant	PHO84
CNAG_04209	voltage-gated potassium channel protein beta-2 subunit	N/A
CNAG_04566	beta-flanking protein	N/A
CNAG_06745	Histone H3	H3
CNAG_07361	hypothetical protein	N/A
CNAG_07807	Histone H4	N/A

CNAG_07902	AAT family amino acid transporter	N/A

Table 3.28. Differentially up-regulated *C. neoformans* genes shared between FLC treatment time points based on riboseq.

Differentially up-regulated *C. neoformans* genes shared between 1h, 2h and 4h FLC treatments identified by ribo-seq.

Gene ID	Product Description	Gene Name or Symbol
CNAG_03739	large subunit ribosomal protein L10-like	N/A
CNAG_04011	large subunit ribosomal protein L37a	N/A
CNAG_00077	solute carrier family 26 (sodium-independent sulfate anion transporter), member 11	N/A
CNAG_00315	HHE domain-containing protein	N/A
CNAG_00815	MFS transporter, SIT family, siderophore-iron:H symporter	SIT1
CNAG_01047	hypothetical protein	N/A
CNAG_01666	U6 snRNA-associated Sm-like protein LSm2	N/A
CNAG_04043	hypothetical protein	N/A
CNAG_04663	hypothetical protein	N/A
CNAG_05267	NADH dehydrogenase (ubiquinone) Fe-S protein 5	N/A
CNAG_05696	ubiquitin-conjugating enzyme E2-16 kDa	N/A
CNAG_07965	hypothetical protein	N/A
CNAG_12265	unspecified product	N/A

Table 3.29. Differentially down-regulated *C. neoformans* genes shared between FLC treatment time points based on riboseq.

Differentially down-regulated *C. neoformans* genes after 1, 2 and 4 h incubation with 0.7 μg/ml FLC identified by ribo-seq.

SRT treatment time course

After riboseq on *C. neoformans* treated with SRT for 1hr, 2h and 4h it was observed from the venn-diagram (Fig. 3.15. A) that with time gradually less number of genes were upregulated (Supplementary Table 23). 27 genes which were shared among upregulated sets from all the three time points indicate these genes consistently being modulated by the drug treatment in the time course (Table 3.30). *CNAG_01953*, which is the gene identified from RNA-seq to be highly upregulated, appears in this list. *FZC46* (CNAG_03115) the gene containing the *UPC2* transcription factor domain is another gene that was identified by both RNA-seq and this riboseq time course SRT data. *ERG2, ERG10* and *ERG13* were identified in the SRT riboseq time course which were also found in the RNA-seq data for SRT up-regulated genes. These genes appear to be consistently targeted by SRT even at earlier time points of drug of exposure.

From the venn-diagram (Fig. 3.15. B), it was observed that 1h set had maximum number of down-regulated genes and the numbers gradually decrease with time (Supplementary Table 24). Fifteen genes were shared among SRT riboseq down-regulated sets from all the three time points including the gene encoding translation initiation factor eIF-1A which was also found to be repressed in the SRT RNA-seq data.

A B

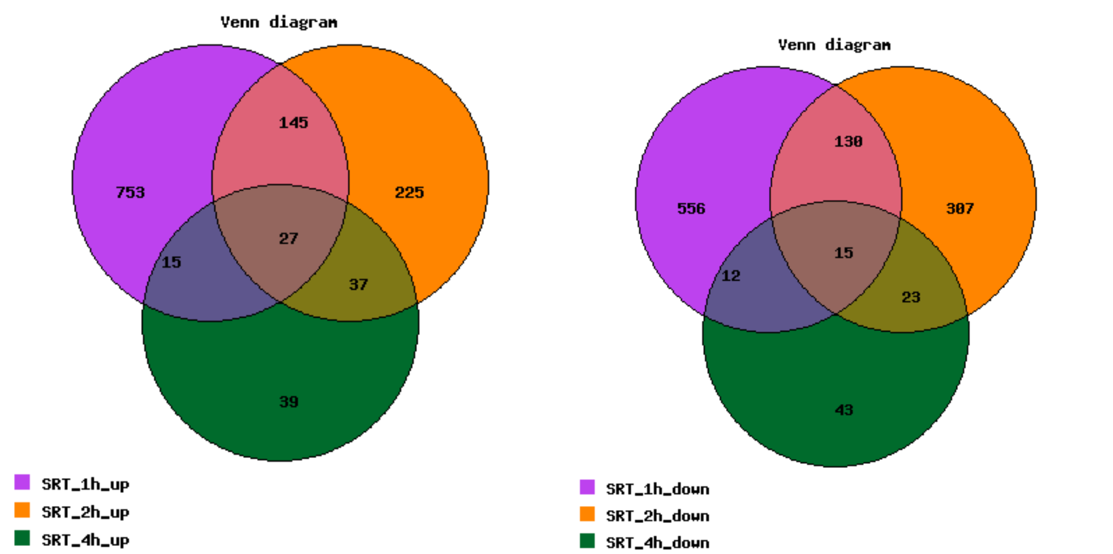

Figure III-14 Venn-diagram showing A, upregulated and B, down-regulated genes in SRT treatments at different time points based on riboseq.

Gene ID	Product Description	Gene Name or Symbol

CNAG_00061	citrate synthase, mitochondrial	CIT1
CNAG_00121	glycerol-3-phosphate dehydrogenase (NAD())	N/A
CNAG_00235	amt family ammonium transporter	AMT1
CNAG_00236	8-Amino-7-oxononanoate synthase	N/A
CNAG_00581	saccharopepsin	N/A
CNAG_00854	C-8 sterol isomerase	ERG2
CNAG_01451	hypothetical protein	N/A
CNAG_01711	glycerol-3-phosphate O- acyltransferase/dihydroxyacetone phosphate acyltransferase	N/A
CNAG_01949	chlorophyll synthesis pathway protein BchC	N/A

Table 3.30. continued

Gene ID	Product Description	Gene Name or Symbol
CNAG_01953	hypothetical protein	N/A
CNAG_01984	transaldolase	TAL1
CNAG_02028	CMGC/SRPK protein kinase	N/A
CNAG_02752	Short-chain dehydrogenase	N/A
CNAG_02768	hypothetical protein	N/A
CNAG_02852	4-aminobutyrate transaminase	N/A
CNAG_02918	Acetyl-CoA C-acetyltransferase	ERG10
CNAG_02974	voltage-dependent anion channel protein 2	N/A
CNAG_03007	hypothetical protein	N/A
CNAG_03114	hypothetical protein	N/A
CNAG_03115	hypothetical protein	FZC46
CNAG_03225	malate dehydrogenase, NAD-dependent	N/A
CNAG_03266	malate dehydrogenase, NAD-dependent	N/A

CNAG_03311	hydroxymethylglutaryl-CoA synthase	ERG13
CNAG_03732	Integral membrane protein	N/A
CNAG_03764	Integral membrane protein	N/A
CNAG_03892	chaperonin GroES	N/A
CNAG_03916	glucose-6-phosphate isomerase	N/A

Table 3.30. Differentially up-regulated *C. neoformans* genes shared between SRT treatment time points based on riboseq.

Differentially up-regulated *C. neoformans* genes shared between 1h, 2h and 4h SRT treatments identified by ribo-seq.

Gene ID	**Product Description**	**Gene Name or Symbol**
CNAG_04147	ATP-dependent rRNA helicase RRP3	N/A
CNAG_04215	sulfate adenylyltransferase	MET3
CNAG_05455	translation initiation factor eIF-1A	N/A
CNAG_05904	small subunit ribosomal protein S14	N/A
CNAG_06367	U3 small nucleolar RNA-associated protein 3	N/A
CNAG_06626	pre-mRNA-splicing factor ATP-dependent RNA helicase DHX15/PRP43	N/A
CNAG_06774	tRNA (guanine-N(7)-)-methyltransferase	N/A
CNAG_07536	DNA-directed RNA polymerase I subunit RPA43	N/A
CNAG_04348	Chaperone	N/A
CNAG_04663	hypothetical protein	N/A

CNAG_05848	splicing factor U2AF 65 kDa subunit	N/A
CNAG_10501	unspecified product	N/A
CNAG_12056	unspecified product	N/A
CNAG_13128	unspecified product	N/A
CNAG_13174	unspecified product	N/A

Table 3.31. Differentially down-regulated *C. neoformans* genes shared between SRT treatment time points based on riboseq.

Differentially up-regulated *C. neoformans* genes shared between 1h, 2h and 4h SRT treatments identified by ribo-seq.

SRT+FLC treatment time course

We found a comparatively small number of genes were identified and shared in all the treatment time points for SRT+FLC treatments in both up-regulated and down-regulated gene categories (Fig.3.16 and Supplementary Tables 25 and 26). 2 genes *CNAG_01953*, the putative MFS transporter and *CNAG_05075*, a phosphate transporter are shared among upregulated sets from all the three time points. *CNAG_01953* as discussed earlier were identified in SRT and SRT+FLC RNA-seq data and in the riboseq data for both SRT and SRT+FLC indicating specific upregulation of this gene by SRT. However, No overlap was found in the SRT+FLC riboseq downregulated sets for all three time points.

A

B

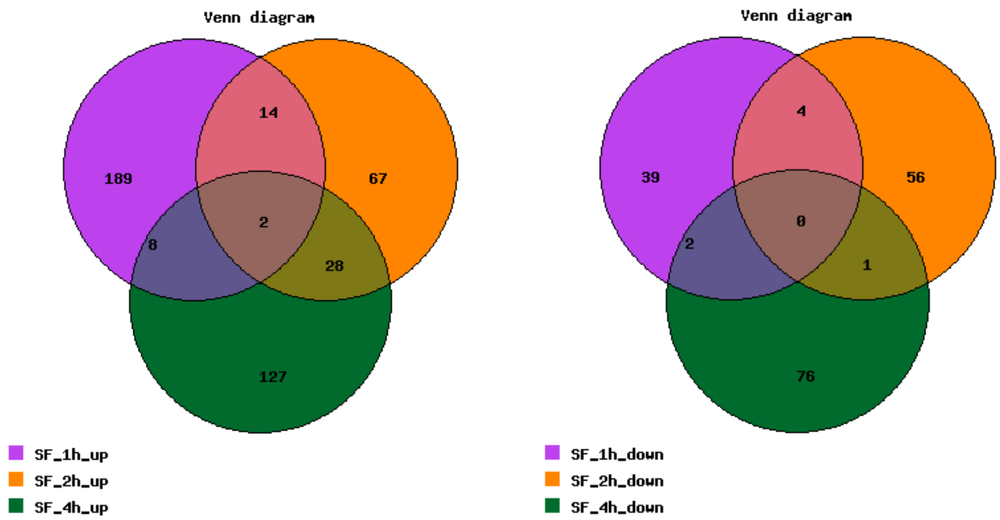

Figure III-15 Venn-diagram showing A, upregulated and B, down-regulated genes in SRT+ FLC treatments at different time points based on riboseq.

CHAPTER IV

CONCLUSIONS AND FUTURE DIRECTIONS

Conclusions

Systemic mycoses are causing millions of deaths worldwide when left untreated and are restricted to a few classes of antifungals [14, 26]. Cryptococcal meningitis is one such infection accounting for a mortality rate of over 60% in HIV-AIDS patients or people having severe immune suppression such as organ transplant patients [2, 5, 30]. Anticryptococcal treatment options are narrowed by the lack of efficacy and active inhibition by drugs or is complicated with cytotoxicity after long term drug exposure. Discovery of the antifungal effect of SRT is a step forward to newer therapeutics. Such alternate therapies are also necessitated by the development of antifungal resistance such as resistance to azoles which are the most well-tolerated and widely used antifungal for cryptococcosis. Major hurdles to find therapies against *C. neoformans* is due to the need for drugs that can cross blood brain barrier and be effective in doses that can be metabolized by the system without generating toxic intermediates.

SRT is a well-suited drug for repurposing because it is an FDA approved antidepressant which has appreciable availability in the central nervous system and has much lesser incidence of adverse effects reported in patients suffering from mental health disorders who are treated with SRT [32, 100, 142, 143]. This is critical since the prolonged time required for drug discovery is completely overcome and the drug being in circulation SRT is already in continuous production and is largely accessible to the society. Additionally SRT is considered to potentiate the activity of FLC, a widely prescribed antifungal [4]. Several studies have also revealed that SRT can inhibit growth of bacteria, other fungi and even cancer cells or tumors [60, 61, 66, 85]. However, the mechanism behind the antiproliferative activity of SRT is not known. Here in this study we aimed to determine the molecular targets of SRT in *C. neoformans* by identifying genome-wide changes specific to drug treatments based on RNA-seq and ribosome profiling or ribo-seq. However, riboseq data is not from the matched cells used for RNA-seq and generated lesser reads overall and has to be considered as a qualitative analysis. FLC being a common antifungal, was a reference standard to serve as a positive control and as expected from several studies, we identified ergosterol biosynthesis genes upregulated by FLC in both RNA-seq and 2h and 4h ribo-seq data [4, 19, 20, 30] . It was interesting to identify that SRT up-reguated half of the genes of the *ERG* pathway in RNA-seq data and some genes such as *SRE1*, *ERG10 ERG13*, *ERG2* and *ERG3* were shared with the SRT riboseq data at all the different time points.

In experiments conducted with SRT+FLC drug combination, all *ERG* genes except *ERG27* were upregulated by RNAseq. SRT+FLC riboseq data could identify *ERG* genes only in 4h time points.

Thus, SRT targets the *ERG* pathway and shows a common branch of antifungal response similar to FLC but to a lesser extent.

The response of SRT does not totally correspond with FLC and reveals its own distinct and unique targets, which are significantly altered in SRT and SRT+FLC treatments but not in FLC. Such SRT specific candidate genes include the putative MFS transporter *CNAG_01953* and *FZC46* (CNAG_03115), the gene containing the *UPC2* transcription factor domain which was consistently upregulated in all SRT experiments including RNA-seq and SRT riboseq time course. *CNAG_03732, CNAG_03764* and *CNAG_02299*, potential paralog of *CNAG_01953* are also identified to be SRT specific membrane proteins induced by SRT in both ribo-seq and RNA-seq. Multiple kinases such as Wee protein kinase (CNAG_03369), CAMK/CAMKL/Kin4 protein kinase (CNAG_05558) and CMGC/MAPK protein kinase (CNAG_04282) were found to SRT specific in the RNA-seq upregulated genes.

Many ribosome biogenesis genes and ribosomal proteins were down-regulated by SRT, FLC and SRT+FLC treatments in RNA-seq results. The decrease in ribosomal protein encoding genes by RNA-seq in FLC treated cells were not reported earlier except for a report in *C. gatti [144]*. Some of these ribosomal proteins including large subunit ribosomal protein L37-A CNAG_03015 and large subunit ribosomal protein L8 CNAG_05232 were specifically downregulated by SRT and not not significantly altered by FLC. Ribosomal protein L37-A also appears in SRT ribo-seq time course. This might also hint at repression of translation by SRT as reported in the literature [4, 66].

Several noncoding RNAs were downregulated by SRT specifically which indicates regulatory roles of these ncRNAs in fungal response to SRT that not clearly understood. Thus our data suggests molecular mechanisms by which SRT changes the gene expression profiles in *C. neoformans* that possibly contributes to killing of the fungi and is substantially distinct from FLC, though shares some common targets.

Future Directions

The genes found to be SRT specific can be investigated by forward genetics. Genes *CNAG_01953*, *CNAG_03115*, *SRE1* are being deleted and overexpressed in *C. neoformans* to investigate cellular response to SRT treatment and identify possible phenotypes. SRT is known to bind lipids and interfere with vesiculogenic membranes, hence, lipid metabolism is another field to study to understand the mode of action of SRT [45, 87]. Resistance to FLC is known to me mediated by aneuploidy to generate more copies of the target gene Erg11 and any such chromosomal aberration could also be studied in case of SRT treatment [20, 22]. Therefore this study has identified interesting SRT specific candidates and genetic and biochemical studies can in future reveal a more comprehensive picture of the antifungal mechanisms employed by SRT against *C. neoformans*

REFRENCES

1. Gatti, F. and R. Eeckels, An atypical strain of Cryptococcus neoformans (San Felice) Vuillemin 1894. I. Description of the disease and of the strain. Ann Soc Belges Med Trop Parasitol Mycol, 1970. **50**(6): p. 689-93.
2. Mitchell, T.G. and J.R. Perfect, *Cryptococcosis in the era of AIDS--100 years after the discovery of Cryptococcus neoformans.* Clinical microbiology reviews, 1995. **8**(4): p. 515-548.
3. Idnurm, A. and X. Lin, *Rising to the challenge of multiple Cryptococcus species and the diseases they cause.* Fungal genetics and biology : FG & B, 2015. **78**: p. 1-6.
4. Zhai, B., et al., *The Antidepressant Sertraline Provides a Promising Therapeutic Option for Neurotropic Cryptococcal Infections.* Antimicrobial Agents and Chemotherapy, 2012. **56**(7): p. 3758-3766.
5. Warnock, D.W., *Cryptococcus neoformans.* Journal of Antimicrobial Chemotherapy, 1999. **44**(1): p. 139-139.
6. Brown, G.D., et al., *Hidden killers: human fungal infections.* Sci Transl Med, 2012. **4**(165): p. 165rv13.
7. Coelho, C., A.L. Bocca, and A. Casadevall, *The intracellular life of Cryptococcus neoformans.* Annu Rev Pathol, 2014. **9**: p. 219-38.
8. Vartivarian, S.E., et al., *Regulation of cryptococcal capsular polysaccharide by iron.* J Infect Dis, 1993. **167**(1): p. 186-90.

9. Aksenov, S.I., I.P. Babyeva, and V.I. Golubev, *On the mechanism of adaptation of micro-organisms to conditions of extreme low humidity.* Life Sci Space Res, 1973. **11**: p. 55-61.

10. Granger, D.L., J.R. Perfect, and D.T. Durack, *Virulence of Cryptococcus neoformans. Regulation of capsule synthesis by carbon dioxide.* J Clin Invest, 1985. **76**(2): p. 508-16.

11. Nosanchuk, J.D., et al., *Evidence that Cryptococcus neoformans is melanized in pigeon excreta: implications for pathogenesis.* Infect Immun, 1999. **67**(10): p. 5477-9.

12. Idnurm, A., et al., *Deciphering the Model Pathogenic Fungus Cryptococcus Neoformans.* Nature Reviews Microbiology, 2005. **3**(10): p. 753-764.

13. Coelho, C. and A. Casadevall, *Cryptococcal therapies and drug targets: the old, the new and the promising.* Cell Microbiol, 2016. **18**(6): p. 792-9.

14. Roemer, T. and D.J. Krysan, *Antifungal drug development: challenges, unmet clinical needs, and new approaches.* Cold Spring Harb Perspect Med, 2014. **4**(5).

15. Pianalto, K.M. and J.A. Alspaugh, *New Horizons in Antifungal Therapy.* J Fungi (Basel), 2016. **2**(4).

16. Odds, F.C., A.J.P. Brown, and N.A.R. Gow, *Antifungal agents: mechanisms of action.* Trends in Microbiology, 2003. **11**(6): p. 272-279.

17. Sangalli-Leite, F., et al., *Amphotericin B mediates killing in Cryptococcus neoformans through the induction of a strong oxidative burst.* Microbes and Infection, 2011. **13**(5): p. 457-467.

18. Perfect, J.R., et al., *Clinical practice guidelines for the management of cryptococcal disease: 2010 update by the infectious diseases society of america.* Clin Infect Dis, 2010. **50**(3): p. 291-322.

19. Spitzer, M., et al., *Cross-species discovery of syncretic drug combinations that potentiate the antifungal fluconazole.* Mol Syst Biol, 2011. **7**: p. 499.

20. Florio, A.R., et al., *Genome-wide expression profiling of the response to short-term exposure to fluconazole in Cryptococcus neoformans serotype A.* BMC Microbiol, 2011. **11**: p. 97.

21. Ngo, H.X., S. Garneau-Tsodikova, and K.D. Green, *A complex game of hide and seek: the search for new antifungals.* Medchemcomm, 2016. **7**(7): p. 1285-1306.

22. Shapiro, R.S., N. Robbins, and L.E. Cowen, *Regulatory circuitry governing fungal development, drug resistance, and disease.* Microbiol Mol Biol Rev, 2011. **75**(2): p. 213-67.

23. Spitzer, M., N. Robbins, and G.D. Wright, *Combinatorial strategies for combating invasive fungal infections.* Virulence, 2017. **8**(2): p. 169-185.

24. Robbins, N., et al., *An Antifungal Combination Matrix Identifies a Rich Pool of Adjuvant Molecules that Enhance Drug Activity against Diverse Fungal Pathogens.* Cell Rep, 2015. **13**(7): p. 1481-1492.

25. Movahed, E., et al., *Triclosan Demonstrates Synergic Effect with Amphotericin B and Fluconazole and Induces Apoptosis-Like Cell Death in Cryptococcus neoformans.* Front Microbiol, 2016. **7**: p. 360.

26. Krysan, D.J., *Toward improved anti-cryptococcal drugs: Novel molecules and repurposed drugs.* Fungal Genet Biol, 2015. **78**: p. 93-8.

27. Gowri, M., et al., *Sertraline as a promising antifungal agent: inhibition of growth and biofilm of Candida auris with special focus on the mechanism of action in vitro.* J Appl Microbiol, 2020. **128**(2): p. 426-437.

28. Rhein, J., et al., *Adjunctive sertraline for HIV-associated cryptococcal meningitis: a randomised, placebo-controlled, double-blind phase 3 trial.* Lancet Infect Dis, 2019. **19**(8): p. 843-851.

29. Tremaine, L.M., W.M. Welch, and R.A. Ronfeld, *Metabolism and disposition of the 5-hydroxytryptamine uptake blocker sertraline in the rat and dog.* Drug Metab Dispos, 1989. **17**(5): p. 542-50.

30. Brown, J.C.S., et al., *Unraveling the biology of a fungal meningitis pathogen using chemical genetics.* Cell, 2014. **159**(5): p. 1168-1187.

31. Nayak, R. and J. Xu, *Effects of sertraline hydrochloride and fluconazole combinations on Cryptococcus neoformans and Cryptococcus gattii.* Mycology, 2010. **1**(2): p. 99-105.

32. Sanchez, C., E.H. Reines, and S.A. Montgomery, *A comparative review of escitalopram, paroxetine, and sertraline: Are they all alike?* Int Clin Psychopharmacol, 2014. **29**(4): p. 185-96.

33. Artigas, F., D.J. Nutt, and R. Shelton, *Mechanism of action of antidepressants.* Psychopharmacology bulletin, 2002. **36 Suppl 2**: p. 123-132.

34. Berger, M., J.A. Gray, and B.L. Roth, *The Expanded Biology of Serotonin.* Annual Review of Medicine, 2009. **60**(1): p. 355-366.

35. Meyer, J.H., et al., *Serotonin transporter occupancy of five selective serotonin reuptake inhibitors at different doses: an [11C]DASB positron emission tomography study.* Am J Psychiatry, 2004. **161**(5): p. 826-35.

36. Zhou, Z., et al., *Antidepressant specificity of serotonin transporter suggested by three LeuT-SSRI structures.* Nat Struct Mol Biol, 2009. **16**(6): p. 652-7.

37. Carvalho, A.F., et al., *The Safety, Tolerability and Risks Associated with the Use of Newer Generation Antidepressant Drugs: A Critical Review of the Literature.* Psychotherapy and Psychosomatics, 2016. **85**(5): p. 270-288.

38. Muñoz-Criado, S., J.L. Muñoz-Bellido, and J.A. García-Rodríguez, *In vitro activity of nonsteroidal anti-inflammatory agents, phenotiazines, and antidepressants against Brucella species.* Eur J Clin Microbiol Infect Dis, 1996. **15**(5): p. 418-20.

39. Munoz-Bellido, J.L., S. Munoz-Criado, and J.A. Garcìa-Rodrìguez, *Antimicrobial activity of psychotropic drugs: selective serotonin reuptake inhibitors.* Int J Antimicrob Agents, 2000. **14**(3): p. 177-80.

40. Krzyżek, P., et al., *In Vitro Activity of Sertraline, an Antidepressant, Against Antibiotic-Susceptible and Antibiotic-Resistant Helicobacter pylori Strains.* Pathogens, 2019. **8**(4): p. 228.

41. Lass-Flörl, C., et al., *Antifungal Activity against Candida Species of the Selective Serotonin-Reuptake Inhibitor, Sertraline.* Clinical Infectious Diseases, 2001. **33**(12): p. e135-e136.

42. Lass-Flörl, C., et al., *Antifungal properties of selective serotonin reuptake inhibitors against Aspergillus species in vitro.* J Antimicrob Chemother, 2001. **48**(6): p. 775-9.

43. Costa Silva, R.A., et al., *In vitro anti-Candida activity of selective serotonin reuptake inhibitors against fluconazole-resistant strains and their activity against biofilm-forming isolates.* Microb Pathog, 2017. **107**: p. 341-348.

44. Oliveira, A.S., et al., *Anti-Candida activity of antidepressants sertraline and fluoxetine: effect upon pre-formed biofilms.* Med Microbiol Immunol, 2018. **207**(3-4): p. 195-200.

45. Rainey, M.M., et al., *The Antidepressant Sertraline Targets Intracellular Vesiculogenic Membranes in Yeast.* Genetics, 2010. **185**(4): p. 1221-1233.

46. Chen, J., et al., *Accumulation of an Antidepressant in Vesiculogenic Membranes of Yeast Cells Triggers Autophagy.* PLOS ONE, 2012. **7**(4): p. e34024.

47. Heller, I., et al., *Serotonin (5-HT) enhances the activity of amphotericin B against Aspergillus fumigatus in vitro.* International Journal of Antimicrobial Agents, 2004. **24**(4): p. 401-404.

48. Rossato, L., et al., *In vitro synergistic effects of chlorpromazine and sertraline in combination with amphotericin B against Cryptococcus neoformans var. grubii.* Folia Microbiol (Praha), 2016. **61**(5): p. 399-403.

49. Treviño-Rangel Rde, J., et al., *Activity of sertraline against Cryptococcus neoformans: in vitro and in vivo assays.* Med Mycol, 2016. **54**(3): p. 280-6.

50. Villanueva-Lozano, H., et al., *Evaluation of the expanding spectrum of sertraline against uncommon fungal pathogens.* Journal of Infection and Chemotherapy, 2020. **26**(3): p. 309-311.

51. Romanelli, M.M., et al., *Sertraline Delivered in Phosphatidylserine Liposomes Is Effective in an Experimental Model of Visceral Leishmaniasis.* Frontiers in cellular and infection microbiology, 2019. **9**: p. 353-353.

52. Lima, M.L., et al., *Molecular Basis of the Leishmanicidal Activity of the Antidepressant Sertraline as a Drug Repurposing Candidate.* Antimicrobial agents and chemotherapy, 2018. **62**(12): p. e01928-18.

53. Weeks, J.C., et al., *Sertraline, Paroxetine, and Chlorpromazine Are Rapidly Acting Anthelmintic Drugs Capable of Clinical Repurposing.* Scientific Reports, 2018. **8**(1): p. 975.

54. Ferreira, D.D., et al., *Efficacy of sertraline against Trypanosoma cruzi: an in vitro and in silico study.* The journal of venomous animals and toxins including tropical diseases, 2018. **24**: p. 30-30.

55. Fröbe, A., et al., *Plasma free serotonin as a marker for early detection of breast cancer recurrence.* Anticancer Res, 2014. **34**(3): p. 1167-9.

56. Arreola, R., et al., *Immunomodulatory effects mediated by serotonin.* J Immunol Res, 2015. **2015**: p. 354957.

57. Nannmark, U., et al., *Inhibition of leukocyte phagocytosis by serotonin and its possible role in tumor cell destruction.* Cancer Lett, 1992. **62**(1): p. 83-6.

58. Liang, Y., et al., *Shedding Light on the Role of Neurotransmitters in the Microenvironment of Pancreatic Cancer.* Frontiers in cell and developmental biology, 2021. **9**: p. 688953-688953.

59. Karmakar, S. and G. Lal, *Role of serotonin receptor signaling in cancer cells and anti-tumor immunity.* Theranostics, 2021. **11**(11): p. 5296-5312.

60. Tuynder, M., et al., *Translationally controlled tumor protein is a target of tumor reversion.* Proc Natl Acad Sci U S A, 2004. **101**(43): p. 15364-9.

61. Amson, R., et al., *Reciprocal repression between P53 and TCTP.* Nat Med, 2011. **18**(1): p. 91-9.

62. Malard, F., et al., *Revisiting the molecular interactions between the tumor protein TCTP and the drugs sertraline/thioridazine.* ChemMedChem, 2021.

63. Duarte, D., A. Cardoso, and N. Vale, *Synergistic Growth Inhibition of HT-29 Colon and MCF-7 Breast Cancer Cells with Simultaneous and Sequential Combinations of Antineoplastics and CNS Drugs.* Int J Mol Sci, 2021. **22**(14).

64. Tzadok, S., et al., *In vitro novel combinations of psychotropics and anti-cancer modalities in U87 human glioblastoma cells.* Int J Oncol, 2010. **37**(4): p. 1043-51.

65. Bottega, A.M., et al., *Antimicrobial and Antineoplastic Properties of Sertraline.* American Journal of Therapeutics.

66. Lin, C.-J., et al., *The Antidepressant Sertraline Inhibits Translation Initiation by Curtailing Mammalian Target of Rapamycin Signaling.* Cancer Research, 2010. **70**(8): p. 3199.

67. Jiang, X., et al., *Repurposing sertraline sensitizes non–small cell lung cancer cells to erlotinib by inducing autophagy.* JCI Insight, 2018. **3**(11).

68. Kobayashi, D., et al., *Translationally Controlled Tumor Protein Is a Novel Biological Target for Neurofibromatosis Type 1-associated Tumors **. Journal of Biological Chemistry, 2014. **289**(38): p. 26314-26326.

69. Bommer, U.-A., et al., *Growth-factor dependent expression of the translationally controlled tumour protein TCTP is regulated through the PI3-K/Akt/mTORC1 signalling pathway.* Cellular Signalling, 2015. **27**(8): p. 1557-1568.

70. Bae, S.-Y., et al., *TPT1 (tumor protein, translationally-controlled 1) negatively regulates autophagy through the BECN1 interactome and an MTORC1-mediated pathway.* Autophagy, 2017. **13**(5): p. 820-833.

71. Ye, D., et al., *Targeting SERT promotes tryptophan metabolism: mechanisms and implications in colon cancer treatment.* J Exp Clin Cancer Res, 2021. **40**(1): p. 173.

72. Wang, C., et al., *Inducing and exploiting vulnerabilities for the treatment of liver cancer.* Nature, 2019. **574**(7777): p. 268-272.

73. Hwang, H.Y., et al., *Antidepressant drug sertraline modulates AMPK-MTOR signaling-mediated autophagy via targeting mitochondrial VDAC1 protein.* Autophagy, 2020: p. 1-17.

74. Lin, K.-L., et al., *Effect of sertraline on [Ca2+]i and viability of human MG63 osteosarcoma cells.* Drug and Chemical Toxicology, 2013. **36**(2): p. 231-240.

75. Jajoo, A., et al., *Sertraline induces DNA damage and cellular toxicity in Drosophila that can be ameliorated by antioxidants.* Scientific Reports, 2020. **10**(1): p. 4512.

76. Chen, S., et al., *Sertraline, an antidepressant, induces apoptosis in hepatic cells through the mitogen-activated protein kinase pathway.* Toxicol Sci, 2014. **137**(2): p. 404-15.

77. Chen, S., et al., *Sertraline induces endoplasmic reticulum stress in hepatic cells.* Toxicology, 2014. **322**: p. 78-88.

78. Huang, J.-K., et al., *The Mechanism of Sertraline-induced [Ca2+]i Rise in Human PC3 Prostate Cancer Cells.* Basic & Clinical Pharmacology & Toxicology, 2011. **109**(2): p. 103-110.

79. Chinnapaka, S., V. Bakthavachalam, and G. Munirathinam, *Repurposing antidepressant sertraline as a pharmacological drug to target prostate cancer stem cells: dual activation of apoptosis and autophagy signaling by deregulating redox balance.* Am J Cancer Res, 2020. **10**(7): p. 2043-2065.

80. Kuwahara, J., et al., *Comparison of the Anti-tumor Effects of Selective Serotonin Reuptake Inhibitors as Well as Serotonin and Norepinephrine Reuptake*

Inhibitors in Human Hepatocellular Carcinoma Cells. Biological and Pharmaceutical Bulletin, 2015. **38**(9): p. 1410-1414.

81. Xia, D., et al., *Sertraline exerts its antitumor functions through both apoptosis and autophagy pathways in acute myeloid leukemia cells.* Leukemia & Lymphoma, 2017. **58**(9): p. 2208-2217.

82. Gil-Ad, I., et al., *Evaluation of the potential anti-cancer activity of the antidepressant sertraline in human colon cancer cell lines and in colorectal cancer-xenografted mice.* Int J Oncol, 2008. **33**(2): p. 277-86.

83. Reddy, K.K., et al., *The antidepressant sertraline downregulates Akt and has activity against melanoma cells.* Pigment Cell Melanoma Res, 2008. **21**(4): p. 451-6.

84. Amit, B.H., et al., *Proapoptotic and chemosensitizing effects of selective serotonin reuptake inhibitors on T cell lymphoma/leukemia (Jurkat) in vitro.* Eur Neuropsychopharmacol, 2009. **19**(10): p. 726-34.

85. Di Rosso, M.E., et al., *Beneficial Effect of Fluoxetine and Sertraline on Chronic Stress-Induced Tumor Growth and Cell Dissemination in a Mouse Model of Lymphoma: Crucial Role of Antitumor Immunity.* Frontiers in Immunology, 2018. **9**(1341).

86. Kocaturk, N.M., et al., *Autophagy as a molecular target for cancer treatment.* Eur J Pharm Sci, 2019. **134**: p. 116-137.

87. Ngo, D.T.N., et al., *Thermodynamics of selective serotonin reuptake inhibitors partitioning into 1,2-dioleoyl-sn-glycero-3-phosphocholine bilayers.* RSC Advances, 2020. **10**(64): p. 39338-39347.

88. Wang, J.S., et al., *Sertraline and its metabolite desmethylsertraline, but not bupropion or its three major metabolites, have high affinity for P-glycoprotein.* Biol Pharm Bull, 2008. **31**(2): p. 231-4.

89. Nielsen, C.U., et al., *Sertraline inhibits the transport of PAT1 substrates in vivo and in vitro.* British journal of pharmacology, 2013. **170**(5): p. 1041-1052.

90. Bohnert, J.A., et al., *Efflux inhibition by selective serotonin reuptake inhibitors in Escherichia coli.* J Antimicrob Chemother, 2011. **66**(9): p. 2057-60.

91. Li, L., et al., *Insight into synergetic mechanisms of tetracycline and the selective serotonin reuptake inhibitor, sertraline, in a tetracycline-resistant strain of Escherichia coli.* J Antibiot (Tokyo), 2017. **70**(9): p. 944-953.

92. Hussein, M., et al., *Effective Strategy Targeting Polymyxin-Resistant Gram-Negative Pathogens: Polymyxin B in Combination with the Selective Serotonin Reuptake Inhibitor Sertraline.* ACS Infect Dis, 2020. **6**(6): p. 1436-1450.

93. Kapoor, R., et al., *Antidepressants are modifiers of lipid bilayer properties.* J Gen Physiol, 2019. **151**(3): p. 342-356.

94. Then, C.K., et al., *Antidepressants, sertraline and paroxetine, increase calcium influx and induce mitochondrial damage-mediated apoptosis of astrocytes.* Oncotarget, 2017. **8**(70): p. 115490-115502.

95. Li, Y., et al., *Mitochondrial dysfunction induced by sertraline, an antidepressant agent.* Toxicol Sci, 2012. **127**(2): p. 582-91.

96. Isaac, R., et al., *Selective serotonin reuptake inhibitors (SSRIs) inhibit insulin secretion and action in pancreatic β cells.* J Biol Chem, 2013. **288**(8): p. 5682-93.

97. Chung, C.P., et al., *Increased oxidative stress in patients with depression and its relationship to treatment.* Psychiatry Res, 2013. **206**(2-3): p. 213-6.

98. Battal, D., et al., *Possible role of selective serotonin reuptake inhibitor sertraline on oxidative stress responses.* Eur Rev Med Pharmacol Sci, 2014. **18**(4): p. 477-84.

99. Abdel-Salam, O.M., et al., *Brain and liver oxidative stress after sertraline and haloperidol treatment in mice.* J Basic Clin Physiol Pharmacol, 2013. **24**(2): p. 115-23.

100. Byeon, E., et al., *Two antidepressants fluoxetine and sertraline cause growth retardation and oxidative stress in the marine rotifer Brachionus koreanus.* Aquatic Toxicology, 2020. **218**: p. 105337.

101. Ilgin, S., et al., *Evidence for cardiotoxicity associated with sertraline in rats.* Toxicology Research, 2018. **7**(5): p. 817-825.

102. Arihan, O., et al., *Effects of two selected SSRIs on hemorheological parameters in rats.* Clin Hemorheol Microcirc, 2019. **71**(1): p. 27-38.

103. Atli, O., et al., *Sertraline-induced reproductive toxicity in male rats: evaluation of possible underlying mechanisms.* Asian J Androl, 2017. **19**(6): p. 672-679.

104. Ozgocmen, S., et al., *Antioxidant status, lipid peroxidation and nitric oxide in fibromyalgia: etiologic and therapeutic concerns.* Rheumatol Int, 2006. **26**(7): p. 598-603.

105. Elmorsy, E., et al., *Antidepressants are cytotoxic to rat primary blood brain barrier endothelial cells at high therapeutic concentrations.* Toxicol In Vitro, 2017. **44**: p. 154-163.

106. Kumar, P. and A. Kumar, *Possible role of sertraline against 3-nitropropionic acid induced behavioral, oxidative stress and mitochondrial dysfunctions in rat brain.* Prog Neuropsychopharmacol Biol Psychiatry, 2009. **33**(1): p. 100-8.

107. Michalakeas, C.A., et al., *Effects of sertraline on circulating markers of oxidative stress in depressed patients with chronic heart failure: a pilot study.* J Card Fail, 2011. **17**(9): p. 748-54.

108. Pedreañez, A., et al., *Experimental depression induces renal oxidative stress in rats.* Physiology & Behavior, 2011. **104**(5): p. 1002-1009.

109. Kwatra, M., et al., *Naringin and Sertraline Ameliorate Doxorubicin-Induced Behavioral Deficits Through Modulation of Serotonin Level and Mitochondrial Complexes Protection Pathway in Rat Hippocampus.* Neurochemical Research, 2016. **41**(9): p. 2352-2366.

110. Purdel, N.C., et al., *Studies regarding the protective effects exhibited by antidepressants on cell models.* Rom J Morphol Embryol, 2015. **56**(2 Suppl): p. 781-8.

111. Ahmadimanesh, M., et al., *Effects of selective serotonin reuptake inhibitors on DNA damage in patients with depression.* J Psychopharmacol, 2019. **33**(11): p. 1364-1376.

112. Istifli, E.S., et al., *In vitro cytogenotoxic evaluation of sertraline.* Interdisciplinary toxicology, 2018. **11**(3): p. 181-188.

113. Spadari, C.d.C., et al., *New Approaches for Cryptococcosis Treatment.* Microorganisms, 2020. **8**(4): p. 613.

114. Wambaugh, M.A., et al., *Synergistic and antagonistic drug interactions in the treatment of systemic fungal infections.* eLife, 2020. **9**: p. e54160.

115. Cong, L., et al., *In Vitro Antifungal Activity of Sertraline and Synergistic Effects in Combination with Antifungal Drugs against Planktonic Forms and Biofilms of Clinical Trichosporon asahii Isolates.* PLOS ONE, 2016. **11**(12): p. e0167903.

116. McGlincy, N.J. and N.T. Ingolia, *Transcriptome-wide measurement of translation by ribosome profiling.* Methods, 2017. **126**: p. 112-129.

117. Basenko, E.Y., et al., *FungiDB: An Integrated Bioinformatic Resource for Fungi and Oomycetes.* J Fungi (Basel), 2018. **4**(1).

118. Kim, J., et al., *A defect in iron uptake enhances the susceptibility of Cryptococcus neoformans to azole antifungal drugs.* Fungal Genet Biol, 2012. **49**(11): p. 955-66.

119. Bhattacharya, S., B.D. Esquivel, and T.C. White, *Overexpression or deletion of ergosterol biosynthesis genes alters doubling time, response to stress agents, and drug susceptibility in Saccharomyces cerevisiae.* mBio, 2018. **9**(4).

120. Hughes, A.L., et al., *4-Methyl sterols regulate fission yeast SREBP-Scap under low oxygen and cell stress.* J Biol Chem, 2007. **282**(33): p. 24388-96.

121. Ward, D.M., et al., *Altered sterol metabolism in budding yeast affects mitochondrial iron-sulfur (Fe-S) cluster synthesis.* The Journal of biological chemistry, 2018. **293**(27): p. 10782-10795.

122. Ghannoum, M.A. and L.B. Rice, *Antifungal agents: mode of action, mechanisms of resistance, and correlation of these mechanisms with bacterial resistance.* Clin Microbiol Rev, 1999. **12**(4): p. 501-17.

123. Rodrigues, M.L., *The Multifunctional Fungal Ergosterol.* mBio, 2018. **9**(5).

124. Hu, Z., et al., *Recent Advances in Ergosterol Biosynthesis and Regulation Mechanisms in Saccharomyces cerevisiae.* Indian J Microbiol, 2017. **57**(3): p. 270-277.

125. Jorda, T. and S. Puig, *Regulation of ergosterol biosynthesis in Saccharomyces cerevisiae.* Genes (Basel), 2020. **11**(7).

126. Branco, J., et al., *Impact of ERG3 mutations and expression of ergosterol genes controlled by UPC2 and NDT80 in Candida parapsilosis azole resistance.* Clinical Microbiology and Infection, 2017. **23**(8): p. 575.e1-575.e8.

127. Chang, Y.C., et al., *Conservation of the sterol regulatory element-binding protein pathway and its pathobiological importance in Cryptococcus neoformans.* Eukaryot Cell, 2009. **8**(11): p. 1770-9.

128. Hughes, B.T., C.C. Nwosu, and P.J. Espenshade, *Degradation of sterol regulatory element-binding protein precursor requires the endoplasmic*

reticulum-associated degradation components Ubc7 and Hrd1 in fission yeast. The Journal of biological chemistry, 2009. **284**(31): p. 20512-20521.

129. Lee, K.-T., et al., *Fungal kinases and transcription factors regulating brain infection in Cryptococcus neoformans.* Nature Communications, 2020. **11**(1): p. 1521.

130. Lee, C.Y., et al., *Oxygen-dependent binding of Nro1 to the prolyl hydroxylase Ofd1 regulates SREBP degradation in yeast.* Embo j, 2009. **28**(2): p. 135-43.

131. Karnani, N., et al., *SRE1 and SRE2 are two specific steroid-responsive modules of Candida drug resistance gene 1 (CDR1) promoter.* Yeast, 2004. **21**(3): p. 219-39.

132. Hwang, L.H., et al., *SRE1 regulates iron-dependent and -independent pathways in the fungal pathogen Histoplasma capsulatum.* Eukaryotic cell, 2012. **11**(1): p. 16-25.

133. Chao, L.Y., M.A. Marletta, and J. Rine, *Sre1, an Iron-Modulated GATA DNA-Binding Protein of Iron-Uptake Genes in the Fungal Pathogen Histoplasma capsulatum.* Biochemistry, 2008. **47**(27): p. 7274-7283.

134. Chang, Y.C., et al., *Sre1p, a regulator of oxygen sensing and sterol homeostasis, is required for virulence in Cryptococcus neoformans.* Mol Microbiol, 2007. **64**(3): p. 614-29.

135. Blatzer, M., et al., *SREBP Coordinates Iron and Ergosterol Homeostasis to Mediate Triazole Drug and Hypoxia Responses in the Human Fungal Pathogen Aspergillus fumigatus.* PLOS Genetics, 2011. **7**(12): p. e1002374.

136. Hughes, A.L., B.L. Todd, and P.J. Espenshade, *SREBP pathway responds to sterols and functions as an oxygen sensor in fission yeast.* Cell, 2005. **120**(6): p. 831-42.

137. Bien, C.M. and P.J. Espenshade, *Sterol regulatory element binding proteins in fungi: hypoxic transcription factors linked to pathogenesis.* Eukaryot Cell, 2010. **9**(3): p. 352-9.

138. Gutiérrez, M.S., et al., *Sterol Regulatory Element-Binding Protein (Sre1) Promotes the Synthesis of Carotenoids and Sterols in Xanthophyllomyces dendrorhous.* Frontiers in microbiology, 2019. **10**: p. 586-586.

139. Brown, H.E., et al., *Sterol-Response Pathways Mediate Alkaline Survival in Diverse Fungi.* mBio, 2020. **11**(3): p. e00719-20.

140. Maguire, S.L., et al., *Zinc finger transcription factors displaced SREBP proteins as the major Sterol regulators during Saccharomycotina evolution.* PLoS genetics, 2014. **10**(1): p. e1004076-e1004076.

141. Ma, B.X., et al., *Rate-limiting steps in the Saccharomyces cerevisiae ergosterol pathway: towards improved ergosta-5,7-dien-3β-ol accumulation by metabolic engineering.* World J Microbiol Biotechnol, 2018. **34**(4): p. 55.

142. Huddart, R., et al., *PharmGKB summary: sertraline pathway, pharmacokinetics.* Pharmacogenetics and genomics, 2020. **30**(2): p. 26-33.

143. Saletu, B., J. Grünberger, and L. Linzmayer, *On central effects of serotonin re-uptake inhibitors: Quantitative EEG and psychometric studies with sertraline and zimelidine.* Journal of Neural Transmission, 1986. **67**(3): p. 241-266.

144. Chong, H.S., et al., *Time-Course Proteome Analysis Reveals the Dynamic Response of Cryptococcus gattii Cells to Fluconazole.* PLOS ONE, 2012. **7**(8): p. e42835.

APPENDIX A

SUPPLEMENTARY INFORMATION

List of Supplementary tables with web links

Source Folder:

https://drive.google.com/drive/folders/1VYD5KRpQpW049cieSPtFhMtf8mhBC2N0?usp=sharing

Tables	Content	Link
1	RNAseq Up Venn-diagram	https://docs.google.com/spreadsheets/d/1xgs0tKZcMidizALq5jfIfKWtR4Oj69b-/edit?usp=sharing&ouid=110521100861719320194&rtpof=true&sd=true
2	RNAseq down Venn-diagram	https://docs.google.com/spreadsheets/d/1_VWds6yQfsyyF4pumnYRozh_WHeqgkF-/edit?usp=sharing&ouid=110521100861719320194&rtpof=true&sd=true
3	RNAseq FLC upregulated genes	https://docs.google.com/spreadsheets/d/1EdBKYuUVo1v0A7O4WHdhdoXnJI_1V3_J/edit?usp=sharing&ouid=110521100861719320194&rtpof=true&sd=true
4	RNAseq FLC Up GO analysis	https://docs.google.com/spreadsheets/d/1msxqXpqF7o1osS_VlLgIDG2B3YH9RH5D/edit?usp=sharing&ouid=110521100861719320194&rtpof=true&sd=true
5	RNAseq FLC downregulated genes	https://docs.google.com/spreadsheets/d/13LekNIYRHAExX5gglIX7IpIIvu6wbwwP/edit?usp=sharing&ouid=110521100861719320194&rtpof=true&sd=true
6	RNAseq FLC down GO analysis	https://docs.google.com/spreadsheets/d/1RT_Lk_xf8uuDimHp04w_ccOAB4rAf47V/edit?usp=sharing&ouid=110521100861719320194&rtpof=true&sd=true
7	RNAseq SRT upregulated genes	https://docs.google.com/spreadsheets/d/1AQ1snc-_ZgsTn87HIA0J6ZcClIAbV5Vp/edit?usp=sharing&ouid=110521100861719320194&rtpof=true&sd=true
8	RNAseq SRT Up GO analysis	https://docs.google.com/spreadsheets/d/1OWJ2vH6r0_B8dlF7OXIqOUhKlJI63pBE/edit?usp=sharing&ouid=110521100861719320194&rtpof=true&sd=true
9	RNAseq SRT downregulated genes	https://docs.google.com/spreadsheets/d/1tDbJDjurPgYWikZUbg8vsFBAaJ4XKiDc/edit?usp=sharing&ouid=110521100861719320194&rtpof=true&sd=true
10	RNAseq SRT down GO analysis	https://docs.google.com/spreadsheets/d/12ZwDpM9ir3D2qDexE7Ov9NNkWZ0uR1r_/edit?usp=sharing&ouid=110521100861719320194&rtpof=true&sd=true

11	RNAseq SRT+FLC upregulated genes	https://docs.google.com/spreadsheets/d/1UmvPBcW5KTjBMujq8ITE36ZiC6gYTWL8/edit?usp=sharing&ouid=110521100861719320194&rtpof=true&sd=true
12	RNAseq SRT+FLC Up GO analysis	https://docs.google.com/spreadsheets/d/1SpTwHpGPUH5xcwedpjz_lDsy0R_Nx8_p/edit?usp=sharing&ouid=110521100861719320194&rtpof=true&sd=true
13	RNAseq SRT+FLC downregulated genes	https://docs.google.com/spreadsheets/d/1Bv48MP04SWp2guRo8cy2yOh-PPPMiku-/edit?usp=sharing&ouid=110521100861719320194&rtpof=true&sd=true
14	RNAseq SRT+FLC down GO analysis	https://docs.google.com/spreadsheets/d/18QP_aSOszs29WbiVZ12pga4hlp-BdCKJ/edit?usp=sharing&ouid=110521100861719320194&rtpof=true&sd=true
15	Riboseq 4h FLC upregulated genes	https://docs.google.com/spreadsheets/d/14d0x75_TKYbVdbqGe472EXE-uhX34umP/edit?usp=sharing&ouid=110521100861719320194&rtpof=true&sd=true
16	Riboseq 4h FLC downregulated genes	https://docs.google.com/spreadsheets/d/1MyZZ3vj3IqrkOmPAS4JAqU6opO2jDrGg/edit?usp=sharing&ouid=110521100861719320194&rtpof=true&sd=true
17	Riboseq 4h SRT upregulated genes	https://docs.google.com/spreadsheets/d/1E_4HCD595Cht-l-VyJoggTUlox55HgJ9/edit?usp=sharing&ouid=110521100861719320194&rtpof=true&sd=true
18	Riboseq 4h SRT downregulated genes	https://docs.google.com/spreadsheets/d/1kJUWROaEYnKEy-kiDhK5RidnFH7yvJWp/edit?usp=sharing&ouid=110521100861719320194&rtpof=true&sd=true
19	Riboseq 4h SRT+FLC upregulated genes	https://docs.google.com/spreadsheets/d/1KcKSAAjvvRtDNp_q18R4egyTb7g4JoyI/edit?usp=sharing&ouid=110521100861719320194&rtpof=true&sd=true
20	Riboseq 4h SRT+FLC downregulated genes	https://docs.google.com/spreadsheets/d/1NLyDPRl9Dcw7mhEwddqhMF96u7pJVx3m/edit?usp=sharing&ouid=110521100861719320194&rtpof=true&sd=true
21	Riboseq FLC Up Venn-diagram	https://docs.google.com/spreadsheets/d/1sv2Go6qdAOKHSIh25ALn6kJHU3eUOoZw/edit?usp=sharing&ouid=110521100861719320194&rtpof=true&sd=true

22	Riboseq FLC down Venn-diagram	https://docs.google.com/spreadsheets/d/16PqXPgRaE16v-2o7MJth0WuwGzknVJER/edit?usp=sharing&ouid=110521100861719320194&rtpof=true&sd=true
23	Riboseq SRT Up Venn-diagram	https://docs.google.com/spreadsheets/d/14UGGM-efSMb9MRRqgKA1XPubT_wzodOg/edit?usp=sharing&ouid=110521100861719320194&rtpof=true&sd=true
24	Riboseq SRT down Venn-diagram	https://docs.google.com/spreadsheets/d/1cQGOdG06UQfA8m9zFJVzy7Td79j9I8tF/edit?usp=sharing&ouid=110521100861719320194&rtpof=true&sd=true
25	Riboseq SRT+FLC Up Venn-diagram	https://docs.google.com/spreadsheets/d/1mrjJO6J7Kzd2rsQAqUBZCh3rSBFsAJ2u/edit?usp=sharing&ouid=110521100861719320194&rtpof=true&sd=true
26	Riboseq SRT+FLC down Venn-diagram	https://docs.google.com/spreadsheets/d/1PfFGq8gwg8kifFi6AagcalaXLv8xTuUC/edit?usp=sharing&ouid=110521100861719320194&rtpof=true&sd=true